Theses and Dissertations--Civil Engineering

Civil Engineering

2016

CIRCULAR RC COLUMNS PARTIALLY CONFINED WITH FRP

Sahar Y. Ghanem
University of Kentucky, sayghanem@yahoo.com
Digital Object Identifier: http://dx.doi.org/10.13023/ETD.2016.124

STUDENT AGREEMENT:

I represent that my thesis or dissertation and abstract are my original work. Proper attribution has been given to all outside sources. I understand that I am solely responsible for obtaining any needed copyright permissions. I have obtained needed written permission statement(s) from the owner(s) of each third-party copyrighted matter to be included in my work, allowing electronic distribution (if such use is not permitted by the fair use doctrine) which will be submitted to UKnowledge as Additional File.

I hereby grant to The University of Kentucky and its agents the irrevocable, non-exclusive, and royalty-free license to archive and make accessible my work in whole or in part in all forms of media, now or hereafter known. I agree that the document mentioned above may be made available immediately for worldwide access unless an embargo applies.

I retain all other ownership rights to the copyright of my work. I also retain the right to use in future works (such as articles or books) all or part of my work. I understand that I am free to register the copyright to my work.

REVIEW, APPROVAL AND ACCEPTANCE

The document mentioned above has been reviewed and accepted by the student's advisor, on behalf of the advisory committee, and by the Director of Graduate Studies (DGS), on behalf of the program; we verify that this is the final, approved version of the student's thesis including all changes required by the advisory committee. The undersigned agree to abide by the statements above.

<div align="right">

Sahar Y. Ghanem, Student

Dr. Issam E. Harik, Major Professor

Dr. Yi T. Wang, Director of Graduate Studies

</div>

CIRCULAR RC COLUMNS PARTIALLY CONFINED WITH FRP

―――――――――――――――――――――

DISSERTATION

―――――――――――――――――――――

A dissertation submitted in partial fulfillment of the
requirements for the degree of Doctor of Philosophy in the
College of Engineering
at the University of Kentucky

By

Sahar Yousef Ghanem

Lexington, Kentucky

Director: Dr. Issam Elias Harik, Professor of Civil Engineering
Lexington, Kentucky
2016

ABSTRACT OF DISSERTATION

CIRCULAR RC COLUMNS PARTIALLY CONFINED WITH FRP

Wrapping reinforced concrete (RC) columns with Fiber Reinforced Polymer (FRP) composites is effective in increasing their capacity. The current state of art concentrates primarily on fully wrapped RC columns and few studies dealt with partially wrapped columns. The majority of the studies did not account for the influence of the existing steel reinforcement on the column's behavior. Other studies estimated the total confinement pressure as the sum of the confinement pressure due to the external FRP jacketing and due to the internal transverse steel reinforcement. Few models dealt with the coupled effect of the confinement from steel and partial FRP wrapping of RC columns. The objective herein is to evaluate the effectiveness of partial wraps (or strips) and to develop a confined concrete compressive stress-strain (f_c – ε_c) model that accounts for partial wrapping. Three dimensional finite element (FE) models are generated to evaluate the influence of different parameters on the behavior of concentrically loaded RC circular columns that are partially and fully wrapped with FRP. The influence of FRP volumetric ratio, concrete compressive strength, transverse steel reinforcement ratio, longitudinal steel reinforcement ratio, and strip arrangement, are evaluated. The results indicated an increase in ductility as the number of FRP strips was increased, and showed that longitudinal steel had little influence on the confined f_c – ε_c relationship. The proposed f_c – ε_c model, derived from the parametric study, accounts for the effect of partial and full confinement, the unconfined concrete strength f_c', and yielding of transverse steel. Comparison of the results generated using the proposed model with FE and experimental results are in good agreement. The finite element method (FEM) is also used to evaluate the effectiveness of RC columns, wrapped with carbon FRP, subjected to an eccentric load, with a case study of a bridge column wrapped with FRP.

KEYWORDS: Reinforced concrete; columns; confinement; stress–strain; finite element; ductility, partial FRP Wrap

Sahar Ghanem

_____

Student's Signature

_____

Date

CIRCULAR RC COLUMNS PARTIALLY CONFINED WITH FRP

By

Sahar Yousef Ghanem

Dr. Issam E. Harik
Director of Dissertation

Dr. Yi-Tin Wang
Director of Graduate Studies

_____
Date

To my husband, my parents, and my wonderful children

ACKNOWLEDGEMENTS

TABLE OF CONTENTS

LIST OF TABLES

LIST OF FIGURES

x

xi

xiii

CHAPTER 1
INTRODUCTION

1.1   Background

As structures age and their serviceability life is reached, engineers have to either demolish them and build new structures or restore them so they can still serve their purpose. Old structures are restored for a number of different reasons, such as improving the seismic performance, changing the facility's intended use, strengthening of deficient elements, or revisions of code requirements.

The selection of the materials to for restoration is challenging and the overall retrofit can be very costly. Consequently, engineers look for unconventional repair materials, in particular, Fiber-Reinforced Polymer (FRP) composites.

FRP has several advantages compared to traditional materials used for strengthening, such as light weight, high stiffness, and resistance to corrosion which creates minimal architecture impact due to low thickness and ease of repair. However, it is expensive and has a linear stress-strain relationship leading to a brittle failure behavior. Currently, one of the major applications of FRP in civil infrastructure is retrofitting structural reinforced concrete components with FRP composites.

Reinforced concrete (RC) columns, that are critical structural components, are the subject of this dissertation.   One method for increasing the capacity of RC columns is by confining the concrete. This is generally carried out by providing lateral or hoop steel around the longitudinal reinforcing steel bars. A concrete cover is applied around the lateral steel to protect it from the elements. The initial method of confining RC columns was by using steel jackets which wrapped around the concrete cover. Consequently, the

1

concrete core inside the lateral hoop steel is being confined by the hoops and the steel jacket while the core is confined by the jacket. This increases the column capacity considerably. One limitation for steel jacketing is that they have to be prefabricated for the specific columns.

FRP jacketing of RC columns was an extension of the steel jacketing. Its advantage is its adaptability to any column shape when applied through wet layup in the field. Application of FRP jacketing is currently an established and efficient technique for enhancing the capacity of columns. FRP wraps can be applied in different arrangements, from covering the entire column (full wrap) or covering part of the column with FRP strips (partial wrap).

Columns that are fully wrapped with FRP showed an increase in ductility, moment and ultimate compressive load capacity, ultimate deformability, and energy absorption compared to unconfined columns (Mirmiran and Shahawy 1997, Spoelstra and Monti 1999, Toutanji 1999). Several studies focusing on fully wrapped FRP confined concrete columns have been carried out to generate models for predicting their behavior (Nanni, A., and Bradford 1995, Samaan et al 1998, Lam and Teng 2003). Research on columns partially wrapped with FRP sheets (or strips) is very limited (Saadatmanesh et al 1994, Barros and Ferreira 2008, Wu et al 2009).

The majority of the studies did not account for the influence of the existing steel reinforcement on the column's behavior (Lam and Teng 2003), or simply estimated the total confinement pressure as the sum of the confinement pressure due to the external FRP sheets and the confinement pressure due to the internal transverse steel reinforcement (Barros and Ferreira 2008, Harajli et al 2006). Few models dealt with concrete confined by

2

both FRP and transverse steel (Eid and Paultre 2008, Lee et al 2010). The consideration of the interaction between existing internal steel and external FRP reinforcement in partially wrapped RC columns is an area requiring further evaluation and it is the focus of this dissertation.

1.2   Research Objectives

The objective of this research is to derive a confined concrete compressive stress-strain model for concentrically loaded RC circular columns that are partially and fully wrapped with Fiber Reinforced Polymer composites.

1.3   Research Significance

The study introduces a new analytical stress strain model to accurately predict the behavior of concentrically loaded RC circular columns wrapped with FRP strips while taking into account the interaction between internal steel and external FRP reinforcement.

Based on the current state of the art, the proposed work will allow a better understanding of the behavior of using FRP Strips for wrapping RC columns and the parameters that influence the effectiveness of partial wraps. Throughout this work, circular specimens are studied, and all fibers are oriented in the hoop direction. This is achieved by developing a three dimensional finite element (FE) model, which is capable of describing the behavior of these structures.

3

1.4   Organization of Dissertation

This dissertation is organized in six chapters. The main body of the work, which includes FE analysis and analytical investigations of the effectiveness of RC column wrapped with FRP is presented in chapters 3, 4, and 5. An outline of the contents of the chapters is presented in the following sections:

Chapter 2:   Literature Review

An overview of current researches regarding steel-confined concrete, FRP confined concrete, and steel-and-FRP-confined concrete have been reviewed in this chapter, as well as the concrete models in literature. The review included concentrically and eccentrically loaded columns, and Finite Element Analysis Models (FEAM) for confined columns.

Chapter 3:   Finite Element Analysis for Concentrically Loaded RC Circular Columns Confined with FRP

A Finite Element Model (FEM) of circular reinforced concrete (RC) columns partially and fully wrapped with FRP are generated using ANSYS 14 (ANSYS 2012) finite element program. The results from the analysis are compared with published experimental results to validate the model. They are listed in term of stress-strain relationships. The influence of critical parameters on the confinement effectiveness in concentrically loaded RC columns included the FRP confinement ratio, the compressive strength of unconfined concrete, the

transverse steel reinforcement ratio, the longitudinal steel reinforcement ratio, and the strip arrangement are discussed.

Chapter 4: Model Development for Concentrically Loaded Circular RC Columns Partially Confined with FRP

An analytical model is developed for concentrically loaded RC circular columns that partially and fully wrapped with Fiber Reinforced Polymers (FRP), with fibers oriented in the hoop direction. The reliability of the model is checked by comparing results with experimental results in the current literature and with ones generated by the FE analysis.

Chapter 5: Eccentrically Loaded Confined Columns

The FEM is used in Chapter 3 to analyze concentrically loaded columns, is used in this chapter to study the behavior of eccentrically loaded RC columns wrapped with carbon FRP (CFRP). A case study of a bridge pier that was retrofitted following a truck impact is presented.

Chapter 6: Conclusions

This chapter includes a summary of the dissertation and concludes the major findings of this dissertation. Suggestions for the future work are provided.

CHAPTER 2
LITERATURE REVIEW

2.1   Introduction

This Chapter provides an overview of the current state of the art of the stress-strain models for concrete confined by steel and/or fiber reinforced polymer (FRP) composites. The finite element method, used to verify the accuracy of certain models, is also highlighted in this chapter.

2.2   Concrete Confinement

Confined concrete is achieved by providing internal and/or external reinforcement to concrete, such as internal spirals and hoops, or external steel or FRP jackets.

Two types of confinement are known in civil engineering: (1) Active confinement, which continually provides confining pressure as in the case of fluid pressure, and (2) passive confinement, such as that provided by spiral reinforcement where the pressure is not constant but depends on the lateral expansion of concrete from an axial load and the corresponding response of the confining material.

Passive confinement through fiber reinforced polymer (FRP) wrap is of interest in this dissertation. In the early twentieth century, Richart et al. (1928) pioneered studies regarding beneficial effects of lateral confinement on the strength and deformation characteristics of concrete. It was reported that an increase in lateral pressure leads to significant increase in ductility and strength, and reduces internal cracking. Since then, numerous experimental and analytical studies have been conducted on confined concrete.

6

2.3   Steel Confined Concrete

2.3.1   General Behavior

Concrete column cross sections, reinforced laterally with steel, have a core portion enclosed or confined with steel and a part that includes the cover of unconfined concrete. At low levels of stress in concrete, both parts behave similarly as unconfined concrete, and steel has no effect. However, as the stress level in concrete is increased and approaches the post-peak loading history, the transverse steel effect increases considerably. Once the compressive strength of the unconfined concrete (f_c') is reached, the concrete cover becomes ineffective. As the stress increases under applied load, the concrete expands outwardly and the internal cracks increase leading to high stress in transverse steel which applies a confining response to the concrete (Kent and Park 1971) and places the core in a state of tri-axial stress.

The behavior of steel confined concrete is affected by variables including amount of lateral reinforcement, distribution of longitudinal and lateral reinforcement configuration, transverse steel spacing, size/dimension, and characteristics of transverse steel (Sheikh and Uzumeri 1980).

Between the locations of transverse steel, or within the spacing, the confinement is less significant depending on the spacing and amount of transverse steel due to arching between them. The arching effect is caused by the spalling of ineffectively confined concrete and is greatest midway between transverse steel reinforcement. The strength of the column is then governed by the smallest area of a section which is midway between the transverse reinforcement (Mander, et al. 1988), and larger spacing between them results in a smaller confined area of concrete as shown in Figure 2.1. (Sheikh and Uzumeri 1980).

7

Where $f_{l,s,\max}$ is the maximum lateral confining pressure due to transverse steel and f_y

is the specified yield strength of transverse steel reinforcement.
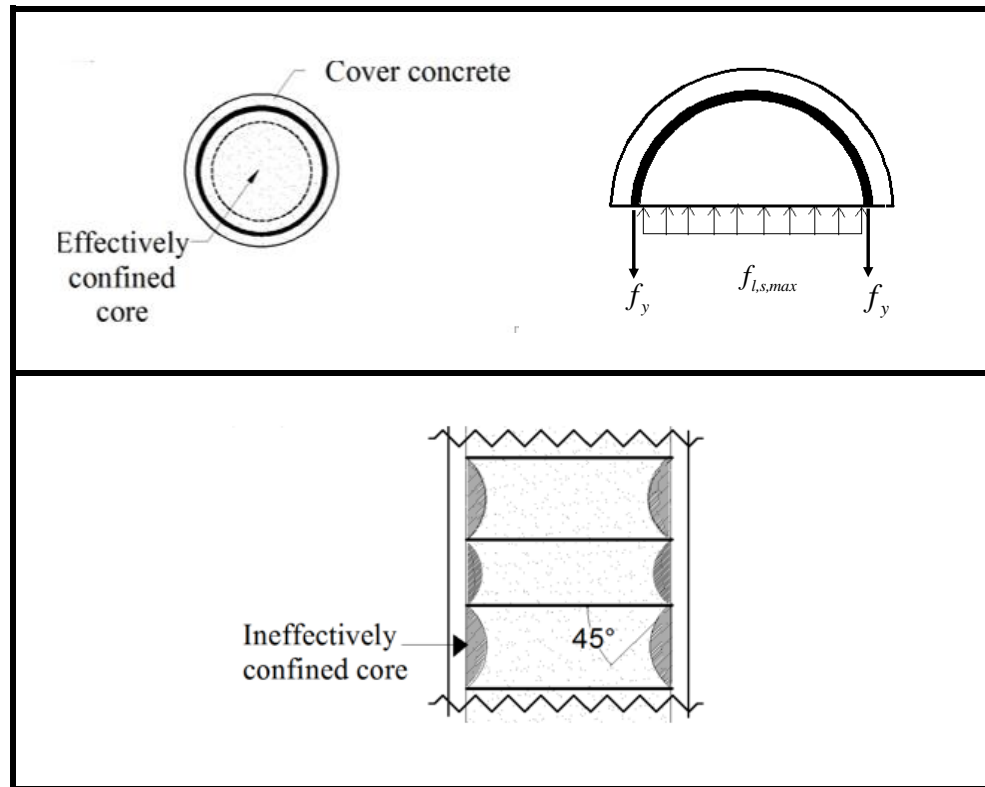
Figure 2.1-Concrete effectively confined by steel

Circular transverse steel is more effective than square or rectangular ones, since non circular transverse steel applies confining pressure only near the corners, while the pressure of the concrete on the sides causes the steel to bend. Therefore, the strength enhancement in confined rectangular columns is not significant.

8

2.3.2   Steel Confinement Models

Numerous stress-strain models for steel confined concrete have been proposed (Kent and Park 1971, Scott et al 1982, Mander et al 1988, and Hoshikuma et al 1997). Most of the models are composed of an ascending branch and a descending branch, and each branch is represented by a different equation. Studies were conducted on columns having rectangular cross sections (Mander et al 1988, Scott et al 1982), or circular cross-sections (Mander et al 1988, Hoshikuma et al 1997).

Two stress strain models are discussed in the following sections. The Kent and Park model (1971) and the Mander model (1988).

2.3.2.1   Kent and Park (1971)

This model was developed for concrete confined with transverse steel hoops or spirals. The proposed stress strain relationship for unconfined and confined concrete is defined by three regions as shown in Figure 2.2.

The first region (from A-B) initiates at a concrete compressive strain of $\varepsilon_c = 0$ and extends to a strain level of $\varepsilon_c = 0.002$. This region is expressed as Eq. 2.1. Confinement does not influence this region. .

$$f_c = f_c' \left[\frac{2\varepsilon_c}{0.002} - \left(\frac{\varepsilon_c}{0.002} \right)^2 \right] \tag{2.1}$$

Where f_c is compressive stress in concrete; f_c' is the compressive strength of unconfined and ε_c is the axial strain level in concrete.

9
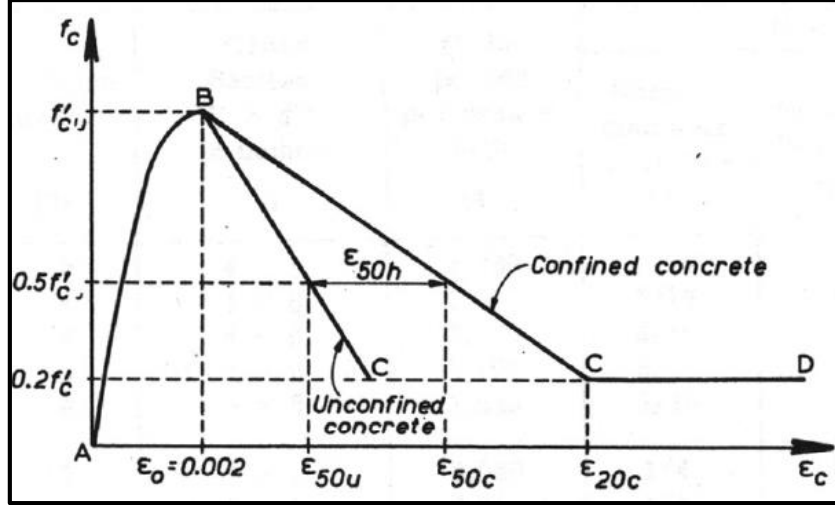
Figure 2.2- Kent and Park stress strain model (Kent and Park1971)

The second region (from B-C) is the descending linear curve for unconfined concrete that initiates at $\varepsilon_c = 0.002$ and extends to the point where it intersects with horizontal at compressive concrete stress level $f_c = 0.2 f_c^{'}$, where $f_c^{'}$ is compressive strength of unconfined concrete at 28 days. The equation for this region is expressed as follows:

$$f_c = f_c^{'} \times [1 - Z(\varepsilon_c - 0.002)]$$ (2.2)

Where Z is the slope of descending curve and is expressed as

$$Z = \frac{0.5}{\varepsilon_{50u} + \varepsilon_{50h} - 0.002}$$ (2.3)

in which,

$$\varepsilon_{50u} = \frac{3 + 0.002 f_c^{'}}{f_c^{'} - 1000}$$ (2.4)

$$\varepsilon_{50h} = \frac{3}{4} \rho_s \sqrt{\frac{b''}{s}}$$ (2.5)

10

Where ε_{50u} is strain at 50% of compressive strength of unconfined concrete (f_c') and ε_{50h} is the strain increment due to the effects of confinement for confined concrete, also at 50% f_c'. ε_{50u} and ε_{50h} are shown in Figure 2.2. ρ_s is the ratio of the volume of transverse reinforcement to the volume of the concrete core; b'' is the width of the confined core; s is the spacing between the transverse reinforcement.

The third region from B to C to D is the descending linear curve for confined concrete that initiates at $\varepsilon_c = 0.002$ and extends to the point where it intersects with horizontal at compressive concrete stress level $f_c = 0.2f_c'$ and levels off at a constant stress level of $f_c = 0.2f_c'$ until it reaches point D (Figure 2.2).

2.3.2.2 Mander et al. (1988)

One of the most widely used models in analyzing reinforced concrete columns is Mander's Model (1988). The model is presented in Figure 2.3 for unconfined and confined concrete. f_c-ε_c relationship and is expressed by Eq. 2.6

$$f_c = f_{cc}' \frac{(\varepsilon_c / \varepsilon_{ccu}) r_s}{r_s - 1 + (\varepsilon_c / \varepsilon_{ccu})^{r_s}} \tag{2.6}$$

in which,

$$\varepsilon_{ccu} = \varepsilon_c' \left[1 + 5 \left(\frac{f_{cc}'}{f_c'} - 1 \right) \right] \tag{2.7}$$

$$r_s = \frac{E_c}{\left(E_c - f_{cc}' / \varepsilon_{ccu} \right)} \tag{2.8}$$

$$E_c = 5000 \sqrt{f_c'} \tag{2.9}$$

11

where E_c is the modulus of elasticity of concrete; r_s is a steel constant that accounts for the brittleness of concrete; ε_c' is the unconfined strain that can be approximated as being equal to 0.002; ε_{ccu} confined concrete ultimate axial strain corresponding to ultimate compressive stress in confined concrete f_{cc}'
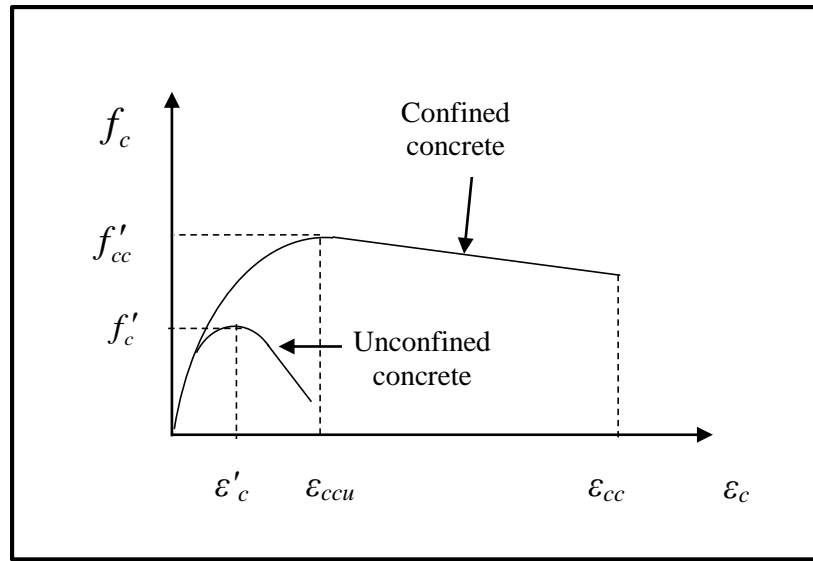
Figure 2.3- Mander Stress-Strain Model 1988 for Monotonic loading
of confined concrete

The ultimate compressive stress in confined concrete, f_{cc}', is determined by Mander (1988) using the five parameter failure criterion proposed by William and Warnke 1975, and the triaxial test data of Schickert and Winkler 1977, and expressed as

$$f_{cc}' = f_c'\left(2.254\sqrt{1 + 7.94\frac{f_{l,s,\max}'}{f_c'}} - 2\frac{f_{l,s,\max}'}{f_c'} - 1.254 \right) \tag{2.10}$$

in which, $f_{l,s,max}'$ = effective lateral confining pressure due to transverse steel, and

12

$$f'_{l,s,\max} = k_{e,s} f_{l,s,\max} \tag{2.11}$$

where $k_{e,s}$ is the confinement effectiveness coefficient, and $f_{l,s,\max}$ is the maximum confining pressure due to transverse steel.

For circular columns,

$$\rho_{st} = \frac{4A_{st}}{sd_s} \tag{2.12}$$

$$f_{l,s,\max} = \frac{1}{2}\rho_{st}f_y \tag{2.13}$$

$$k_{e,s} = \begin{cases} \dfrac{\left(1-\dfrac{s'}{2d_s}\right)^2}{1-(A_{sl}/A_{core})} & \text{for hoops} \\[4ex] \dfrac{1-\dfrac{s'}{2d_s}}{1-(A_{sl}/A_{core})} & \text{for spirals} \end{cases} \tag{2.14}$$

where A_{core} is the core area of the column measured to the centerline of transverse steel; A_{st} is the area of transverse steel; A_{sl} is the total area of longitudinal reinforcement; d_s is the diameter of the section between the transverse steel centers; f_y is the specified yield strength of nonprestressed reinforcement; s is the center to center spacing between transverse steel; s' is the clear spacing between transverse steel ; ρ_{st} is the transverse steel reinforcement ratio.

13

2.4   FRP Confined Concrete

2.4.1   General Behavior

FRP wrapping of columns provides a passive confinement. Under an applied concentric axial load, P, on a column, and as P is increased from 0 to P_n, where P_n is the nominal axial capacity of the column, the concrete starts to crack and expand laterally until failure. The lateral expansion is partially resisted by the FRP leading to the concrete being placed in a state of triaxial confining stress. This condition serves to significantly increase the compressive strength and the ductility of brittle concrete.

The concrete confined by unidirectional FRPs exhibits different behavior than concrete confined by transverse steel due to the nature of FRP whose stress-strain relationship is linear up to failure. Consequently, the confining pressure provided by FRP increases with the lateral strain until rupture of FRP (Lam and Teng 2003).

FRP usually begins to confine the concrete shortly after the unconfined concrete stress reaches $f_c^{'}$. Failure of FRP-confined concrete in circular columns is governed by FRP rupture in the hoop direction. This phenomenon has been observed by many studies conducted on FRP confined circular concrete cylinders (Karbhari and Gao 1997; Xiao and Wu 2000). Compared to steel, FRP materials generally have higher strength than the yield strength of steel and lower strain at failure. Pressure provided by FRP wraps is uniform around the circumference of circular column (Figure 2.4).

14
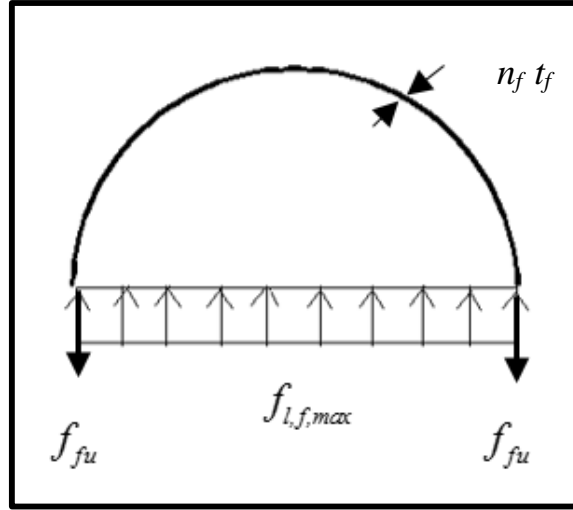
Figure 2.4: Confining action of FRP wrap

$$f_{l,f,\max} = \frac{\rho_f E_f \ \varepsilon_{fu}}{2} \tag{2.15}$$

Where E_f is the tensile modulus of elasticity of the FRP composite; f_{fu} ultimate strength of FRP material; $f_{l,f,\max}$ maximum lateral confining pressure due to FRP only; n_f number of FRP sheets; t_f is thickness of FRP sheet; ε_{fu} is the design rupture strain of FRP wrap; ρ_f is the FRP reinforcement ratio   .

FRP confinement can be achieved using different arrangements of the wraps (or fabrics, or sheets). Wraps can be applied to cover the entire column surface (or full wrap) or to cover part of the column with FRP strips (or partial wrap). Current studies are primarily focusing on fully wrapping concrete columns with FRP (Mirmiran et al.1997, Spoelstra et al.1999, Toutanji 1999, Xiao et al.2000). Studies dealing with partially confined columns (or partially wrapped columns using FRP) are very limited (Saadatmanesh et al. 94, Barros and Ferreira 2008, Colomb et al. 2008, Wu et al. 2009).

15

Fully wrapped circular columns are under even confinement pressure while partially wrapped columns are under uneven confinement pressure due to the discontinuity in the FRP wraps. There exists both confined and unconfined zones over the height of the column. The FRP reinforcement ratio, ρ_f, for both fully and partially confined columns can be expressed as follows

$$\rho_f = \frac{4t_f w_f n_f N_f}{D l_u} \qquad (2.16)$$

Where D is circular column diameter, l_u is the column unsupported length; n_f is the number of FRP sheets per strip; N_f is the number of FRP strips along the column; t_f is the thickness of FRP sheet; w_f is the FRP strip width.

In the literature, partially wrapped columns are usually modeled as fully wrapped columns with an effectiveness coefficient based on an arch action assumption between the transverse steel used by Sheikh and Uzumeri (1982) and Mander et al. (1988b). The arching action theory assumes that concrete is fully confined under the strips (Figure 2.5). Midway along the clear distance between the strips, the area of ineffectively confined concrete will be largest (dark shade of gray color) and the area of effectively confined concrete core will be smallest (light shade of gray color). The arching action is assumed to act in the form of a second degree parabola with an initial tangent slope of 45° (Figure 2.5).

16
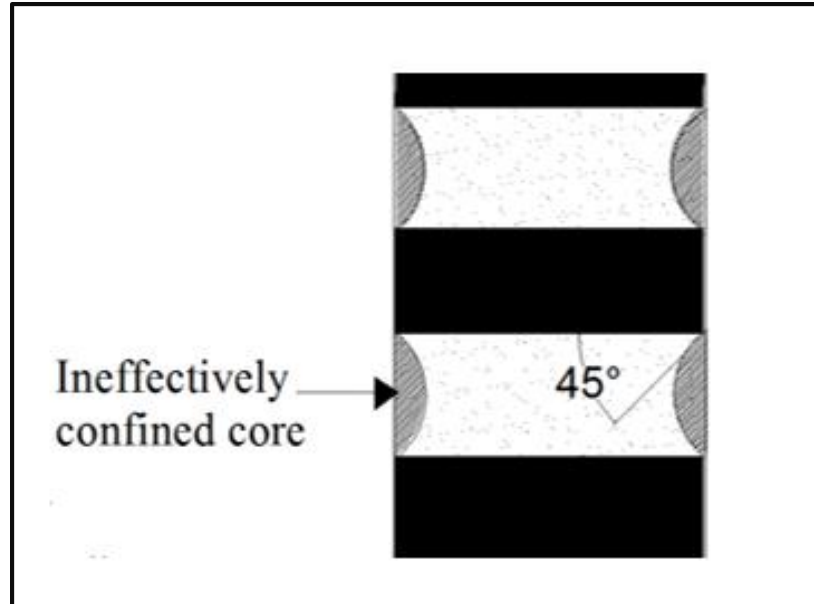
Figure 2.5- Effectively Confined Core for FRP Strips based on
the arching action theory

2.4.2   FRP Confined Concrete Models

The first models proposed to understand the behavior of confined concrete were based on the models derived for steel confined concrete.   Initial studies to model FRP-confined concrete was carried out by Fardis and Khalili (1982). The model is based on the triaxial failure criterion proposed by Richart et al. (1929).   Saadatmanesh et al. (1994) developed a model, based on Mander et al.'s model (1988), for columns that are partially confined using FRP strips.

These models were based on the ultimate strength of the specimen modeled on triaxial tests. The enhancement of the confined concrete was defined as a function of confining pressure, which was considered to be constant throughout the test. However, studies have shown that for FRP confined concrete, steel based confinement models cannot be applied since steel and FRP behave differently under axial loading. Due to the non-

17

yielding behavior of FRP, it exerts a continuously increasing pressure on the concrete core. Mirmiran and Shahawy (1996) and Spoelstra and Monti (1999) have showed the inappropriate implementation of the steel confinement models. Consequently, new models, based on FRP wrapped specimen, were introduced (Nanni and Bradford 1995; Samaan et al. 1998; Spoelstra and Monti 1999, Lam and Teng 2003).

Stress-strain models proposed for FRP-confined concrete in circular columns can be classified into two categories (Teng and Lam 2004): (a) analysis-oriented models (e.g. Mirmiran and Shahawy 1997; Spoelstra and Monti 1999; Fam and Rizkalla 2001; Teng et al. 2007), and (b) design-oriented models (e.g. Fardis and Khalili 1982; Samaan et al.1998; Toutanji 1999; Xiao and Wu 2000, Lam and Teng 2003; Harajli 2006)

In analysis-oriented models, the stress-strain curves of FRP-confined concrete are generated using an incremental numerical procedure which accounts for the interaction between the FRP wrap and the concrete core. The accuracy of analysis-oriented models depends mainly on the modeling of the lateral-to-axial strain relationship of FRP-confined concrete. Analysis-oriented models are more suitable for incorporation in computer-based numerical analysis such as nonlinear finite element analysis.

Design-oriented models generally comprise a closed-form stress-strain equation and ultimate condition equations derived directly from the interpretation of experimental results. The accuracy of design-oriented models highly depends on the definition of the ultimate condition of FRP-confined concrete. The simple form of design-oriented models makes them convenient for design use.

18

2.4.2.1 Lam and Teng (2003)

Lam and Teng's (2003) model presents the stress–strain curve as a parabolic first portion and a linear second portion (Figure 2.6). The model's first portion includes the contribution of the FRP.

The initial slope of the parabolic portion is the elastic modulus of unconfined concrete, and the confined concrete stress, f_c, is expressed as

$$f_c = E_c \ \varepsilon_c - \frac{\left(E_c - E_2\right)^2}{4 f_0} \ \varepsilon_c^{\ 2} \quad , \ 0 \le \varepsilon_c \le \varepsilon_t \qquad (2.17)$$
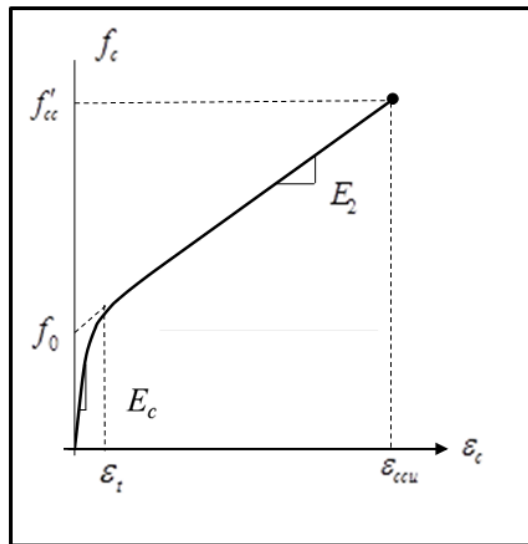
Figure 2.6- Lam and Teng 2003 stress- strain model

The parabolic first portion meets the linear portion without a change in slope. The point at which both portions intersect is defined by

$$f_0 = f_c' \qquad (2.18)$$

19

$$\varepsilon_t = \frac{2f_0}{E_c - E_2} \tag{2.19}$$

$$E_2 = \frac{f'_{cc} - f_0}{\varepsilon_{ccu}} \tag{2.20}$$

Where f_0 is the intercept of the stress axis by the linear second portion; ε_t is the strain level at which the parabolic first portion meets the linear second portion smoothly; and E_2 is the slope of the linear second portion.

The linear portion terminates when the ultimate confined concrete compressive strength is reached.

$$f_c = f_0 + E_2 \varepsilon_c \quad , \varepsilon_c \geq \varepsilon_t \tag{2.21}$$

The ultimate conditions are

$$f'_{cc} = f'_c \left(1 + 3.3 \frac{f_{l,a}}{f'_c} \right) \tag{2.22}$$

$$\varepsilon_{ccu} = \varepsilon'_c \left[1.75 + 12 \left(\frac{f_{l,a}}{f'_c} \right) \left(\frac{\varepsilon_{fe}}{\varepsilon'_c} \right)^{0.45} \right] \tag{2.23}$$

$$f_{l,a} = \frac{\rho_f E_f \varepsilon_{fe}}{2} \tag{2.24}$$

Where $f_{l,a}$ is actual maximum confining pressure; ε_{fe} is the effective strain level in FRP wrap attained at failure.

2.5   Steel-FRP Confined Concrete

2.5.1   General Behavior

When wrapping RC columns with FRP, the core is confined by two materials: the internal steel and the external FRP wrap, while the cover only confined by FRP (Figure

20

2.7). Both materials contribute to the enhancement of strength and ductility in different manners due to the difference of material properties.
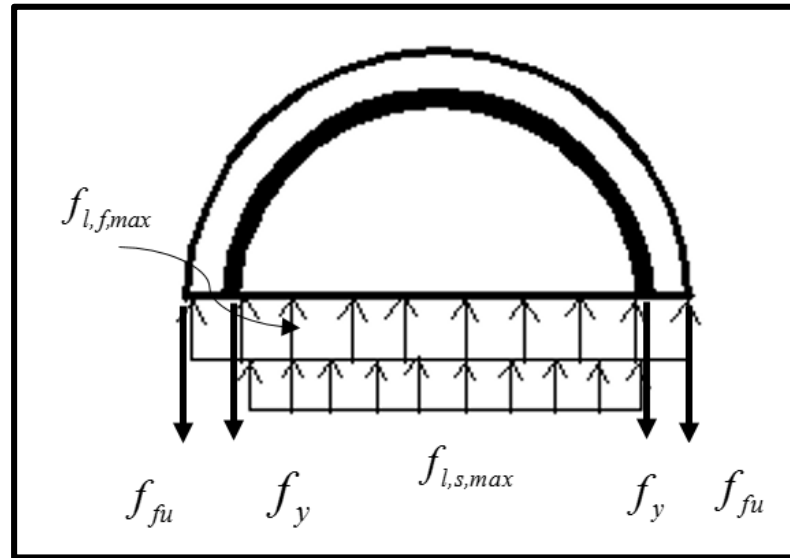
Figure 2.7- Confinement in column with internal steel and FRP wrap

Although studies found that transverse steel reinforcement does contribute to the response of RC columns wrapped with FRP (Demers and Neale 1999; Chastre and Silva, 2010), most researches simply use FRP-confined concrete model, or ignore the contribution of steel confinement (Lam and Teng 2003). Failure of columns with steel-and-FRP-confinement is governed by rupture of the FRP confinement in the hoop direction (Chastre and Silva 2010).

www.manaraa.com

2.5.2 Steel-FRP Confinement Models

The majority of existing studies considered the confinement pressure equal to that due to FRP only and neglected the contribution of the internal transverse steel reinforcement (Shao et al. 2005). Recently, some analytical models estimated the total confinement pressure as the sum of the confinement pressure due to FRP wrap and the confinement pressure due to steel reinforcement (Li et al. 2003; Ilki et al. 2008). Harajli et al. (2006) proposed a model for circular and rectangular concrete columns, Eid and Paultre (2008) and Lee et al. (2010) proposed a new analytical model. Chastre and Silva (2010) proposed a model using Richard and Abbott stress–strain relationship. Two models will be presented in more details in the following section.

2.5.2.1 Lee et al (2010)

The study tested twenty four concrete cylinders subjected to pure compression with various confinement ratios and types of confining material. It found that the models developed for concrete confined with FRP alone or steel alone do not predict well the behaviour of concrete confined with mixed material, and after exceeding the unconfined stress the cylinders showed a behavior between steel confinement and FRP confinement. A new empirical stress strain model for column confined with FRP and spirals is proposed (Eq. 2.25 – Eq. 2.30). The model accounts for the transverse steel confining pressure and the yielding of transverse steel (Figure 2.8)

$$f_c = E_c \varepsilon_c + (f_c' - E_c \varepsilon_c') \left(\frac{\varepsilon_c}{\varepsilon_c'} \right)^2 \quad 0 \le \varepsilon_c \le \varepsilon_c' \tag{2.25}$$

22

$$f_c = f_c' + (f_{c,s} - f_c')\left(\frac{\varepsilon_c - \varepsilon_c'}{\varepsilon_{c,s} - \varepsilon_c'}\right)^{0.7} \quad \varepsilon_c' \le \varepsilon_c \le \varepsilon_{c,s} \tag{2.26}$$

$$f_c = f_{c,s} + (f_{cc}' - f_{c,s})\left(\frac{\varepsilon_c - \varepsilon_{c,s}}{\varepsilon_{ccu} - \varepsilon_{c,s}}\right)^{0.7} \quad \varepsilon_{c,s} \le \varepsilon_c \le \varepsilon_{ccu} \tag{2.27}$$

Where

$$E_c = 4700\sqrt{f_c'} \quad (Mpa) \tag{2.28}$$

$$\varepsilon_{c,s} = \varepsilon_{ccu}\left[0.85 + 0.03\left(\frac{f_{l,f,\max}}{f_{l,s,\max}}\right)\right] and \quad f_{c,s} = 0.95 f_{cc}' \quad f_{l,f,\max} \ge f_{l,s,\max} \tag{2.29}$$

$$\varepsilon_{c,s} = 0.7\,\varepsilon_{ccu}\,and \quad f_{c,s} = \left(\frac{\varepsilon_{c,s}}{\varepsilon_{ccu}}\right)^{0.4} f_{cc}' \quad f_{l,f,\max} \prec f_{l,s,\max} \tag{2.30}$$

Where $f_{c,s}$ and $\varepsilon_{c,s}$ are compressive stress and axial in confined concrete at yielding of transverse steel respectively.
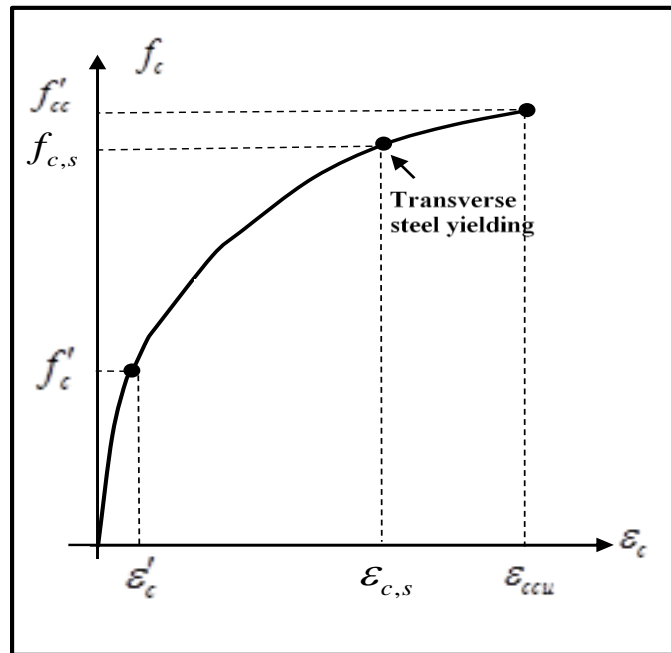
Figure 2.8– Stress –Strain model for concrete
confined with transverse steel and FRP

23

Lam and Teng's model (2002) was adopted and modified to determine the stress and strain at ultimate conditions. The strength of cylinders can be taken as the sum of increments of the compressive strength of carbon FRP (CFRP) confined concrete and spiral confined concrete.

2.5.2.2   Pellegrino and Modena (2010)

This model is based on the experimental results presented in the literature on tests conducted on axially and concentrically loaded FRP confined concrete columns. Pelligrino and Modena studied the results for 354 FRP confined circular columns without steel reinforcement and 233 FRP confined circular columns with steel reinforcement.

The partial wraps are accounted for by modifying the discontinuity coefficient used for transverse steel in Mander's model 1988. Although the model by Pellegrino and Modena accounts for the transverse steel, its influence cannot be separated from that of the FRP strips since the total lateral confining pressure, f_l, combines the transverse steel and FRP pressures in one single equation.

2.6   FRP Confined Concrete under Eccentric Load

The current state of art concentrates on FRP confined columns subjected to concentric axial loads. The behavior of FRP confined reinforced concrete columns subjected to eccentric loads are not well understood and the majority of studies concentrated on plain concrete (Wu and Jiang 2014, Parvin and Wang 2001).

Eccentrically loaded FRP confined concrete showed an increase in strength and ductility compared with unconfined concrete, although the increase was not as significant

24

as for columns loaded concentrically (Li and Hadi 2003). The increase in the stiffness of the FRP wrap would result in an increase in strength and flexural ductility of the column (Li and Hadi 2003, Fitzwilliam and Bisby 2006).

Yuan et al. (2001) conducted a comparative study of stress-strain models for confined concrete. The models were used to develop axial load-moment interaction diagrams, and a layer-by-layer approach was implemented. The strength and ductility were increased for all confined columns when compared to unconfined specimens. It was observed that the effectiveness of the confinement decreased with the increase in load eccentricity.

Fam et al. (2003b) studied, both experimentally and analytically, the performance of concrete filled GFRP tubes under eccentric loading. It was observed that FRP-confined columns display an increase in axial strength and flexural ductility over unconfined columns; although relative strength and ductility gains are apparently reduced with increasing initial load eccentricity. Based on their observations, the authors proposed a variable FRP confinement model to account for load eccentricity.

2.7   Finite Element Modeling for Confined Concrete

Two and three dimensional finite element (FE) models are employed to simulate the structural behavior under any type of load. It has been used to understand the behavior of confined columns. Rochette and Labossiere (1996) used the FE models to evaluate the response of FRP wrapped concrete columns by applying Drucker - Prager failure criteria (Drucker and Prager 1952).

25

Mirmiran et al. (2000) developed a nonlinear finite element model for confined concrete using non-associative Drucker – Prager plasticity model, which takes in to account the pressure sensitivity of the material. The study tested several parameters including cohesion, angle of internal friction and the dilatancy angle. The FE program ANSYS was tused o develop one quarter model of the circular and the square specimen specimens. The results show that the Drucker –Prager plasticity effectively predicts the axial stress-strain response of the FRP confined columns.

Wu et al. (2009) tested 60 high strength concrete (HSC) circular columns confined with continuous and discontinuous AFRP wrapping. The study assumed the confining stress between the adjacent AFRP wrap is distributed by arching action. A 3D nonlinear finite-element model, with a Drucker–Prager plasticity model for the concrete core and an elastic model for the AFRP, is developed by using the finite-element program ANSYS. The model successfully simulated the behavior of HSC circular columns confined by AFRP wrap.

The aforementioned studies show that using FE models can effectively predict the behavior of the FRP confined concrete columns.

2.6   Conclusions

This chapter presented a review of existing studies on concrete columns confined by steel and/or Fiber Reinforced Polymer (FRP) composites subjected to concentric and eccentric axial loads. The available related experimental studies along with available predictive models and finite element models were presented and discussed.

26

It can be concluded that the focus in the literature is on fully wrapped FRP confined concrete columns and several models were proposed to predict their behavior. Columns partially wrapped with FRP strips are analyzed by smearing the FRP to produce and equivalent fully wrapped column and accounted for the partial FRP wrap discontinuity by using coefficients based on steel confinement models. Therefore, more investigations are needed on columns partially wrapped with FRP strips.

The majority of the studies did not account for the influence of the existing steel reinforcement on the column's behavior, or estimated the total lateral confining pressure by combining that of the transverse steel and FRP. Only one model addressed the transverse steel yielding and its effect on RC column's behavior. Consequently, it is important to understand the interaction between internal steel reinforcement and partial or full external FRP wrap/reinforcement and their influence on concrete confinement.

Most of the previous research was conducted in column tests under concentric compressive load. However, in practice most columns are actually loaded eccentrically, which can be attributed to construction errors or material non-homogeneities or deficiencies, or with some combination of axial load and bending moment. Only limited research has been reported investigating the behavior of FRP fully wrapped columns subjected to eccentric axial compressive loading. Considering that, it is clear that additional research is required in this area.

Several studies confirmed that FE models can be used successfully to simulate the behavior of columns wrapped by FRP sheets.

CHAPTER 3
FINITE ELEMENT ANALYSIS FOR CONCENTRICALLY LOADED RC CIRCULAR COLUMN CONFINED WITH FRP

3.1   Introduction

The basic concept behind the finite element (FE) method is that the structure, or structural component, is divided into smaller elements of finite dimensions called 'finite elements'. The original structure is then considered as an assemblage of these elements at a finite number of joints called nodes. The properties of the elements are formulated and combined to obtain the solution for the entire structure.

Two and three dimensional FE models have been deployed understand the behavior of confined columns. Rochette and Labossiere (1996) evaluated the response of FRP wrapped concrete columns by applying the Drucker-Prager failure criteria (Drucker and Prager 1952). A nonlinear finite element model for confined concrete, using non-associative Drucker–Prager plasticity model (Drucker and Prager 1952) was presented in Mirmiran et al. (2000). The model was developed in ANSYS and used one quarter model of the circular and square column specimens. It was concluded that the Drucker–Prager plasticity model (Drucker and Prager 1952) does effectively predict the axial stress-strain response of the FRP confined columns. Sixty high strength concrete (HSC) circular columns confined with continuous and discontinuous AFRP wrapping were tested by Wu et al. 2009. The study assumed the confining stress between the adjacent AFRP sheets is distributed by arching action. A 3D nonlinear finite-element model, with a Drucker–Prager plasticity model (Drucker and Prager 1952) for the concrete core and an elastic model for the AFRP, is developed by using the finite-element program ANSYS. The model successfully simulates the behaviors of HSC circular columns confined by AFRP sheets.

www.manaraa.com

These models show that using the finite element method can effectively predict the behavior of the FRP confined concrete columns.

In this Chapter, a finite element (FE) model of FRP confined circular RC columns is developed, calibrated, and validated using published experimental results. The FE software ANSYS 14 (2012) is used to simulate the behavior of partially and fully confined columns. Four groups of nine (9) columns each are studied in this chapter. A FE model was generated for each column in each of the groups.

3.2   Finite Element Model

3.2.1   Element Types

Selection of the proper element types is an important criterion in finite element analysis. For RC columns, the modeling includes three different materials: concrete, steel and FRP, and each material requires a specific element.

For concrete, the solid element (SOLID 65) is adopted. SOLID 65 is used for the 3-D modeling of solids. The element has three degrees of freedom at each node, translations in the global X, Y, and Z directions, and it is capable of plastic deformation, cracking in three orthogonal directions, crushing, and creep (ANSYS 2012).

The Link180 element is used to model the steel reinforcement. It is a 3-D spar element with uniaxial tension-compression and has three translational degrees of freedom at each node in the nodal x, y, and z directions. This element has the capability of predicting plasticity, large deflection, and large strain (ANSYS 2012).

For FRP wrapping, the SHELL181 element is used. It is suitable for analyzing thin to moderately thick shell structures. It has 4 nodes with three translational degrees of

29

freedom at each node when used as a membrane. The element works for both linear and nonlinear layered applications up to 250 layers (ANSYS 2012).

3.2.2 Material Models

The Drucker–Prager plasticity model (Drucker and Prager 1952) has been successfully adopted to simulate concrete wrapped with FRP (Rochette and Labossière 1996; Mirmiran et al. 2000; Shahawy et al. 2000). The model assumes an elastic-perfectly plastic material response with an associative or non- associative flow rule. The model will be used in this study for confined concrete. The yield criterion of the Drucker–Prager plasticity model is a modification of the von Mises yield criterion that accounts for the influence of the hydrostatic stress components: the higher the hydrostatic stress (confinement pressure), the higher the yield strength.

For a triaxial state of stress in concrete, the equivalent stress for the Drucker–Prager plasticity model is (ANSYS 2012)

$$\sigma_e = 3\beta\sigma_m + \left[\frac{1}{2}\{s_v\}^T [M_{DP}]\{s_v\}\right]^{\frac{1}{2}} \tag{3.1}$$

Where σ_m is the mean or hydrostatic stress; s_v is the deviatoric stress vector; M_{DP} is a special diagonal matrix; β is material constant given as

$$\beta = \frac{2\sin\phi}{\sqrt{3}(3-\sin\phi)} \tag{3.2}$$

Where ϕ is the angle of internal friction; and the yield parameter of the material (σ_y) is defined as

$$\sigma_y = \frac{6c_{DP}\cos\phi}{\sqrt{3}(3-\sin\phi)} \tag{3.3}$$

30

Where c_{DP} is the cohesion value of the material

In the present study, the values suggested for c_{DP} and ϕ by Rochette and Labossiere (1996) are used. This method was successfully used by Mirmiran et al. (2000)

$$\phi = \sin^{-1} \frac{3}{1+1.59 f_c'} \qquad\qquad (f_c' \text{ in } ksi) \qquad\qquad (3.4)$$

$$c_{DP} = (f_c' - 1256) \frac{3 - \sin \phi}{6 \cos \phi} \qquad\qquad (f_c' \text{ and } c_{DP} \text{ in } psi) \qquad\qquad (3.5)$$

For steel confined concrete, the Mander compressive stress-axial strain relationship for steel confined concrete (Mander 1988) is adopted to define the multilinear isotropic stress-strain curves required by ANSYS, and for unconfined concrete Kent and Park 1971 model is used. These models were discussed in details in Chapter 2.

A failure criteria is needed to define the failure type of concrete; either in cracking (for regions under tensile stresses) or crushing (for regions under compressive stresses).

ANSYS uses the failure criteria proposed by William and Warnke 1975. Other inputs required for modeling concrete material are: Poisson's ratio (v) which is assumed to be 0.2, and shear coefficient for an open and closed crack (β) which is taken as 0.3 (Wolanski 2004).

The FRP warp is assumed to be an elastic material in the hoop direction, where modulus of elasticity, number of layers, thickness and orientation of each layer are required. The linear response is assumed to continue until the tensile strength is reached, and failure is assumed after that.

The steel reinforcement stress-strain behavior is modeled as a bi-linear elastic-perfectly plastic relationship with identical response in tension and compression. Perfect

31

bond between the concrete and reinforcing steel, concrete and FRP is assumed in the finite element analyses.

3.2.3   Boundary Conditions and Loading

In the model, the Z-axis of the coordinate system coincides with the axis of the circular column. The X and Y axis represent the radial and hoop directions of the column respectively. At the bottom of the column, the six degrees of freedom are constrained at all nodes. At the top of the column, the axial compressive load was applied on the top nodes as a displacement to simulate the displacement control mode. The loads will be determined from the displacement.

A nonlinear structural analysis is performed and, in order to include the nonlinear material behavior of concrete, the "Newton-Raphson" approach is employed in ANSYS. The displacement can be applied over several steps, and follows an iterative procedure until the problem converges. The time increments and the corresponding load steps were automated and handled by the ANSYS solution algorithm to help the problem to converge (ANSYS 2012).

3.2.4   Validation of the Model

The accuracy of the finite element model was evaluated by comparing the results with ones derived from the experiments conducted by Barros et al (2008). One fully wrapped and one partially wrapped column ate considered. The columns were tested under concentric compressive loading. The material properties are listed in Table 3.1. where f_c' is the compressive strength of unconfined concrete, f_{fu} is the ultimate strength of FRP

32

material and f_y is the yield strength of the steel reinforcement [MPa (ksi)]; E_c is Modulus of elasticity of concrete and E_f is the tensile modulus of elasticity fiber [GPa (ksi)]; t_f is the thickness of FRP Wrap [mm (in)]; A_s is the area of steel reinforcement [mm^2 (in^2)].

The comparison between the FE mod and experimental results is presented in the form of compressive stress (f_c) vs. axial strain (ε_c) in Figure 3.1. The results show a good agreement between FE modeling using ANSYS and the experimental results (Barros 2008). Therefore, the model can capture the compressive stress-strain behavior of concentrically loaded RC columns and will be used to analyze RC columns wrapped with FRP material.

Table 3.1: Material properties of columns used for
FEM validation (Barros et al 2008)

Material	Parameter		
Concrete	f_c'	16 MPa (2.3 ksi)	
	E_c	21.5 GPa (3118 ksi)	
		35.13 GPa (5095 ksi)	
Steel	f_y	413.68 MPa (60 ksi)	
	A_s	$\phi 6$	32 mm^2 (0.044 in^2)
		$\phi 10$	71 mm^2 (0.122 in^2)
FRP	t_f	0.176 mm (0.007 in)	
	f_{fu}	3250 MPa (471.4 ksi)	
	E_f	230 GPa (33358 ksi)	

33

$$
\begin{aligned}
f_c' &= 16\ \text{MPa} & (2.32\ \text{ksi}) \\
f_y &= 468.3\ \text{MPa} & (68\ \text{ksi}) \\
f_{fu} &= 3539\ \text{MPa} & (513.3\ \text{ksi}) \\
E_f &= 232\ \text{GPa} & (33649\ \text{ksi})
\end{aligned}
$$
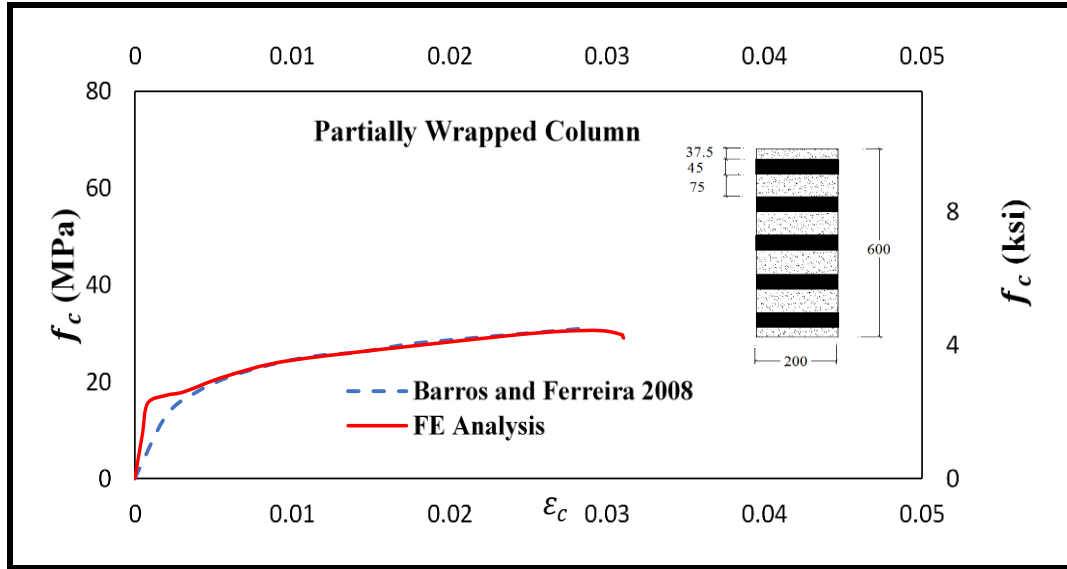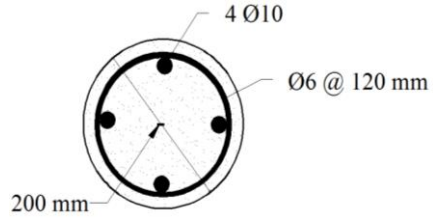
(a)
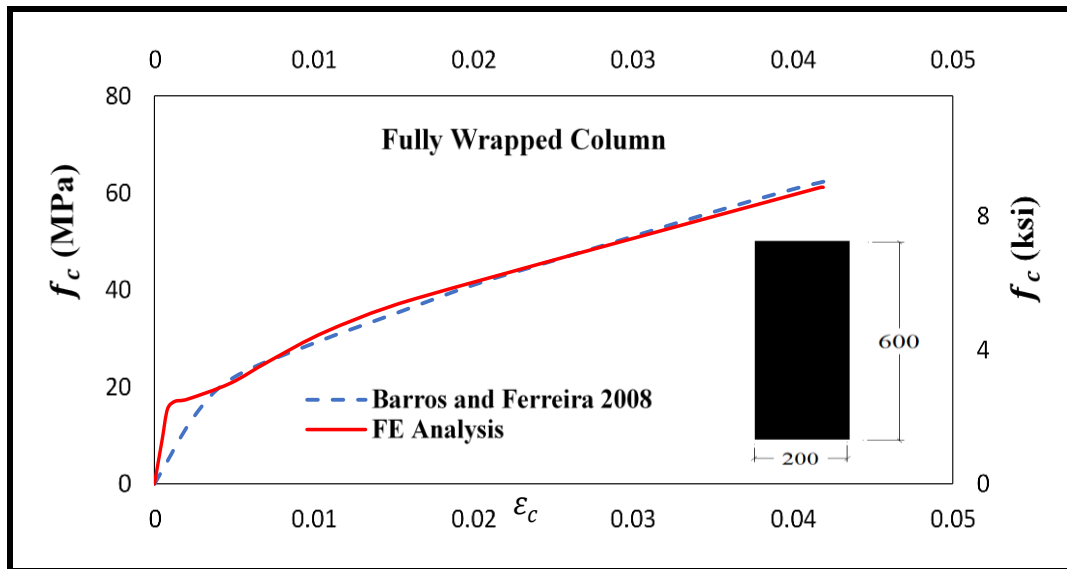
(b)

Figure 3.1- Comparison of compressive stress (f_c) vs. axial strain (ε_c) between FE and experimental results for (a) partially wrapped column (b) fully wrapped column

34

3.3   Test Matrix

The test matrix is composed of four groups of columns and each group consists of nine columns. The objective of the test matrix is to evaluate the influence of different parameters on the confined concrete stress-strain behavior.

3.3.1   Column Groups

All Nine columns in the tested groups (Figures 3.2 and 3.3) have the same unbraced length l_u = 600 mm (23.62 in.) and diameter D = 200 mm (7.9 in.).   One column is unwrapped and is used as the baseline column. The other eight columns are presented in Figure 3.2, one of the columns is fully wrapped (FW) and the remaining seven are partially wrapped with strips varying from one strip (N_f =1) on column S1 to seven strips on column S7 (N_f =7). Each strip has a width w_f = 40 mm (1.6 in.). For the fully wrapped column, $w_f = l_u$ and N_f = 1. The full wrap and each strip has four layers of CFRP fabric (n_f = 4), and the thickness of each layer t_f = 0.15 mm (0.0059 in.).   The FRP volumetric ratio (ρ_f) for each column is determined using the following equation

$$\rho_f = 4\frac{w_f N_f t_f n_f}{Dl_u} \tag{3.6}$$

Where w_f is the FRP strip width; N_f is the number of FRP strips along the column; t_f is the thickness of the FRP wrap; D is the circular column diameter.

It should be noted that the columns wrapped with one, two, or three strips are not of practical interest and are used herein to illustrate the influence of partial wrapping as the

35

analysis transitions from an unwrapped column to a partially wrapped column with one to seven strips, to a fully wrapped column.
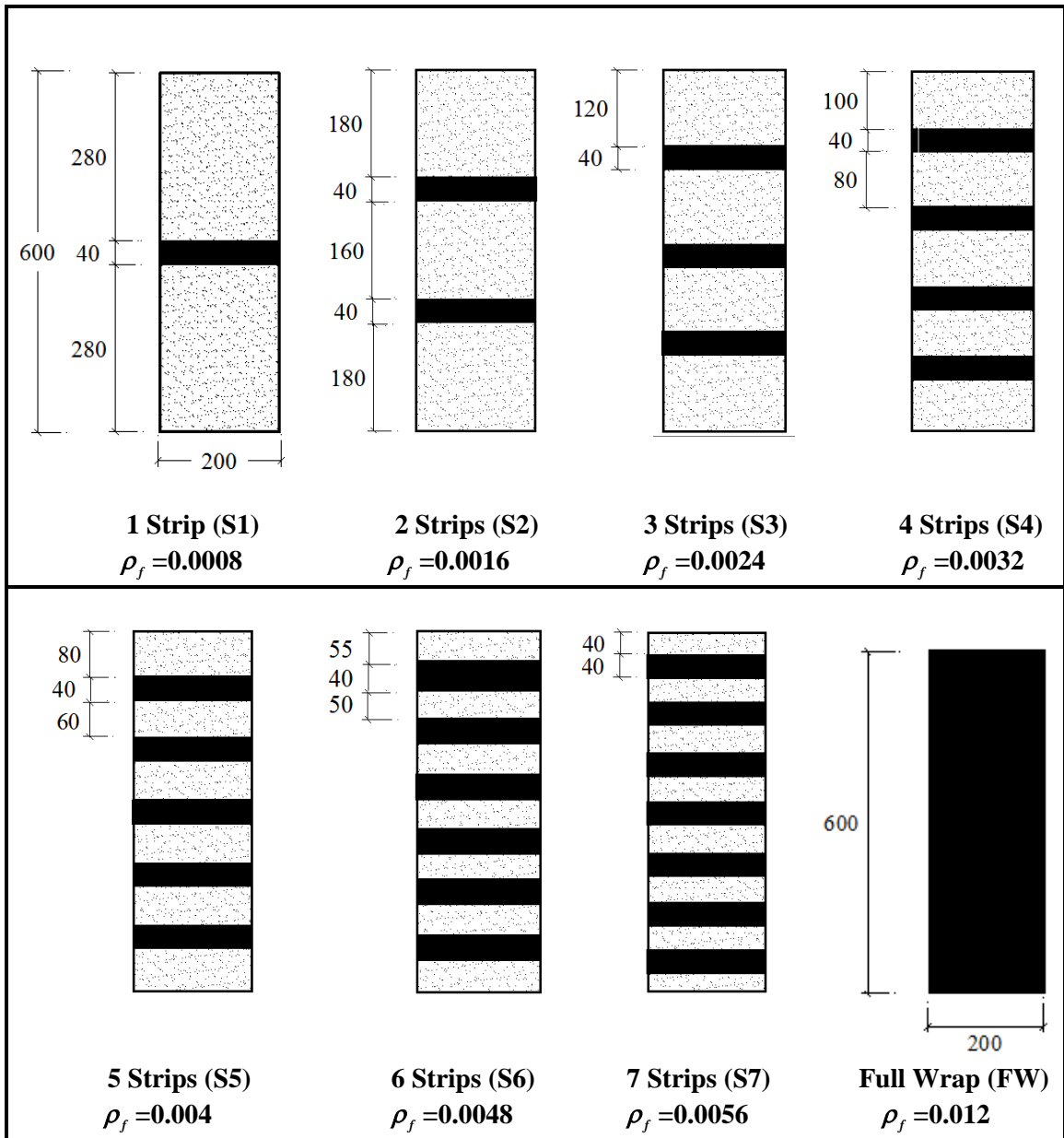
Figure 3.2 – FRP Wrap Layout on circular columns (All dimensions are in mm; 1 mm = 0.039 in.)

Four groups of columns are studied to evaluate the influence of different parameters on the confined concrete stress (f_c), axial strain (ε_c), and lateral strain (ε_l) (Figure 3.3 and Table 3.2). In addition to the unwrapped column, each group contains the eight columns in Figure 3.2, and Group 1 is the baseline group. In Groups 2 to 4, three different parameters are varied: the 28-day compressive strength of unconfined concrete f_c', the transverse steel reinforcement ratio, ρ_{st}, and the longitudinal steel reinforcement ratio, ρ_{sl} (Eq. 3.7)

$$\rho_{st} = V_{st} / V_c \qquad , \qquad \rho_{sl} = A_{sl} / A_g \tag{3.7}$$

Where V_{st} is the volume of transverse steel; V_c is the volume of concrete; A_{sl} is the total area of longitudinal steel; and A_g is the gross area of the column section.
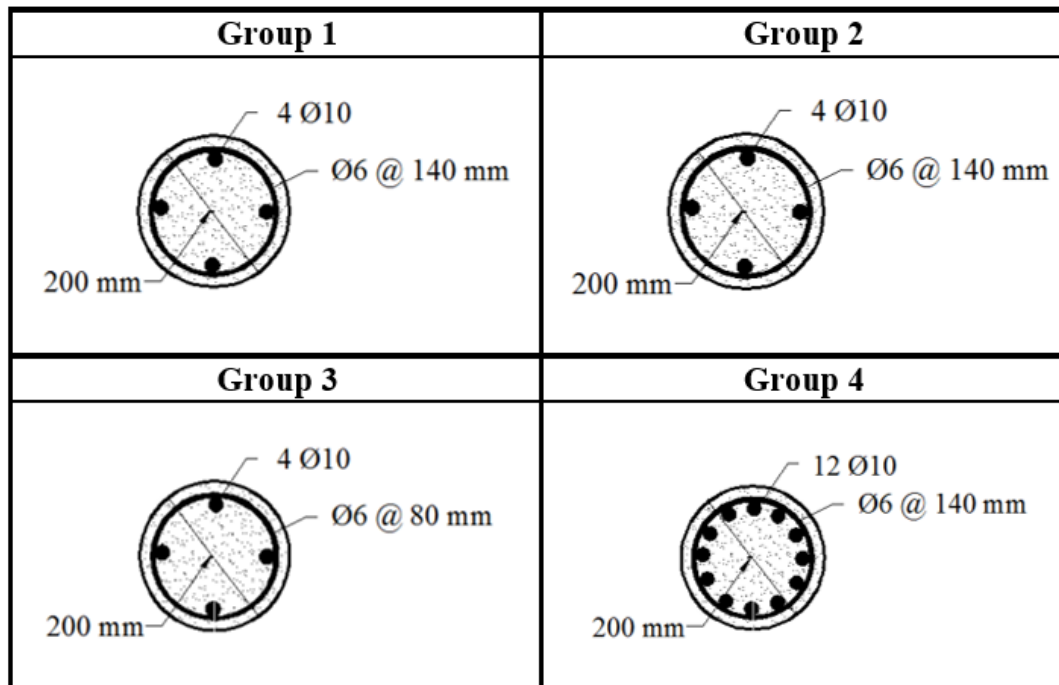
Figure 3.3- Cross sections of tested columns groups

Table 3.2: Column Groups used in the parametric study

Group #[a]	f_c'		Longitudinal steel ϕ 10 mm (#3)		Transverse steel stirrups ϕ 6 mm (#2)		
	MPa	ksi	Number of Bars	ρ_{sl}	Spacing		ρ_{st}
					mm	in	
1	20.68	3	4	0.011	140	5.50	0.004
2	55.16	8	4	0.011	140	5.50	0.004
3	20.68	3	4	0.011	80	3.15	0.0064
4	20.68	3	12	0.027	140	5.50	0.004

[a] Each Group contains, in addition to the unwrapped column, the eight columns in Figure. 3.2

3.3.2 Material Properties

For concrete, two unconfined concrete compressive strength are used here 20.68 MPa (3 ksi) and 55.16 MPa (8 ksi) to evaluate the effect of the compressive strength of unconfined concrete (f_c').

The steel reinforcement was modeled as having bi-linear elastic-perfectly plastic material model with a yield strength of 413.8 MPa (60 ksi).

The FRP used in the model is a UNI-4.0SM non-woven unidirectional carbon fabric (A & P 2014). A summary of the mechanical properties of concrete, FRP, and steel that used to model columns is listed in Table 3.3.

38

Table 3.3: Material properties for the control (or
unwrapped) column and the eight columns in
Figure 3.2

Material	Parameter			
Concrete	f_c'		20.68 MPa	3 ksi
			55.16 MPa	8 ksi
	E_c		21.50 GPa	3118 ksi
			35.13 GPa	5095 ksi
Steel	f_y		413.68 MPa	60 ksi
	A_s	$\phi\,6$	32 mm^2	0.05 in^2
		$\phi\,10$	71 mm^2	0.11 in^2
FRP	t_f		0.15 mm	0.0059 in
	f_{fu}		2848 MPa	413 ksi
	E_f		139 GPa	20160 ksi

3.4   Finite Element Analysis Results

3.4.1   Compressive Stress vs Axial and Lateral Strain Response

Following the analysis of the columns in the four groups using the finite element
program ANSYS, the data from FE time-history analysis was transported into Excel to
develop the compressive stress (f_c) vs axial strain (ε_c) and lateral strain (ε_l)
relationships for the circular columns. The responses are presented in Figures 3.4 to 3.7.
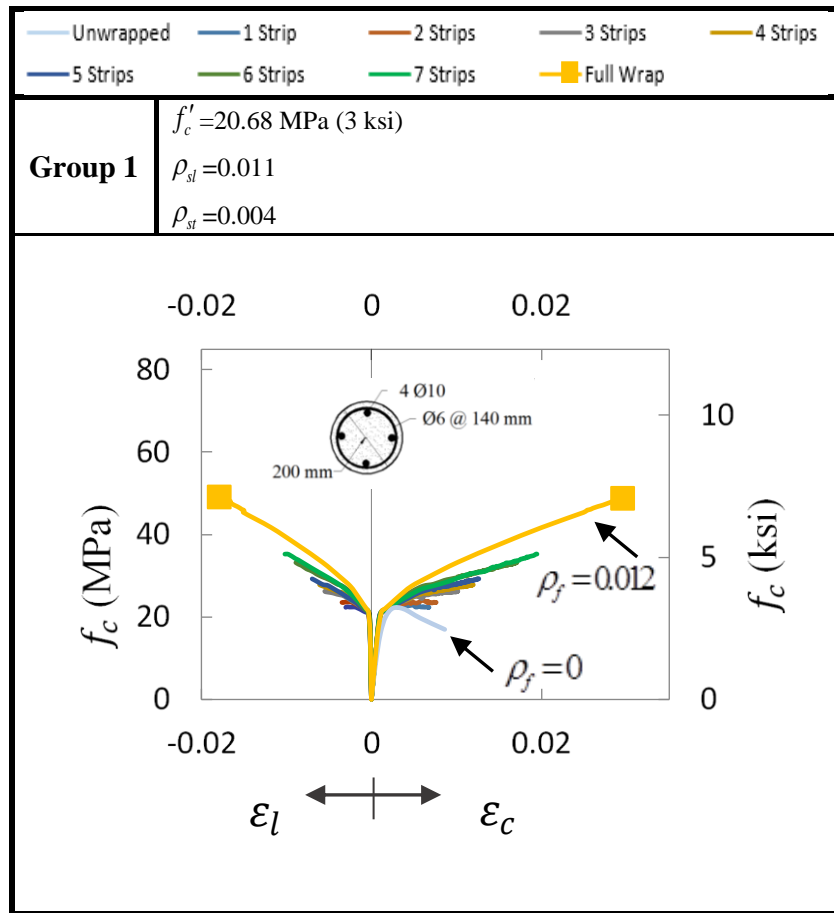
Figure 3.4- Comparison of compressive stress (f_c) vs axial strain (ε_c) and lateral strain (ε_l) for the columns in Group1 (1 mm = 0.039 in.)

40
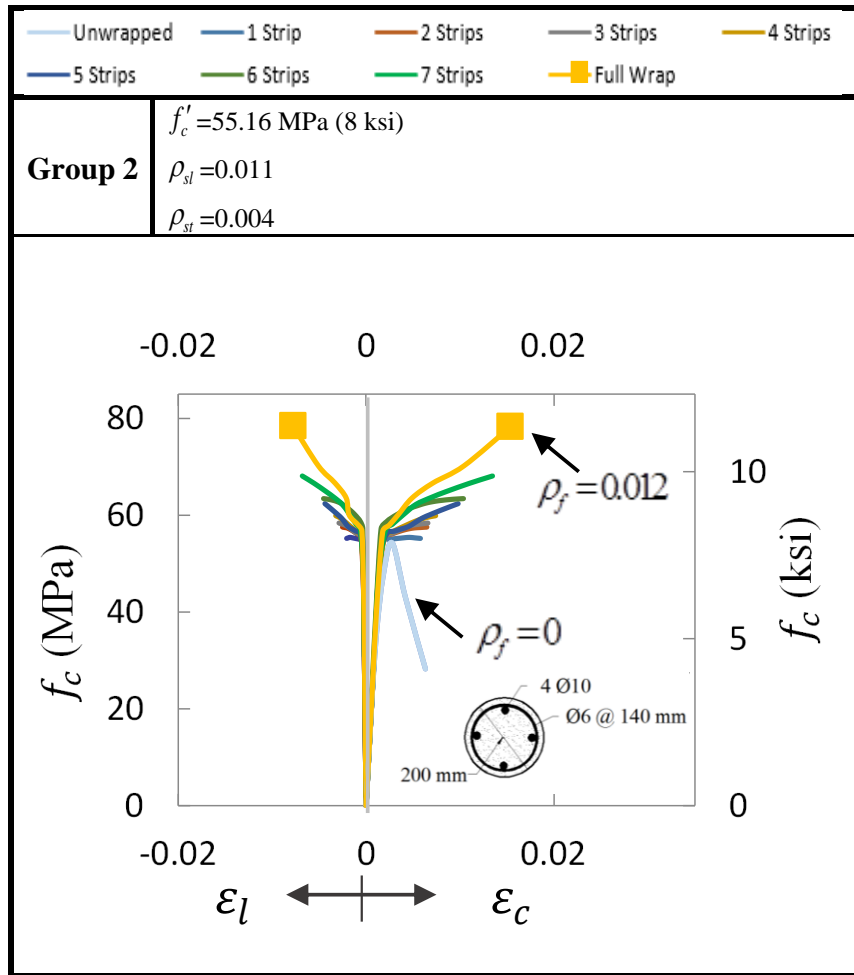
Figure 3.5- Comparison of compressive stress (f_c) vs axial strain (ε_c) and lateral strain (ε_l) for the columns in Group 2 (1 mm = 0.039 in.)

www.manaraa.com
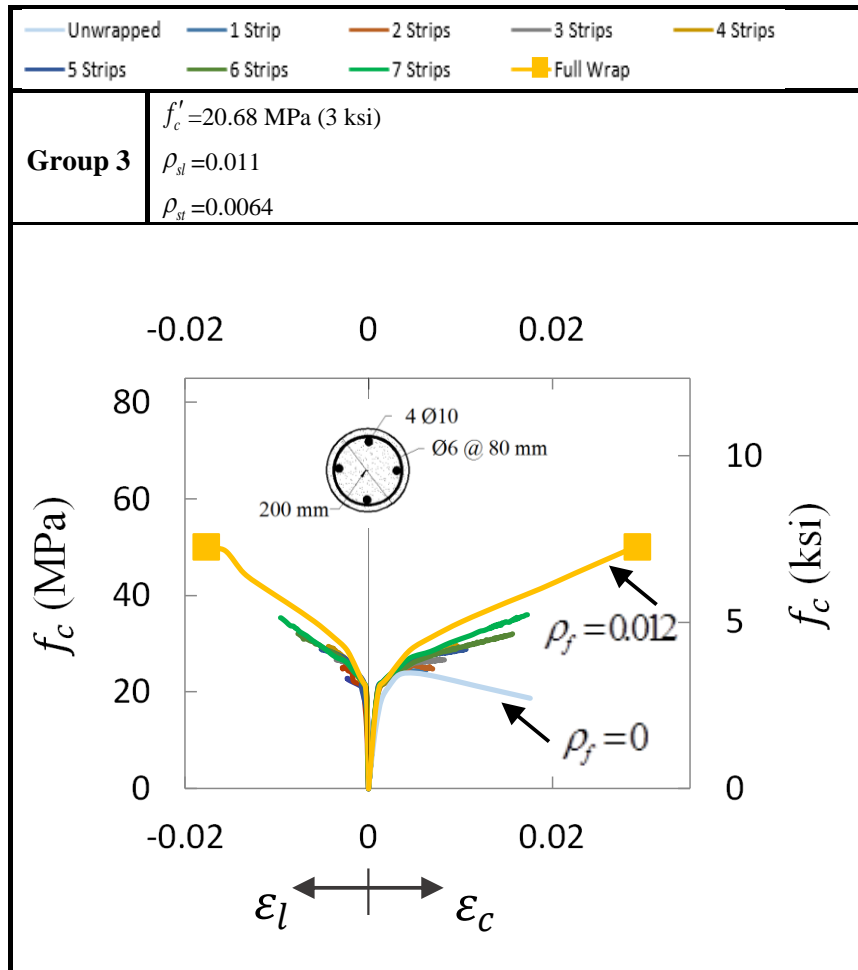
Figure 3.6- Comparison of compressive stress (f_c) vs axial strain (ε_c) and lateral strain (ε_l) for the columns in Group 3 (1 mm = 0.039 in.)
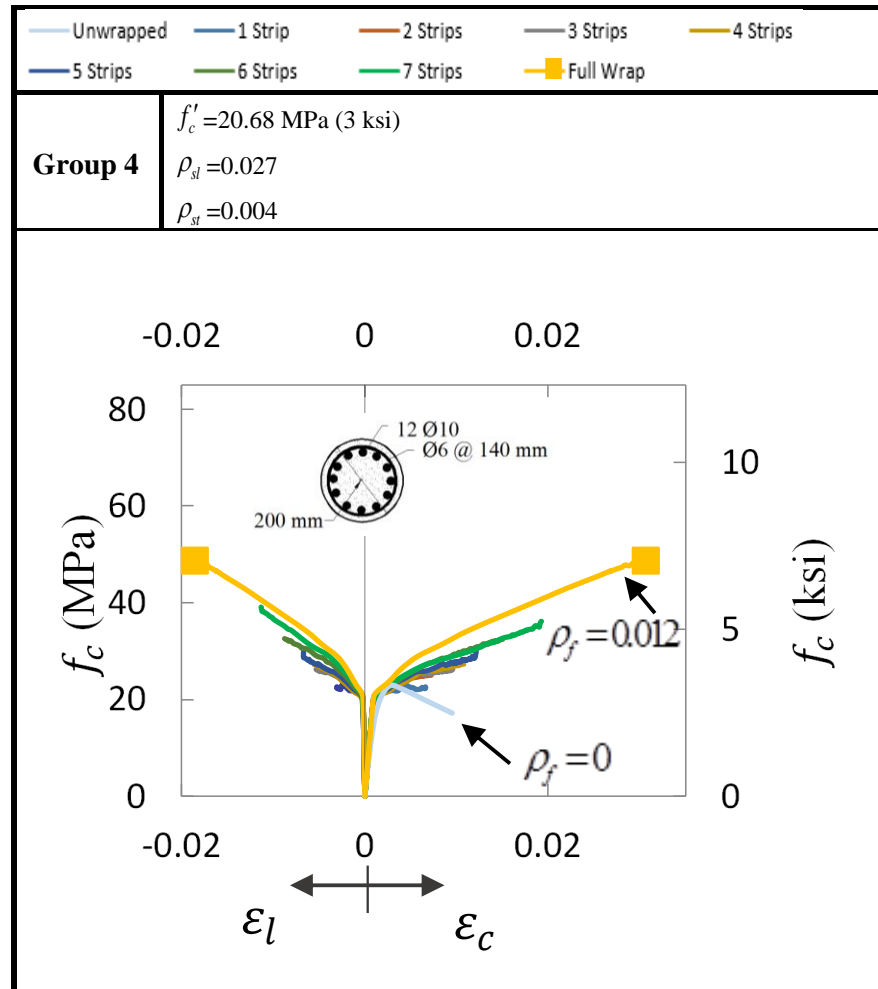
Figure 3.7- Comparison of compressive stress (f_c) vs axial
strain (ε_c) and lateral strain (ε_l) for the columns
in Group 4   (1 mm = 0.039 in.)

To facilitate the analysis and performance of FRP-confined concrete, the following

parameters are introduced in Table 3.4: strengthening ratio (f'_{cc} / f'_c), strain ratio ($\varepsilon_{ccu} / \varepsilon'_c$)

and ductility index (μ)

43

f'_{cc} is the maximum compressive stress of confined concrete; ε_{ccu} ultimate axial strain corresponding to the ultimate confined concrete compressive stress; ε'_c is the axial strain at the peak stress of unconfined concrete.

Ductility is important when evaluating the behavior of confined RC columns. It is of particularly interest when the FRP is used to wrap columns to improve its seismic performance. Therefore, the ductility index (μ) is calculated based on Cui and Sheikh 2010 using the following expression

$$\mu = \frac{\varepsilon_{ccu}}{\varepsilon_1} \tag{3.8}$$

Where ε_1 is ultimate axial strain corresponding to the ultimate confined concrete compressive stress on the initial tangent of the stress strain curve (Figure 3.8).
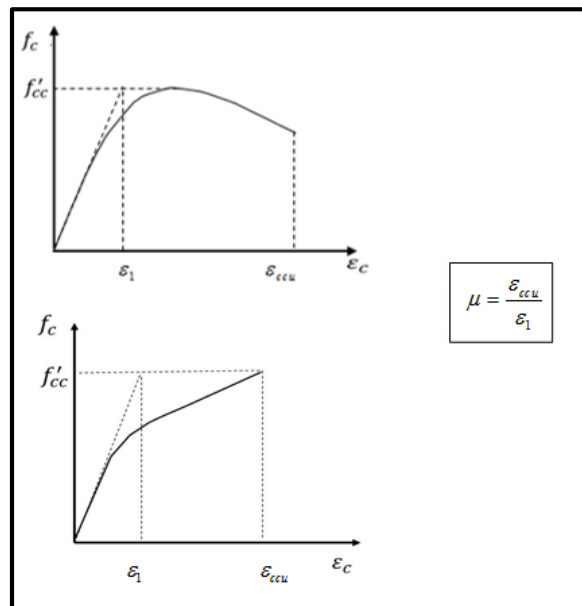
Figure 3.8- Definition of Ductility (μ)

Table 3.4: Stresses, strains and ductility factors for the unwrapped columns (UW) and columns in Groups 1 to 4

Group #		Columns								
		UW	S1	S2	S3	S4	S5	S6	S7	FW
1	f'_{cc} (MPa)[a]	22.13	22.32	23.51	26.22	27.81	29.23	33.18	35.24	48.80
	ε_{ccu}	0.0025	0.0068	0.0076	0.0102	0.0120	0.0126	0.0171	0.0195	0.0303
	ε_{lu}	-	0.003	0.0035	0.0055	0.0061	0.0070	0.0089	0.0102	0.0179
	f'_{cc} / f'_c	1.079	1.070	1.137	1.268	1.345	1.414	1.604	1.704	2.360
	$\varepsilon_{ccu} / \varepsilon'_c$	1.266	3.390	3.808	5.088	5.995	6.321	8.562	9.741	15.166
	μ	5.744	6.357	6.952	8.422	9.215	9.219	10.269	11.266	14.327
2	f'_{cc} (MPa)[a]	55.20	55.22	57.52	28.35	59.86	62.35	63.39	68.06	78.27
	ε_{ccu}	0.0028	0.0058	0.0065	0.0066	0.0074	0.0098	0.0104	0.0135	0.0154
	ε_{lu}	-	0.0021	0.0025	0.0029	0.0032	0.0044	0.0045	0.0068	0.0077
	f'_{cc} / f'_c	1.001	1.001	1.043	1.058	1.085	1.130	1.149	1.234	1.419
	$\varepsilon_{ccu} / \varepsilon'_c$	1.083	2.267	2.534	2.580	2.903	3.840	4.062	5.273	6.036
	μ	3.53	3.552	3.970	4.041	6.177	6.762	6.915	7.087	7.339
3	f'_{cc} (MPa)[a]	23.89	24.55	24.78	26.65	28.80	28.83	32.04	35.99	49.79
	ε_{ccu}	0.0051	0.0066	0.0070	0.0083	0.0084	0.0106	0.0157	0.0173	0.0294
	ε_{lu}	-	0.0023	0.0028	0.0035	0.0044	0.0052	0.0077	0.0096	0.0178
	f'_{cc} / f'_c	1.155	1.187	1.198	1.289	1.393	1.394	1.549	1.740	2.408
	$\varepsilon_{ccu} / \varepsilon'_c$	2.554	3.313	3.491	4.129	4.194	5.309	7.841	8.650	14.717
	μ	5.674	5.796	5.813	6.446	6.983	7.315	9.271	9.765	13.426
4	f'_{cc} (MPa)[a]	22.2	22.38	25.02	26.22	27.31	29.89	32.54	36.16	48.49
	ε_{ccu}	0.0028	0.0066	0.0072	0.0096	0.0108	0.0122	0.0150	0.0193	0.0307
	ε_{lu}	-	0.0031	0.0033	0.0053	0.0056	0.0067	0.0088	0.0113	0.0187
	f'_{cc} / f'_c	1.074	1.082	1.210	1.268	1.320	1.445	1.573	1.749	2.345
	$\varepsilon_{ccu} / \varepsilon'_c$	1.384	3.323	3.618	4.795	5.391	6.082	7.527	9.637	15.374
	μ	5.972	6.205	6.231	7.918	8.415	9.206	10.026	10.697	14.155

[a] 1 MPa= 0.145 ksi

45

In order to evaluate the correlation between the different parameters and the number of strips, the results are plotted in Figures 3.9 (a-d) in terms of the strengthening ratio (f'_{cc} / f'_c), strain ratio ($\varepsilon_{ccu} / \varepsilon'_c$), and ductility ($\mu$) vs number of strips (N_f) for circular columns for all four groups. Three efficiency factors, β, are introduced in Eq. 3.9 compare the fully wrapped (FW) columns to unwrapped columns (UW) in each group.

$$\beta_\mu = \frac{\mu_{FW}}{\mu_{UW}}; \beta_\varepsilon = \frac{(\varepsilon_{ccu})_{FW}}{(\varepsilon_{ccu})_{UW}} \text{ and } \beta_f = \frac{(f'_{cc})_{FW}}{(f'_{cc})_{UW}}$$
(3.9)
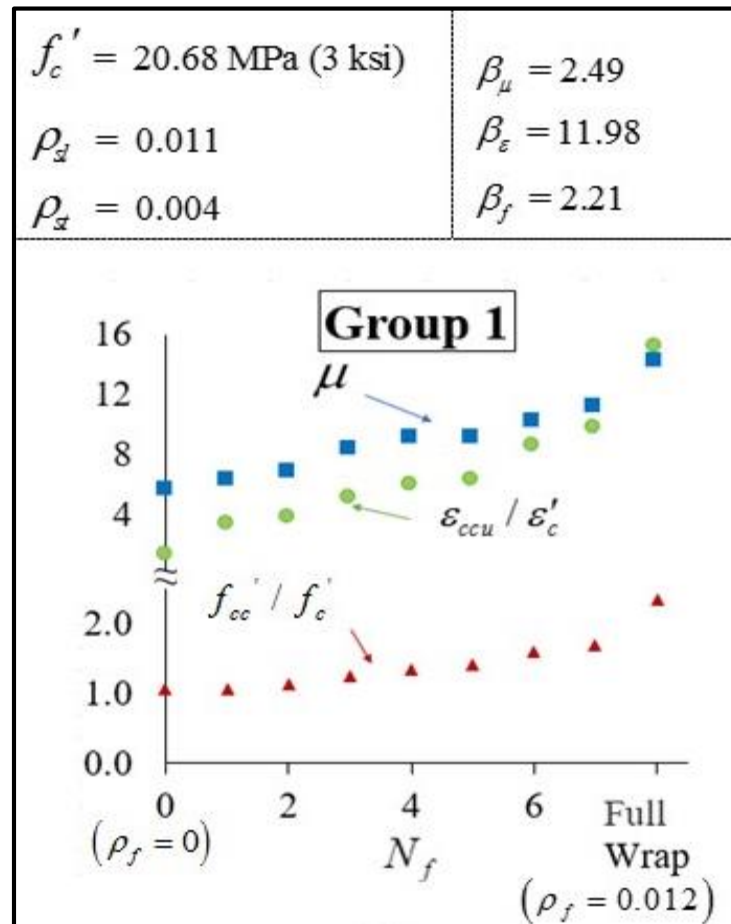
Figure 3.9a - Strengthening ratio (f'_{cc} / f'_c), strain ratio ($\varepsilon_{ccu} / \varepsilon'_c$), and ductility factor (μ) vs number of strips (N_f) for the columns in Group 1

46

Figure 3.9b - Strengthening ratio (f'_{cc} / f'_c), strain ratio
$(\varepsilon_{ccu} / \varepsilon'_c)$, and ductility factor ($\mu$) vs number of
strips (N_f) for the columns in Group 2

$f_c{}' = 20.68$ MPa (3 ksi)	$\beta_\mu = 2.36$
$\rho_{st} = 0.011$	$\beta_\varepsilon = 5.76$
$\rho_{st} = 0.0064$	$\beta_f = 2.08$
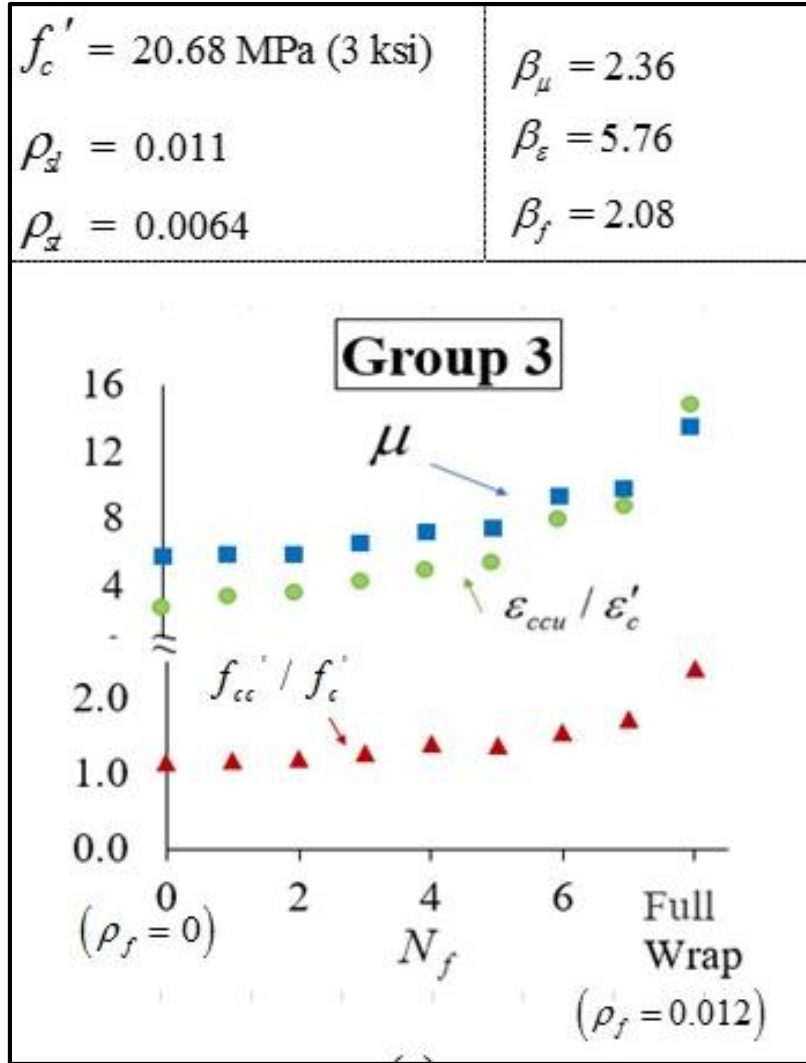
Figure 3.9c - Strengthening ratio (f_{cc}' / f_c'), strain ratio
$(\varepsilon_{ccu} / \varepsilon_c')$, and ductility factor (μ) vs number of strips
(N_f) for the columns in Group 3

48
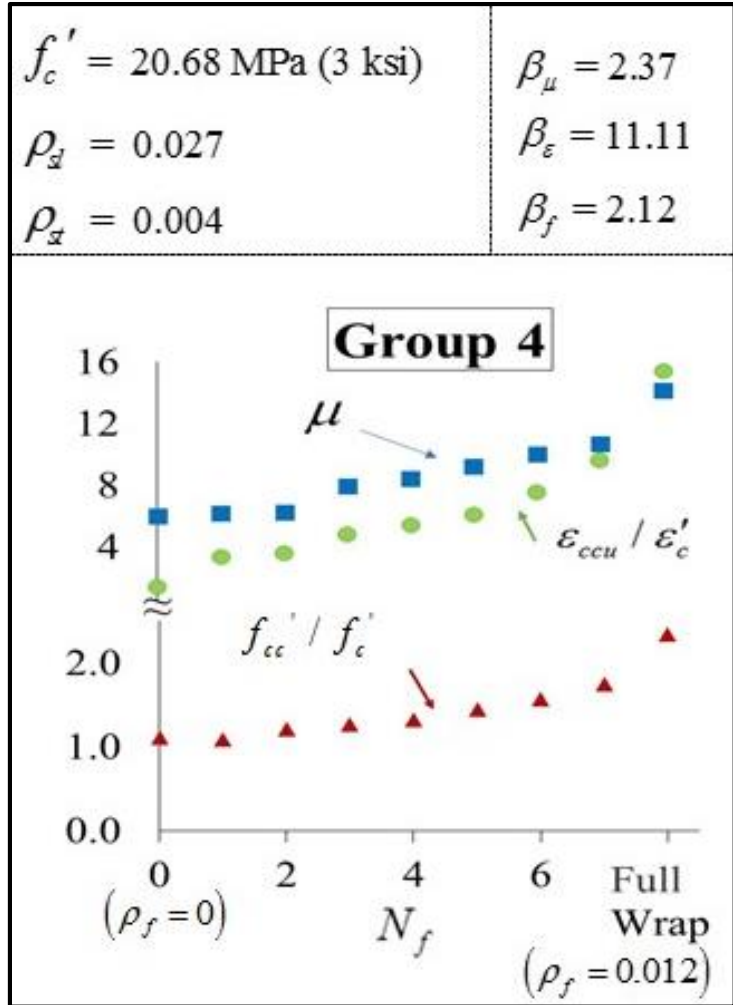
Figure 3.9d - Strengthening ratio (f'_{cc} / f'_c), strain ratio $(\varepsilon_{ccu} / \varepsilon'_c)$, and ductility factor ($\mu$) vs number of strips (N_f) for the columns in Group 4

3.4.2 Influence of the FRP Volumetric Ratio (ρ_f)

In all column groups, as the FRP volumetric ratio (Eq. 3.6) increases from $\rho_f = 0.0$ for the unwrapped column to $\rho_f = 0.012$ for the fully wrapped column in Figures 3.4 to 3.7, and as expected, there is an increase in the ultimate confined concrete compressive stress (f_{cc}'), the ultimate confined axial strain (ε_{ccu}), and the ultimate lateral strain of confined

49

concrete (ε_{lu}). Figures 3.4 to 3.7 and Table 3.4 provide more detailed results that clearly show the influence of the number of strips in Groups 1 to 4 on the strengthening ratio (f'_{cc}/f'_c), strain ratio ($\varepsilon_{ccu}/\varepsilon'_c$), and ductility factor (μ). As the number of strips is increased, the aforementioned ratios also increase.

Although it is clear that the improvements are more significant in fully wrapped columns, using partial wraps shows a noticeable improvements. For example, in case of column S7, the strengthening ratio (f'_{cc} / f'_c) and the strain ratio ($\varepsilon_{ccu} / \varepsilon'_c$) reached, 1.75 and 9.74, respectively, compared to 2.408 and 15.374 for fully wrapped columns. Comparing the ductility ratio, μ, of the S7 columns with respect to the FW columns, the S7 columns ductility ratio ranged between 75.6%-96% of that of the FW columns. It should be noted that for the columns under consideration in this particular FE analysis, the average ductility increase by 10.7% with each additional strip.

The ultimate lateral concrete strains $\left(\varepsilon_{lu} \right)$ increases with the increase in the FRP volumetric ratio in all groups. This implies a higher effective lateral confining pressure as presented in Table 3.4. None of the lateral strains reached the maximum FRP tensile strain reported by the manufacturer. The ultimate lateral strain to FRP maximum tensile strain ratio varied widely with the number of strips, averaging 0.758 and 0.462 for FW columns and S7 columns, respectively.

Since the interest in this research is the reinforced concrete columns, it is important to study the effect of the number of strips on the behavior of the internal longitudinal and lateral steel. Therefore, the points at which the longitudinal and transverse steel yield were determined for the different columns.   Three columns are selected from Group 1:

50

unwrapped column (UW), column wrapped with five strips (S5) and fully wrapped column (FW) and are presented in Figure 3.10. Studying the effect of the FRP volumetric ratio (ρ_f) on these key points in the stress strain relationship shows that, with increasing ρ_f, the transverse steel yields at higher compressive stresses and strains in concrete. It can be seen that the slope of the stress strain curves decreases after the yield of transverse steel.

51

Legend box (top left):

f_c' — 20.68 MPa (3 ksi)

f_y — 413.68 MPa (60 ksi)

f_{fu} — 2848 MPa (413 ksi)

E_f — 139 GPa (20160 ksi)

Cross-section (top right): 4 ⌀10; ⌀6 @ 140 mm; 200 mm

Legend: − − − Unwrapped Column (UW) — · · · 5 Strips (5S) ——— Full Wrap (FW)

Unwrapped (UW) (a) — f_c (MPa) / f_c (ksi) vs ε_c

5 Strips (5S) (b) — f_c (MPa) / f_c (ksi) vs ε_c

Full Wrap (FW) (c) — f_c (MPa) / f_c (ksi) vs ε_c

All Columns (d) — f_c (MPa) / f_c (ksi) vs ε_c

	Unwrapped (UW)		5 Strips (5S)		Full Wrap (FW)	
	ε_c	f_c (MPa)	ε_c	f_c (MPa)	ε_c	f_c (MPa)
△ (Long. Steel Yield)	0.0022	22.03	0.0021	22.13	0.0023	23.16
□ (Trans. Steel Yield)	0.0025	22.13	0.0045	24.82	0.0047	27.29
○ (Ultimate Point)	0.0025	22.13	0.0126	29.16	0.0303	48.80

Figure 3.10- Compressive stress (f_c) vs axial strain (ε_c) relationships showing longitudinal steel yield, transverse steel yield and ultimate points for circular columns in group 1 (a) Unwrapped (b) 5 Strips (c) Full Wrap (d) All columns (1 mm = 0.039 in.; 1MPa= 0.145 ksi)

52

3.4.3 Unconfined concrete compressive strength ($f_c{}'$)

The influence of $f_c{}'$ is studied by comparing Group 1 and Group 2 (Figures 3.11 (a-h), and Table 3.6). Group 2 has the same cross section as the basic group (Group 1) except the value of unconfined concrete compressive strength (f_c'), which is increased from 20.68 MPa (3 ksi) to 55.158 MPa (8 ksi).

Figures 3.11 (a-h) show the increase in ultimate confined concrete compressive stress ($f_{cc}{}'$) and the reduction in the ultimate confined axial strain (ε_{ccu}) as the unconfined concrete compressive strength $f_c{}'$ is increased. All nine columns in Group 1 have strengthening ratios ($f_{cc}{}'/f_c{}'$), strain ratios ($\varepsilon_{ccu}/\varepsilon_c{}'$), ductility factors (μ), and efficiency factors, β (Eq. 3.9), larger than the one for the corresponding columns in Group 2 (Figure 3.9a , Figure 3.9b).

The influence of the unconfined concrete compressive strength in the column strength is more noticeable in case of the fully wrapped columns, where the strengthening ratios were 2.36 and 1.42 for FW columns in Group1 and Group 2 respectively.
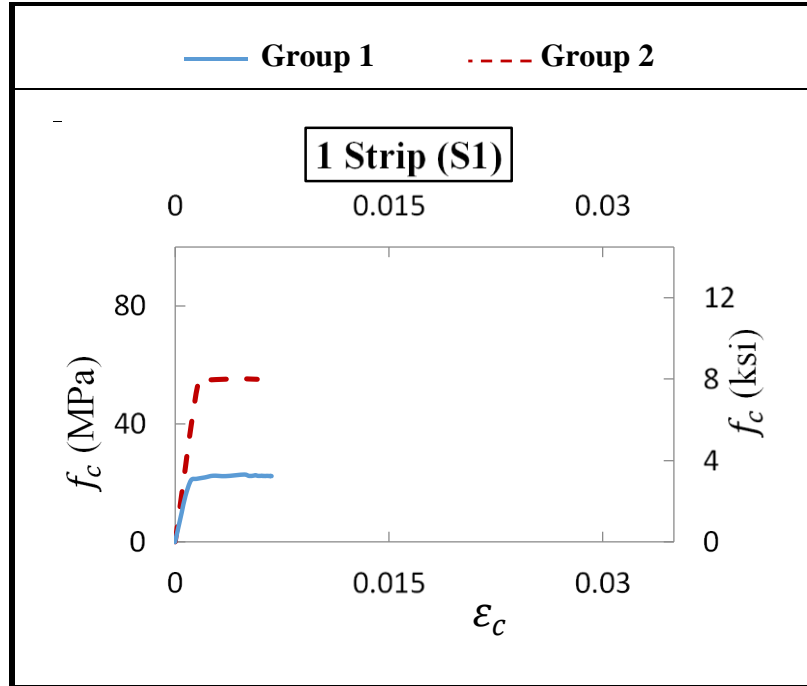
Figure 3.11 a- Comparison of compressive stress (f_c) vs axial
strain (ε_c) for Group1 and Group 2 column with 1 Strip (S1)
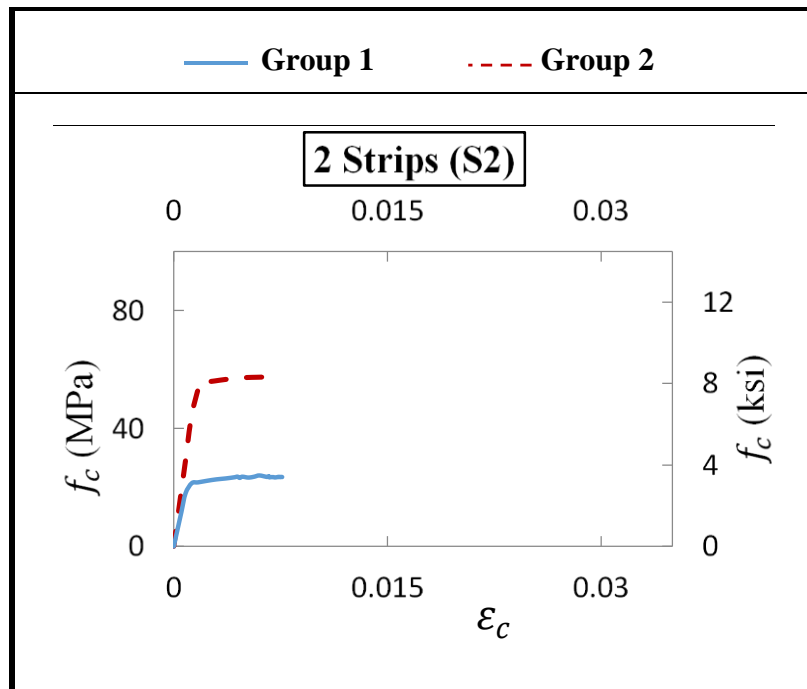
Figure 3.11 b - Comparison of compressive stress (f_c) vs axial
strain (ε_c) for Group1 and Group 2 column with 2 Strips (S2)

54
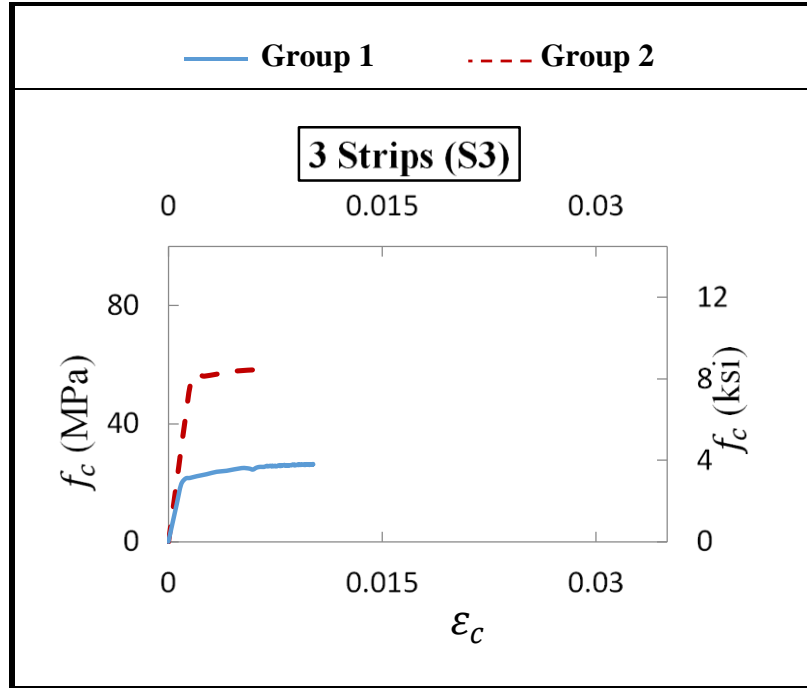
Figure 3.11 c - Comparison of compressive stress (f_c) vs axial strain (ε_c) for Group1 and Group 2 column with 3 Strips (S3)
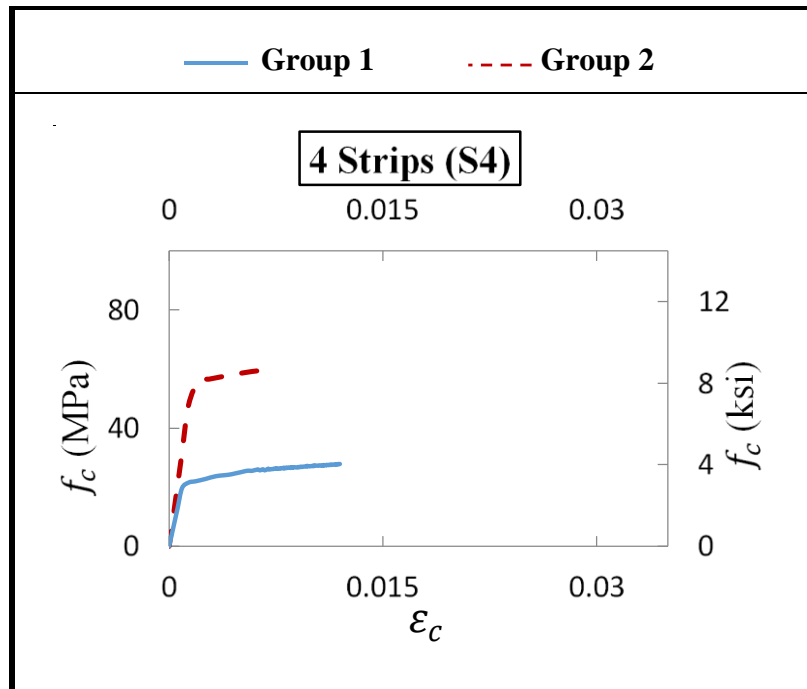
Figure 3.11 d - Comparison of compressive stress (f_c) vs axial strain (ε_c) for Group1 and Group 2 column with 4 Strips (S4)

55
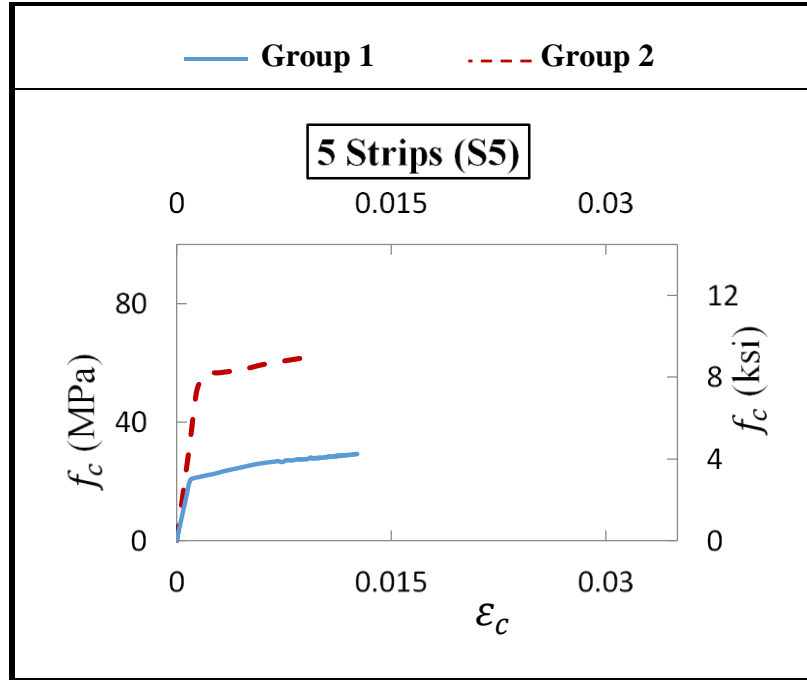
Figure 3.11 e - Comparison of compressive stress (f_c) vs axial
strain (ε_c) for Group1 and Group 2 column with 5 Strips (S5)
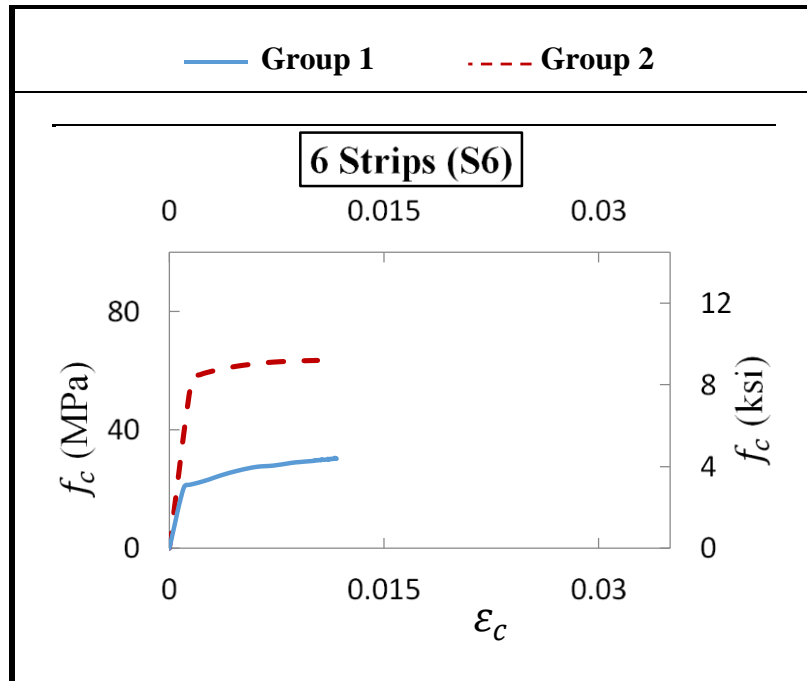
Figure 3.11 f - Comparison of compressive stress (f_c) vs axial
strain (ε_c) for Group1 and Group 2 column with 6 Strips (S6)

56
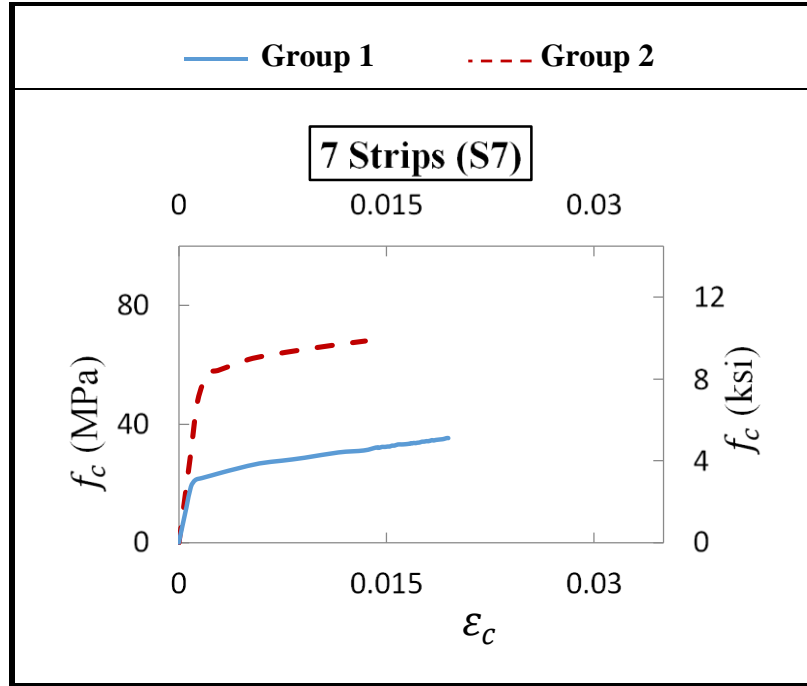
Figure 3.11 g - Comparison of compressive stress (f_c) vs axial
strain (ε_c) for Group1 and Group 2 column with 7 Strips (S7)
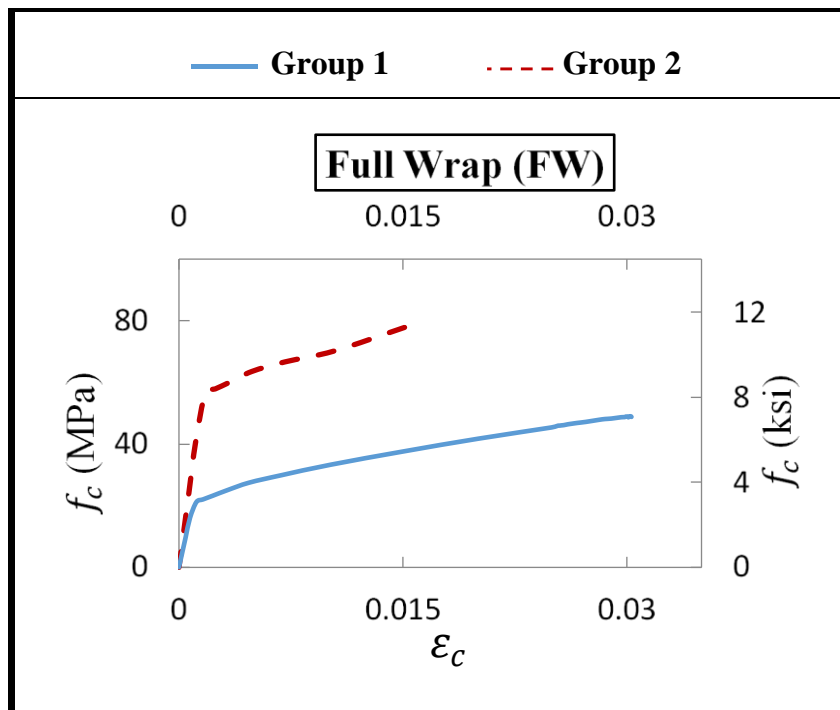
Figure 3.11 h - Comparison of compressive stress (f_c) vs axial
strain (ε_c) for Group1 and Group 2 fully wrapped columns

57

3.4.4   Transverse Steel Reinforcement Ratio (ρ_{st})

The influence of ρ_{st} is studied by comparing the columns in Group 1 with $\rho_{st} = 0.004$, and Group 3 with $\rho_{st} = 0.0064$ (Figures 3.12 (a-h), and Table 3.6).

Except for columns S5 and S6, the columns in Group 1 have a lower ultimate confined concrete compressive stress $f_{cc}{}'$. For columns S5 and S6 in Group 3, there is an overlap between the FRP and transverse steel leading to a decrease in the volume of confined concrete, and in turn to a lower $f_{cc}{}'$. The columns in Group 1 also have a higher ultimate confined concrete axial strain, ε_{ccu}, compared to the ones in Group 3 (Table 3.4). The ductility factor, μ, and the efficiency factors, β in Eq. 3.9, are reduced by increasing ρ_{st} (Figure 3.9a, Figure 3.9c).As the number of strips or the lateral FRP confinement (ρ_f) increases, the influence of the transverse steel confinement (ρ_{st}) decreases as can be seen from the post linear behavior when the f_c-ε_c curve for Group 1 ($\rho_{st} = 0.004$) approaches that of Group 3 ($\rho_{st} = 0.0064$).

58
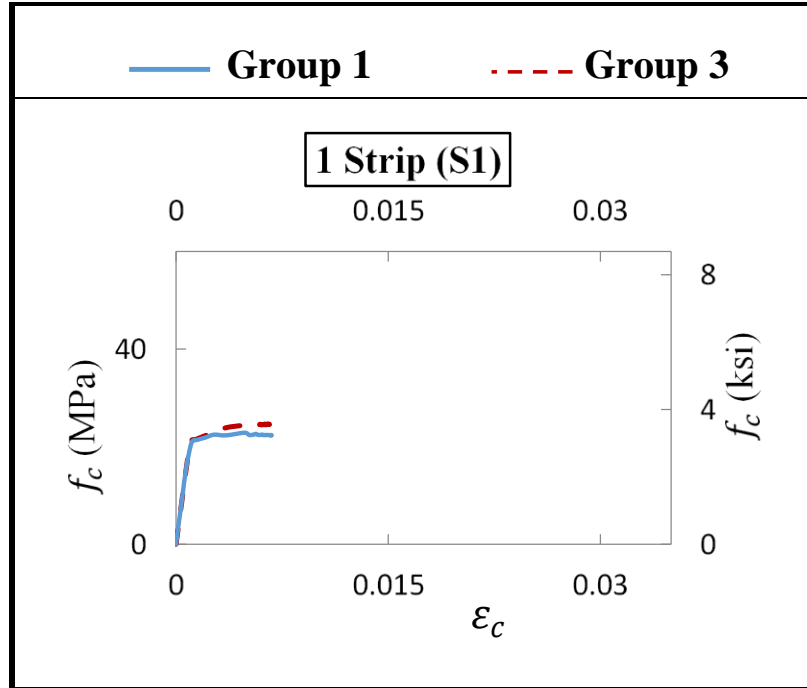
Figure 3.12 a - Comparison of compressive stress (f_c) vs axial strain (ε_c) for Group1 and Group 3 column with 1 Strip (S1)
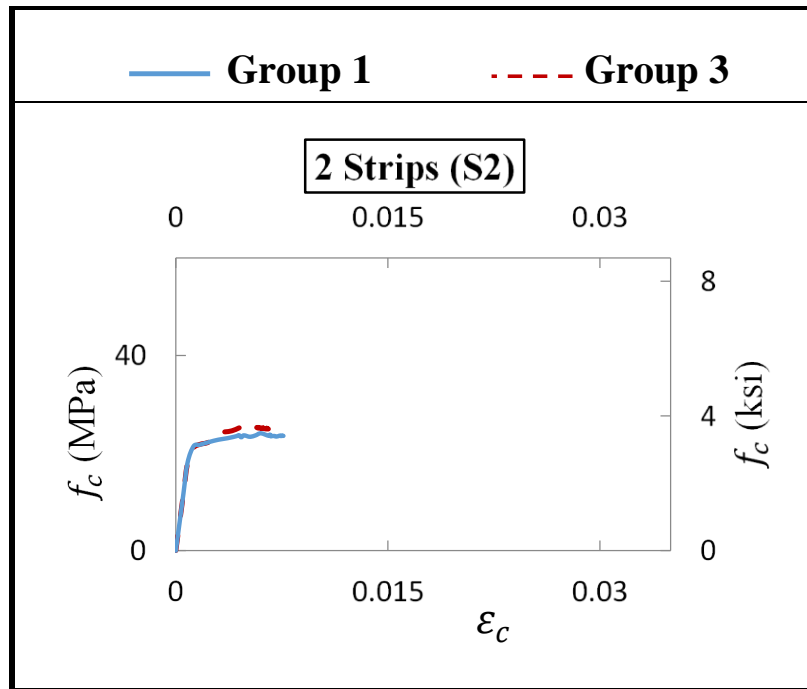
Figure 3.12 b - Comparison of compressive stress (f_c) vs axial strain (ε_c) for Group1 and Group 3 column with 2 Strips (S2)

59
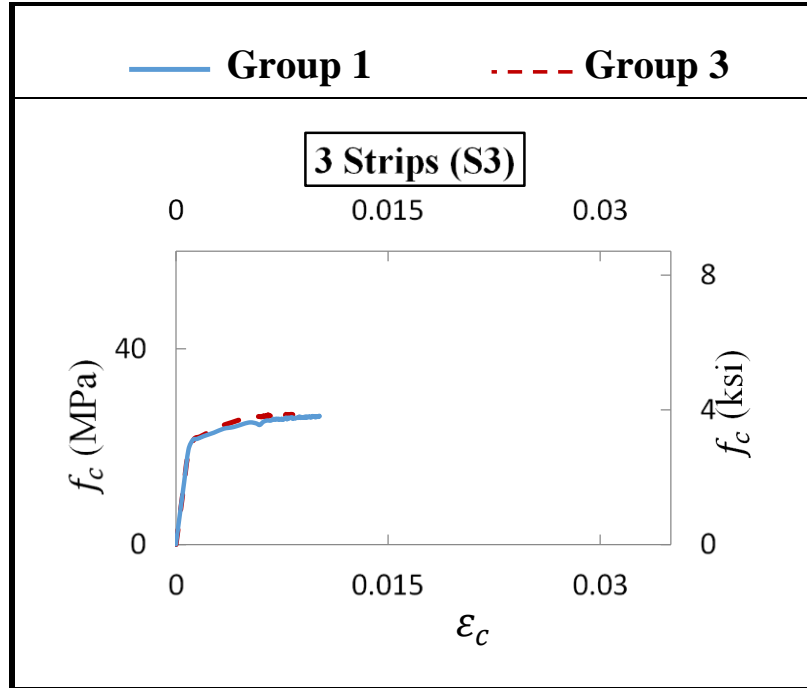
Figure 3.12 c - Comparison of compressive stress (f_c) vs axial
strain (ε_c) for Group1 and Group 3 column with 3 Strips (S3)
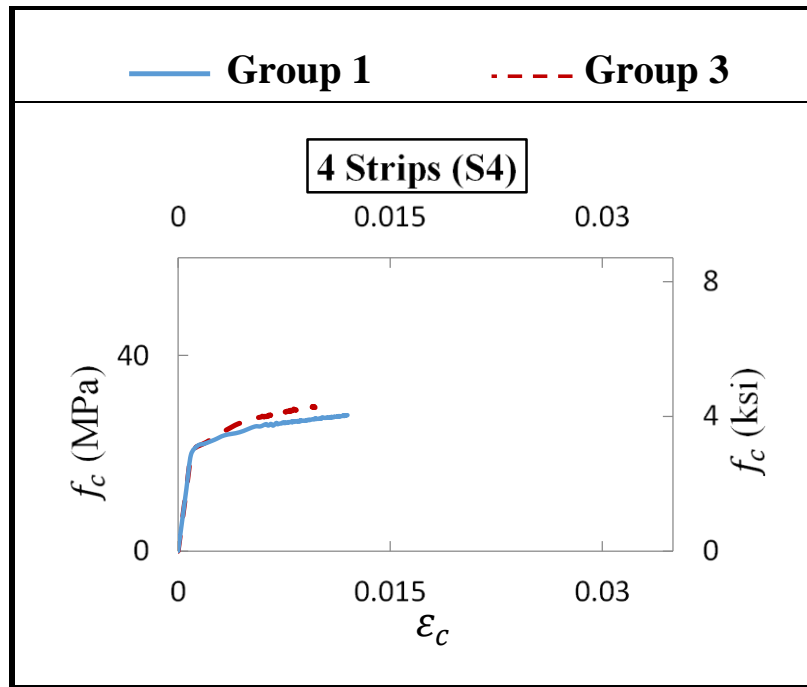
Figure 3.12 d - Comparison of compressive stress (f_c) vs axial
strain (ε_c) for Group1 and Group 3 column with 4 Strips (S4)

60
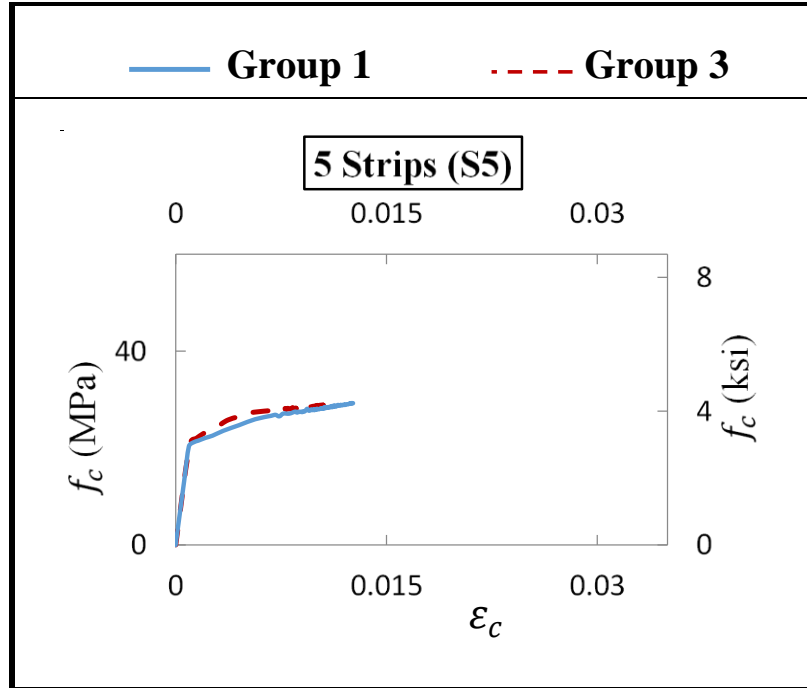
Figure 3.12 e - Comparison of compressive stress (f_c) vs axial strain (ε_c) for Group1 and Group 3 column with 5 Strips (S5)
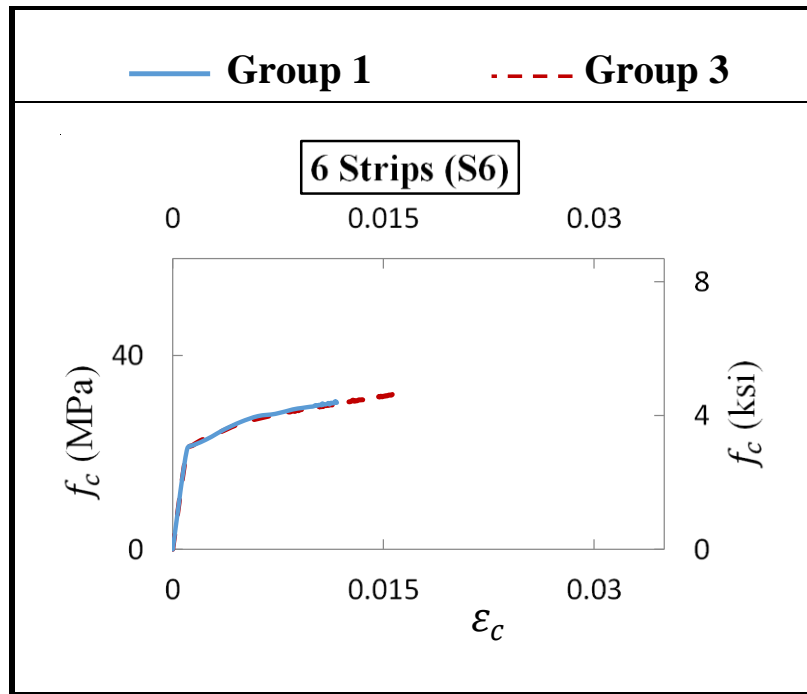
Figure 3.12 f - Comparison of compressive stress (f_c) vs axial strain (ε_c) for Group1 and Group 3 column with 6 Strips (S6)

61
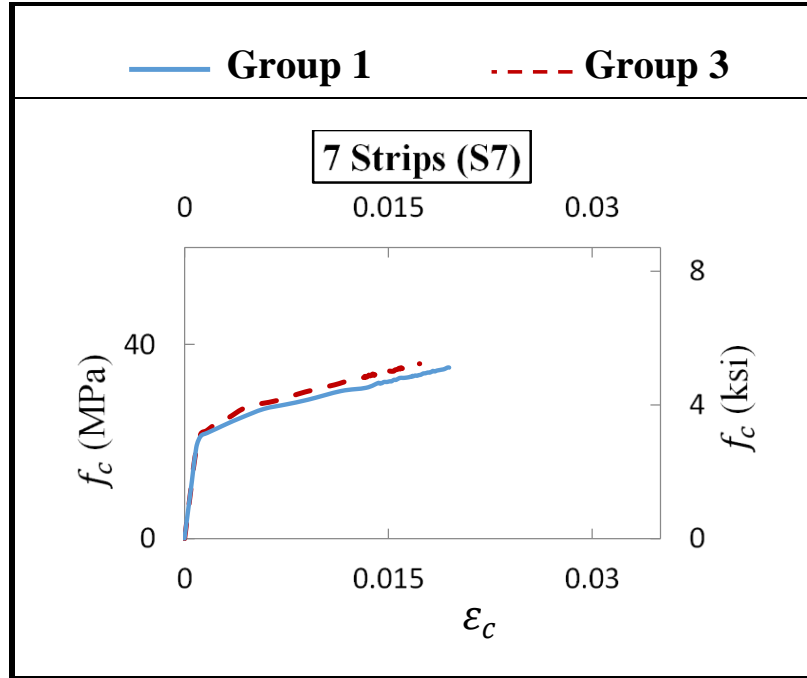
Figure 3.12 g - Comparison of compressive stress (f_c) vs axial
strain (ε_c) for Group1 and Group 3 column with 7 Strips (S7)
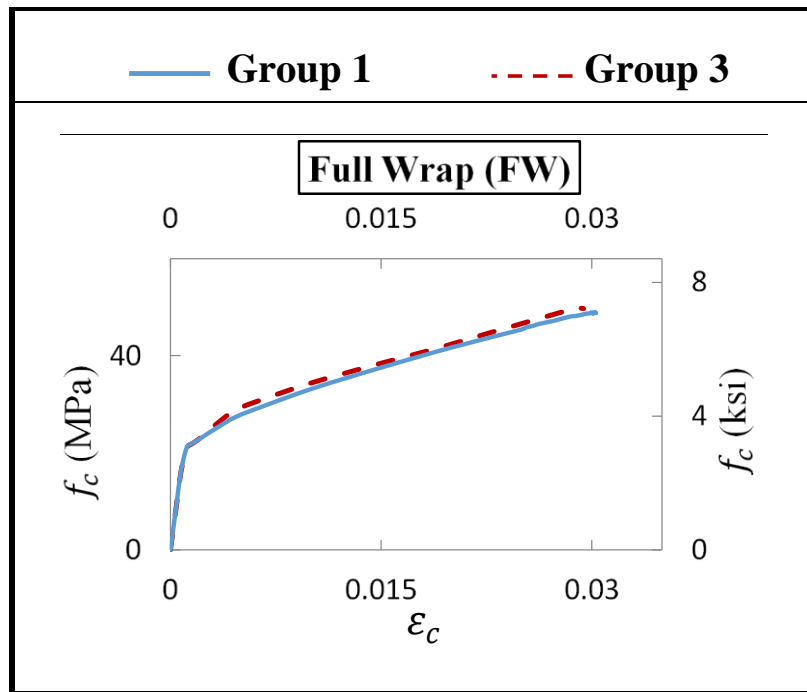
Figure 3.12 h - Comparison of compressive stress (f_c) vs axial
strain (ε_c) for Group1 and Group 3 fully wrapped columns

62

3.4.5 Longitudinal Steel Reinforcement Ratio (ρ_{sl})

The effect of ρ_{sl} is studied by comparing the columns in Group 1 ($\rho_{sl} = 0.011$) and Group 4 ($\rho_{sl} = 0.027$) (Figures 3.13 (a-h), and Table 3.6).

At ultimate conditions, the columns in Group 1 have a slightly lower ultimate confined concrete compressive stress and higher ultimate axial concrete strain (Table 3.6). The efficiency factors, β (Eq. 3.9), for Group 1 are slightly larger than the ones for Group. In general, the change in th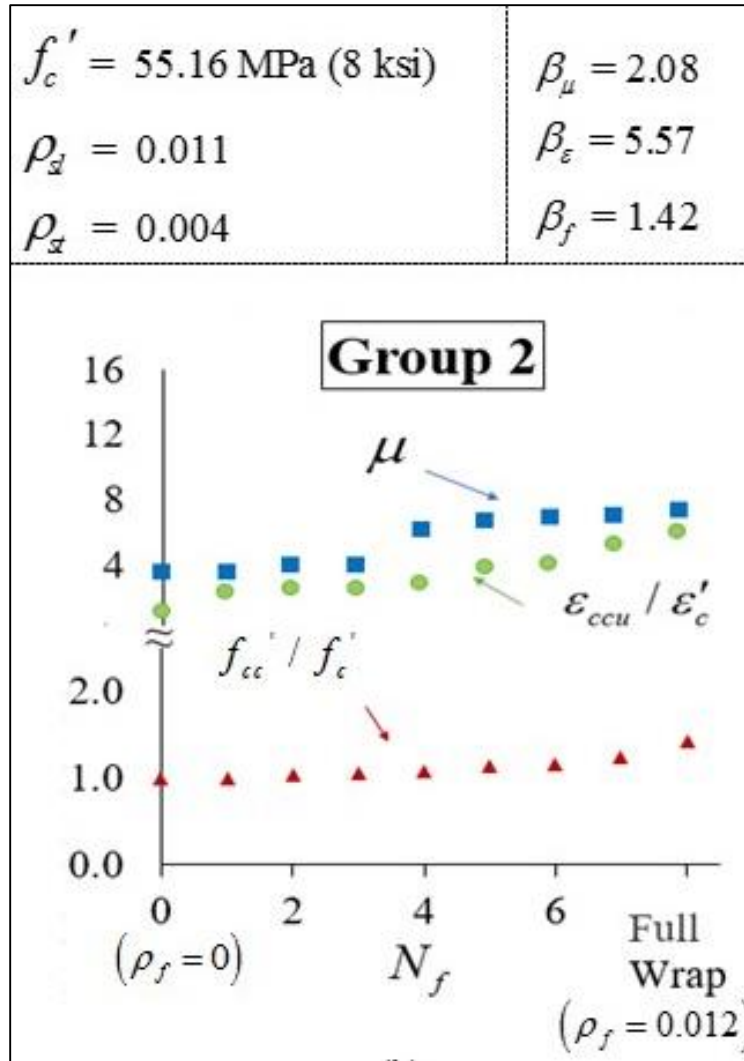e strengthening ratios (f_{cc}'/f_c'), strain ratios ($\varepsilon_{ccu}/\varepsilon'_c$), and ductility factors (μ), due to the increase in the longitudinal steel reinforcement ratio has a little influence on concrete confinement for the columns under consideration (Figure 3.9a, Figure 3.9d). Figures 3.13 (a-h) clearly show that the f_c-ε_c plots for Groups 1 and 4 are difficult to separate. Consequently, the contribution of the longitudinal steel is neglected in the derivation of the confined concrete stress-strain model in the following sections.
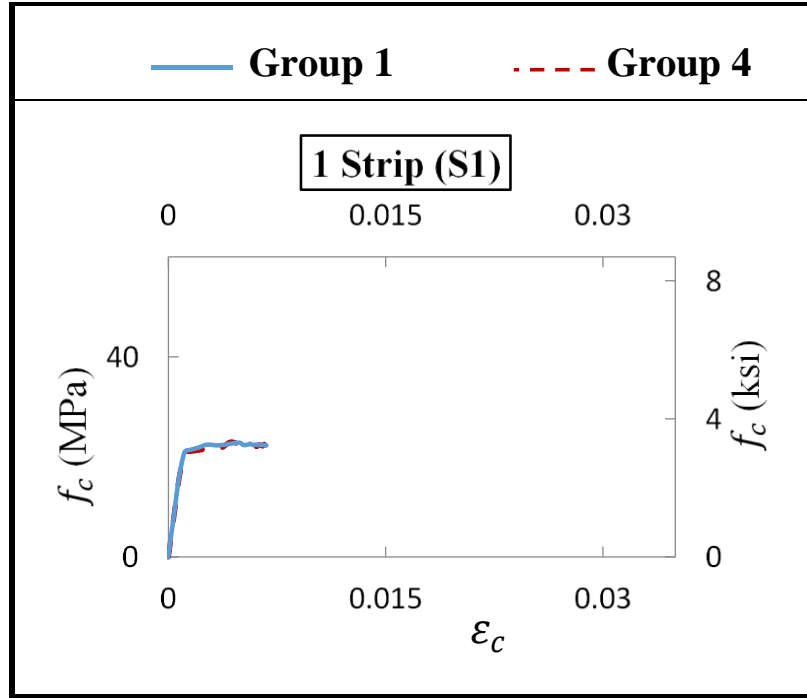
Figure 3.13 a - Comparison of compressive stress (f_c) vs axial strain (ε_c) for Group1 and Group 4 column with 1 Strip (S1)
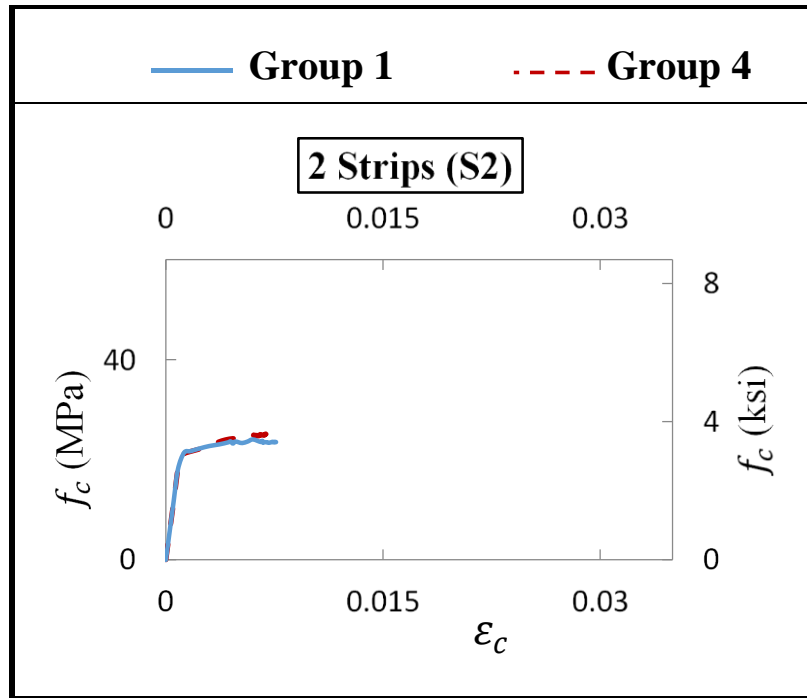
Figure 3.13 b - Comparison of compressive stress (f_c) vs axial strain (ε_c) for Group1 and Group 4 column with 2 Strips (S2)

64
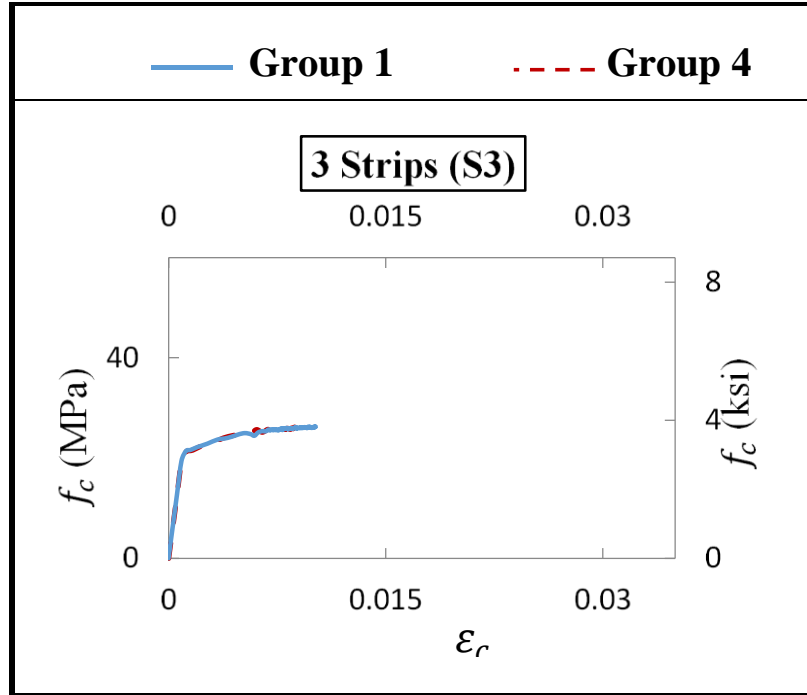
Figure 3.13 c - Comparison of compressive stress (f_c) vs axial
strain (ε_c) for Group1 and Group 4 column with 3 Strips (S3)
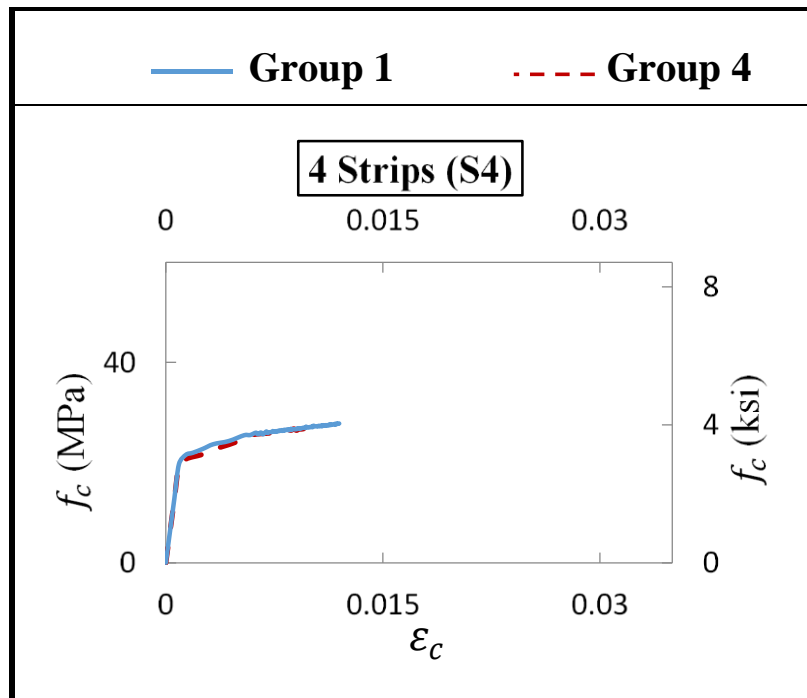
Figure 3.13 d - Comparison of compressive stress (f_c) vs axial
strain (ε_c) for Group1 and Group 4 column with 4 Strips (S4)

65
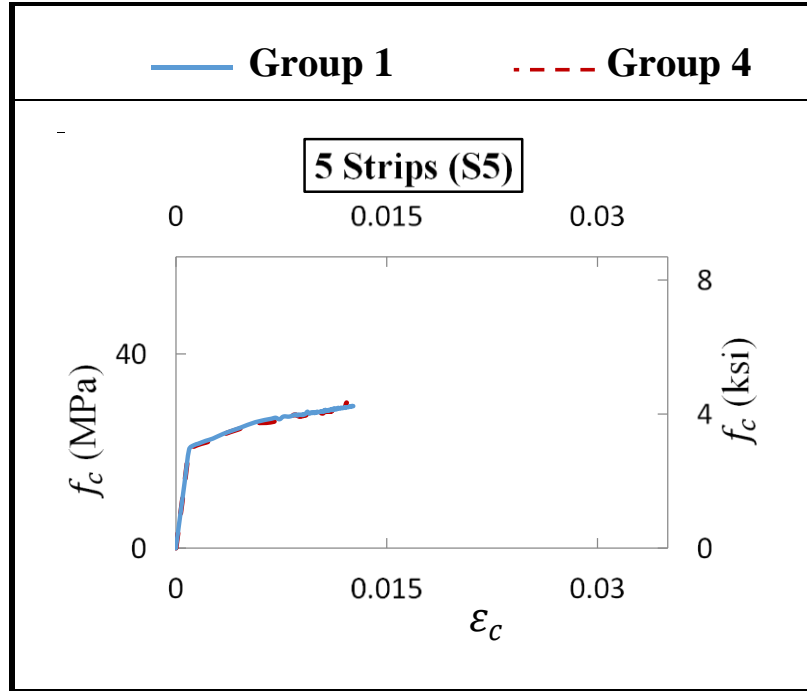
Figure 3.13 e - Comparison of compressive stress (f_c) vs axial strain (ε_c) for Group1 and Group 4 column with 5 Strips (S5)
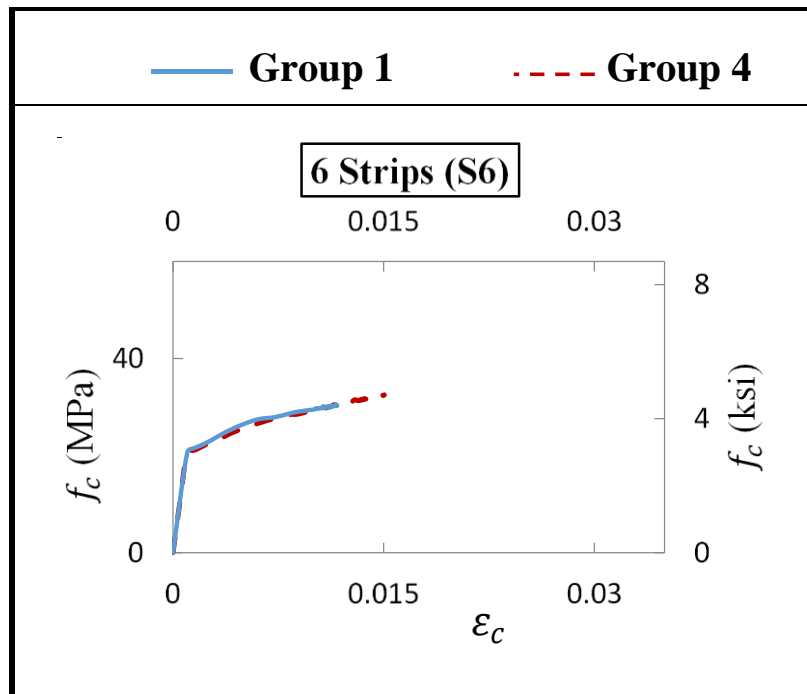
Figure 3.13 f - Comparison of compressive stress (f_c) vs axial strain (ε_c) for Group1 and Group 4 column with 6 Strips (S6)
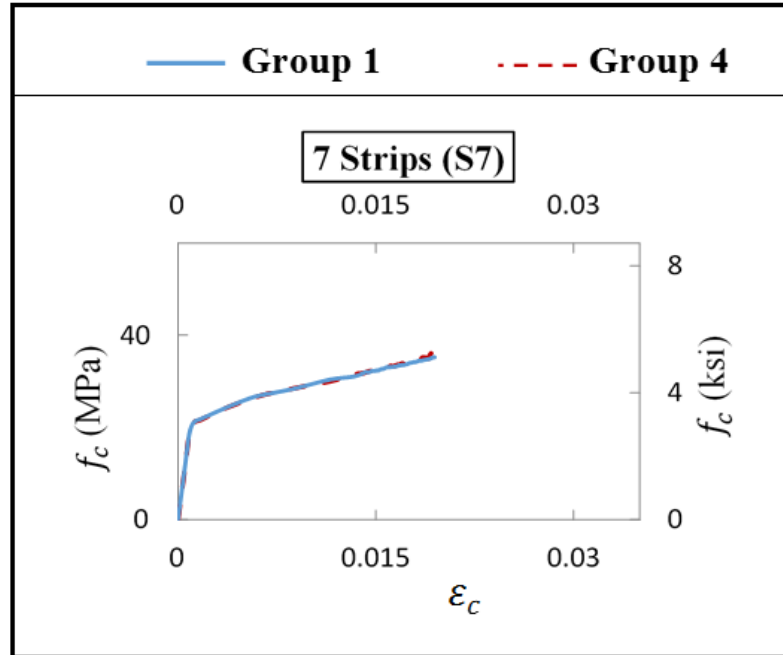
Figure 3.13 g - Comparison of compressive stress (f_c) vs axial strain (ε_c) for Group1 and Group 4 column with 7 Strips (S7)
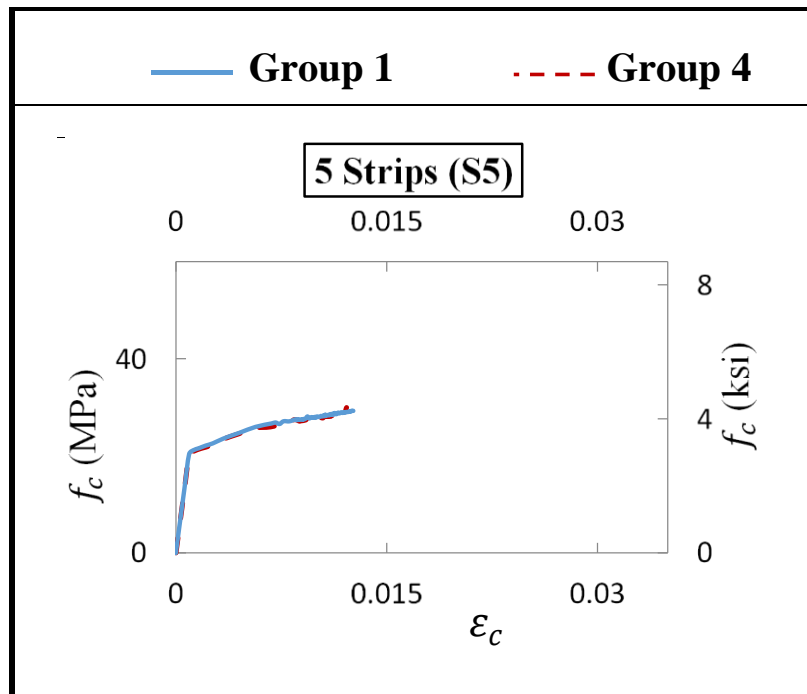
Figure 3.13 h - Comparison of compressive stress (f_c) vs axial strain (ε_c) for Group1 and Group 4 fully wrapped columns

67

3.5   Strip Arrangement

In this section, the effect of the number of strips on the behavior of confined columns is evaluated by using different strip arrangement while keeping the FRP volumetric ratio constant for all columns.

Two groups of RC columns with FRP volumetric ratios of 0.003 and 0.006 are considered. Each group has four columns with different strip arrangement in order to evaluate the effect of the strip arrangement on the confined stress-strain behavior. The columns are wrapped with 1, 3, 6 strips and full wrap (Figure 3.14), and have the same cross section and material properties as the columns in Group 1 (Figure 3.1 and Table 3.2). The number of FRP layers per strip is varied to achieve the targeted FRP volumetric ratio.

The finite element program ANSYS (ANSYS 14) was used to model the columns to evaluate the effect of the number of strips on the behavior of confined stress-strain. The results are presented in Figure 3.15 for two FRP volumetric ratios (Eq. 3.6), $\rho_f = 0.003$ and $\rho_f = 0.006$.   One unwrapped ($\rho_f = 0.0$) and one fully wrapped column, and three columns wrapped with 1, 3, and 6 strips are compared in Figure 3.15.   It is clearly seen that, for the same volume of CFRP material bonded to the column, the fully wrap is more effective in increasing the ultimate compressive stress and strain, and thus, ductility. The effectiveness is more pronounced when the CFRP volumetric ratio is increased to 0.006 in Figure 3.15b. Although the fully wrapped column is more effective, in certain instances, a specific number of strips could satisfy the design requirements. This may be of interest when retrofitting columns that are not easily accessible (e.g. over a waterway) where the placement of strips maybe more economical than placing a full wrap.

68
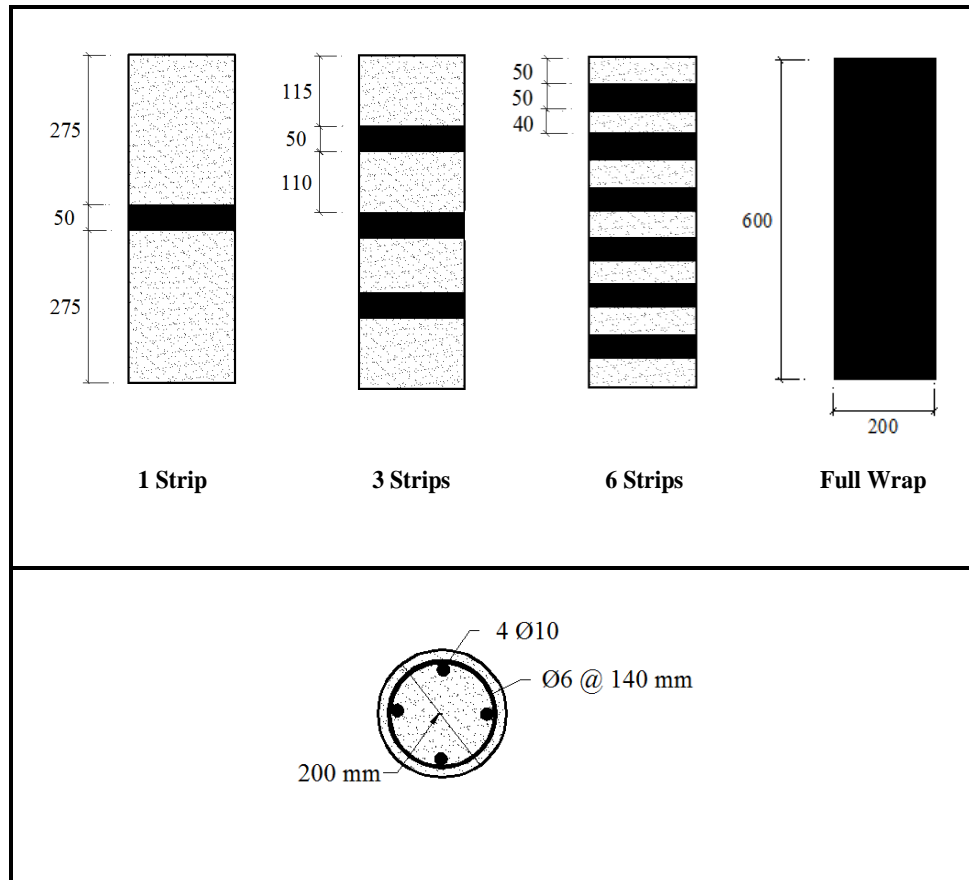
Figure 3.14- FRP Wraps Layouts for columns with the same FRP reinforcement

ratios ρ_f (1 mm = 0.039 in.)

$f_c{}' = 20.68$ MPa (3 ksi)	$f_y = 413.68$ MPa (60ksi)	$f_{fu} = 2848$ MPa (413 ksi)	$E_f = 139$ GPa (20160 ksi)
— · — Unwrapped (UW)	– – – 1 Strip (S1)	– · – · 3 Strips (S3)	
– – – 6Strips (S6)	■ Full Wrap (FW)		

(a)

(b)

Figure 3.15- Comparison of compressive stress (f_c) vs axial strain (ε_c) relationships for the unwrapped column and columns having the same CFRP volumetric ratio, ρ_f: (a) $\rho_f = 0.003$, and (b) $\rho_f = 0.006$

3.6   Conclusions

A comprehensive 3D nonlinear finite element (FE) model was developed in this chapter to simulate the behavior of concentrically loaded RC circular column wrapped with FRP. The (FE) models were generated to study the influence, on the behavior of the concentrically loaded columns, of the unconfined compressive strength ($f_c^{'}$), the number of strips (N_f), the FRP volumetric ratio (ρ_f), the transverse steel reinforcement ratio (ρ_{st}), and the longitudinal steel reinforcement ratio (ρ_{sl}). It should be noted that the columns wrapped with one, two, or three strips are not of practical interest and are used herein to illustrate the influence of partial wrapping as the analysis transitions from an unwrapped column to a partially wrapped column with one to seven strips, to a fully wrapped column.

The following conclusions can be outlined based on the findings of this chapter:

- The increase in the unconfined compressive strength has a pronounced influence of increasing effect on the increase in the confined concrete compressive strength ($f_{cc}^{'}$). As the unconfined compressive strength increases, strengthening ratios ($f_{cc}^{'}/f_c^{'}$), strain ratios ($\varepsilon_{ccu}/\varepsilon_c^{'}$), and ductility factors (μ) decrease.

- As the number of identical strips increases (or ρ_f increases), the influence of the transverse steel confinement (ρ_{st}) decreases.

- The contribution of the longitudinal steel has little influence on the confined concrete stress-strain behavior.

- The increase in the number of strips ($N_f = 1$ to 7), while keeping the FRP volumetric ratio (ρ_f,) constant, leads to an increase in the ultimate compressive stress and strain, and ductility. This indicates that, for a specific ρ_f, it is more effective to fully wrap

71

the column in order to increase the ultimate confined concrete compressive stress

and axial strain.

CHAPTER 4
MODEL DEVELOPMENT FOR CONCENTRICALLY LOADED CIRCULAR RC COLUMNS PARTIALLY CONFINED WITH FRP

4.1 Abstract

Wrapping reinforced concrete (RC) columns with Fiber Reinforced Polymer (FRP) composites is effective in increasing their capacity. The current state of the art concentrates primarily on fully wrapped columns and few studies dealt with partially wrapped ones. The objective herein is to evaluate the effectiveness of partial wraps (or strips) and to develop a confined concrete compressive stress-strain ($f_c - \varepsilon_c$) model that accounts for partial wrapping. Three dimensional finite element (FE) models are generated to evaluate the influence of different parameters on the behavior of concentrically loaded RC circular columns that are partially and fully wrapped with FRP. The results showed an increase in ductility as the number of FRP strips is increased, and indicated that longitudinal steel had little influence on the confined $f_c - \varepsilon_c$ relationship. The proposed $f_c - \varepsilon_c$ model, derived from the parametric study, accounts for the effect of partial and full confinement, the unconfined concrete strength $f_c^{'}$, and yielding of transverse steel. Comparison of the results generated using the proposed model with FE and experimental results are in good agreement.

73

4.2   Introduction

The application of Fiber Reinforced Polymer (FRP) wraps to reinforced concrete (RC) columns is an established and efficient technique for enhancing the capacity of columns. Columns that are fully wrapped with FRP showed an increase in ductility, moment and ultimate compressive load capacity, ultimate deformability and energy absorption compared to unconfined columns (Spoelstra and Monti1999, Toutanji 1999, and Mirmiran, and Shahawy 2007). Several studies focusing on fully wrapped FRP confined concrete columns have been carried out to generate models for predicting their behavior (Nanni and Bradford1995, Samaan et al. 1998, and Lam and Teng 2003).

Research on columns partially wrapped with FRP sheets (or strips) is very limited (Saadatmanesh et al. 1994, Barros and Ferreira 2008, and Wu et al. 2009).   The majority of the studies did not account for the influence of the existing steel reinforcement on the column's behavior (Lam and Teng 2003), or simply estimate the total confinement pressure as the sum of the confinement pressure due to the external FRP jacketing and the confinement pressure due to the internal transverse steel reinforcement (Harajli et al 2006, Barros and Ferreira 2008). Few models dealt with concrete confined by both FRP and transverse steel (Eid and Paultre 2008, and Lee et al. 2010)

The focus of this chapter is to better understand the interaction between internal steel reinforcement and partial or full external FRP wrap/reinforcement and their influence on concrete confinement. A series of finite element (FE) models are developed to analyze the effect of the aforementioned parameters on the confined concrete column. FE models have been successfully used to simulate the behavior of columns wrapped by FRP sheets (Rochette and Labossieren 1996, Mirmiran et al. 1996). The influence of partial wrapping

74

on the increase in strength and ductility is evaluated. The results from the FE parametric analyses were used to derive a new confined concrete compressive stress-strain model for concentrically loaded RC circular columns that are partially and fully wrapped with FRP.

4.3   Research Significance

A new confined concrete compressive stress-strain model is introduced to account for partially and fully FRP wrapped concentrically loaded RC circular columns.
Based on the current state of the art, the proposed work will allow a better understanding of the behavior of partially wrapped RC columns and the parameters that influence their effectiveness. This is achieved by developing a sophisticated three dimensional FE model, which is capable of describing the behavior of these columns.

4.4   Finite Element Modeling

The FE program ANSYS 14.0 (ANSYS 2012) is used to develop a series of 3D nonlinear models for concentrically loaded circular RC columns. The confined concrete is modeled using the Drucker-Prager yield criterion (Wu et al. 2009, Rochette and Labossieren 1996, and Mirmiran et al. 1996), and the steel reinforcement is modeled as a bi-linear elastic-perfectly plastic material. The FRP material is modeled as a linearly elastic material. The mechanical properties of concrete, steel, and FRP are listed in Table 4.1. Due to symmetry, a quarter of the column cross section is modeled, and the load is applied as an equivalent displacement at top of the columns.

75

Table 4.1– Material properties and FE elements for the control (or unwrapped) column and the eight columns in Figure 4.2

Material	Parameter				FE element
Concrete	f_c'		20.68 MPa	3 ksi	SOLID 65
			55.16 MPa	8 ksi	
	E_c		21.50 GPa	3118 ksi	
			35.13 GPa	5095 ksi	
Steel	f_y		413.68 MPa	60 ksi	LINK 180
	A_s	$\phi 6$	32 mm^2	0.05 in^2	
		$\phi 10$	71 mm^2	0.11 in^2	
FRP	t_f		0.15 mm	0.0059 in	SHELL 181
	f_{fu}		2848 MPa	413 ksi	
	E_f		139 GPa	20160 ksi	

The validation of the FE model is carried out by comparing the results of the model with experimental ones presented by Barros and Ferreira 2008 (Figure 4.1). The results show very good agreement between the two.

76

$$f_c' = 16 \text{ MPa} \quad (2.32 \text{ ksi})$$
$$f_y = 468.3 \text{ MPa} \quad (68 \text{ ksi})$$
$$f_{fu} = 3539 \text{ MPa} \quad (513.3 \text{ ksi})$$
$$E_f = 232 \text{ GPa} \quad (33649 \text{ ksi})$$
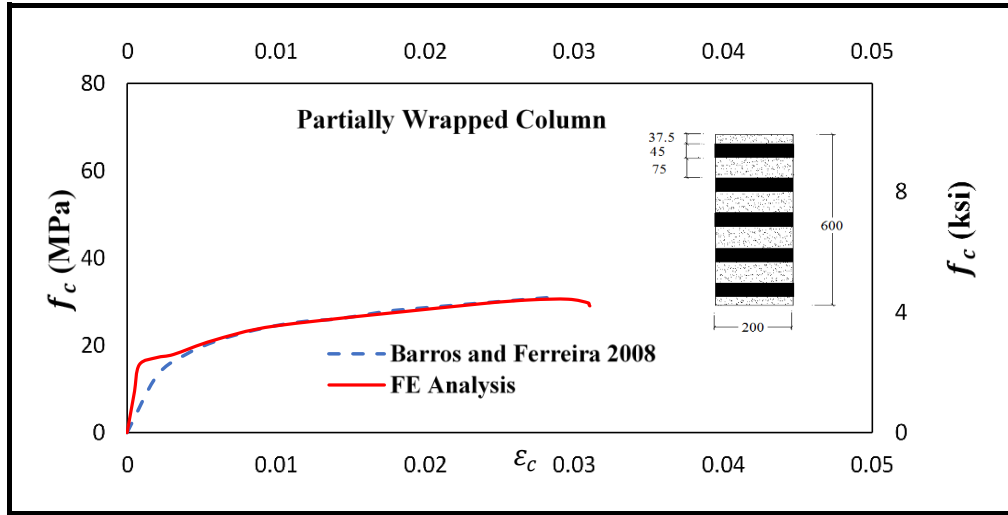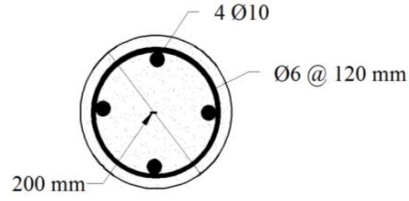
(a)
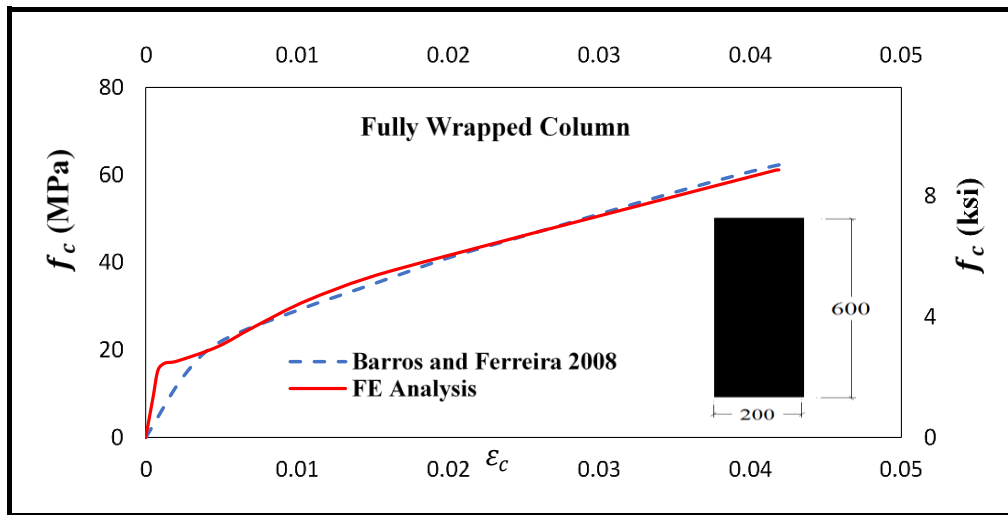
(b)

Figure 4.1– Comparison of compressive stress (f_c) vs. axial strain (ε_c) between FE and experimental results: (a) partially wrapped column; and (b) fully wrapped column (All dimensions are in mm; 1 mm = 0.039 in.)

4.5 Partial FRP Wraps or Strips

Nine columns are considered in the parametric study. All columns have the same unbraced length $l_u = 600$ mm (23.62 in.) and diameter $D = 200$ mm (7.9 in.). One column is unwrapped and is the baseline column. The other eight columns are presented in Figure 4.2, one of the columns is fully wrapped (FW) and the remaining seven are partially wrapped with strips varying from one strip ($N_f = 1$) on column S1 to seven strips on column S7 ($N_f = 7$). Each strip has a width $w_f = 40$ mm (1.6 in.). For the fully wrapped column, $w_f = l_u$ and $N_f = 1$. The full wrap and each strip has four layers of CFRP fabric ($n_f = 4$), and the thickness of each layer $t_f = 0.15$ mm (0.0059 in.). The FRP volumetric ratio (ρ_f) for each column is determined as follows

$$\rho_f = 4\frac{n_f w_f N_f t_f}{D l_u} \tag{4.1}$$

Four groups of columns (Table 4.2) are studied to evaluate the influence of different parameters on the confined concrete stress (f_c), axial strain (ε_c) and lateral strain (ε_l). In addition to the unwrapped column, each group contains the eight columns in Figure 4.2, and Group 1 is the baseline group.

In Groups 2 to 4, three different parameters are varied: the 28-day compressive strength of unconfined concrete $f_c^{'}$, the transverse steel reinforcement ratio, ρ_{st}, and the longitudinal steel reinforcement ratio, ρ_{sl} (Eq. 4.2)

$$\rho_{st} = V_{st} / V_c \qquad , \qquad \rho_{sl} = A_{sl} / A_g \tag{4.2}$$

Where V_{st} is the volume of transverse steel; V_c is the volume of concrete; A_{sl} is the total area of longitudinal steel; and A_g is the gross area of the column section.

78

Table 4.2 – Column Groups used in the parametric study

Group #[a]	f_c'		Longitudinal steel ϕ 10 mm (#3)		Transverse steel stirrups ϕ 6 mm (#2)		
	MPa	ksi	Number of Bars	ρ_{sl}	Spacing		ρ_{st}
					mm	in	
1	20.68	3	4	0.011	140	5.50	0.004
2	55.16	8	4	0.011	140	5.50	0.004
3	20.68	3	4	0.011	80	3.15	0.0064
4	20.68	3	12	0.027	140	5.50	0.004

[a] Each Group contains, in addition to the unwrapped column, the eight columns in Figure 4.2

79

Figure 4.2 – FRP Wrap Layout on circular columns (All dimensions
are in mm; 1 mm = 0.039 in.)

Figure 4.3 presents the results for all four groups in term of compressive stress of
confined concrete (f_c) vs concrete axial strain (ε_c) and concrete lateral strain (ε_l).

80
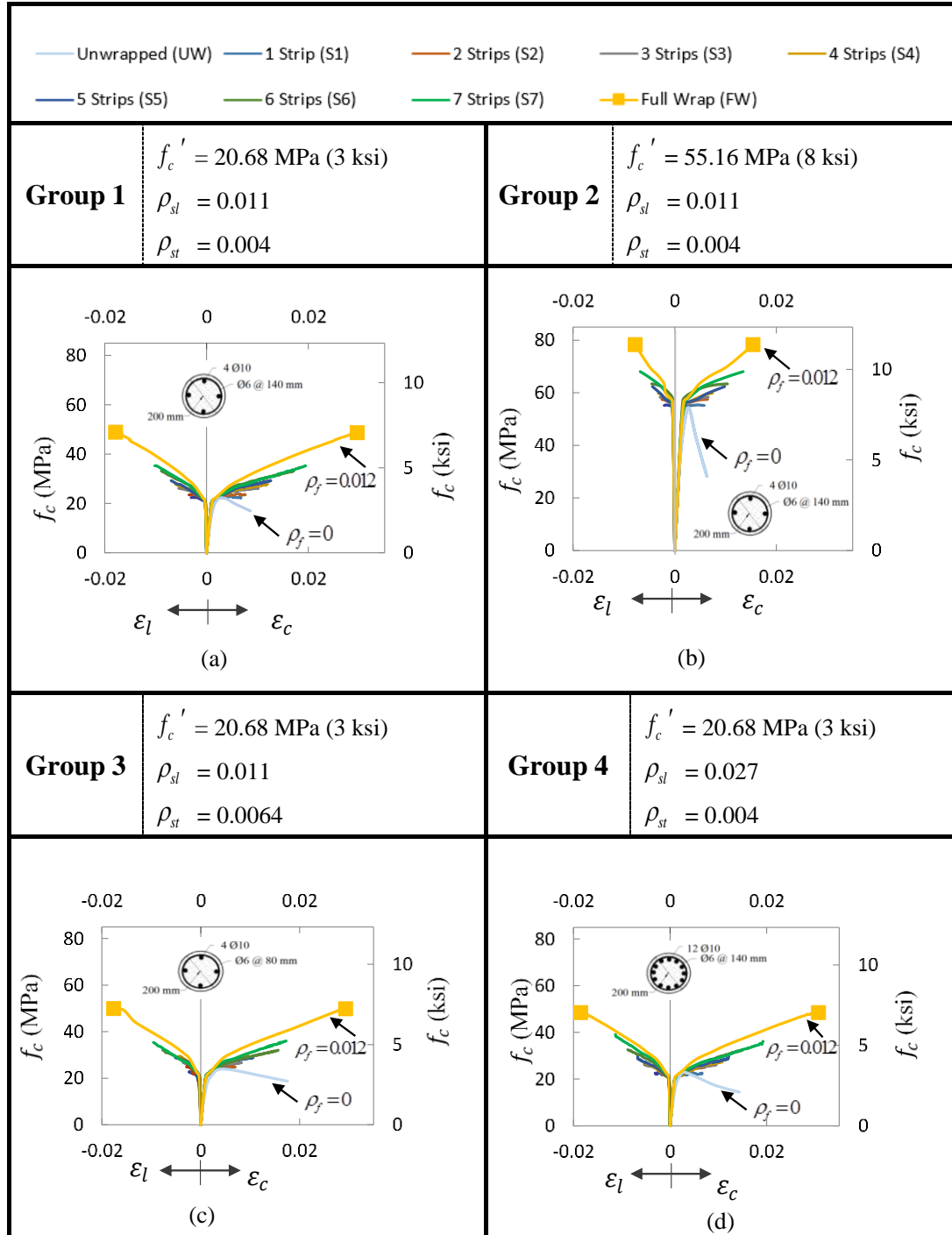
Figure 4.3 – Comparison of compressive stress (f_c) vs axial strain (ε_c) and lateral strain (ε_l) for the columns in Figure 4.2 and Groups 1 to 4 in Table 4.2. Note: Refer to Figure 4.2 for ρ_f values

81

Figure 4.4 presents the variation in the strengthening ratio (f'_{cc}/f'_c), strain ratio ($\varepsilon_{ccu}/\varepsilon_c'$) and ductility factor ($\mu$). f'_{cc} is the ultimate confined concrete compressive stress; ε_{ccu} is the ultimate confined concrete axial strain corresponding to the ultimate confined concrete compressive stress; ε_c' is the concrete axial strain at the unconfined concrete compressive strength (f_c'). These numerical values of these terms are listed in Table 4.3 for all Groups. The derivation of the ductility factor is based on the one proposed by Cui and Sheikh 2010.

Three efficiency factors, β, are introduced in Eq. 4.3 and Figure 4.4 to compare the fully wrapped (FW) columns to unwrapped columns (UW) in each group.

$$\beta_\mu = \frac{\mu_{FW}}{\mu_{UW}}; \beta_\varepsilon = \frac{(\varepsilon_{ccu})_{FW}}{(\varepsilon_{ccu})_{UW}} \text{ and } \beta_f = \frac{(f'_{cc})_{FW}}{(f'_{cc})_{UW}} \tag{4.3}$$

82
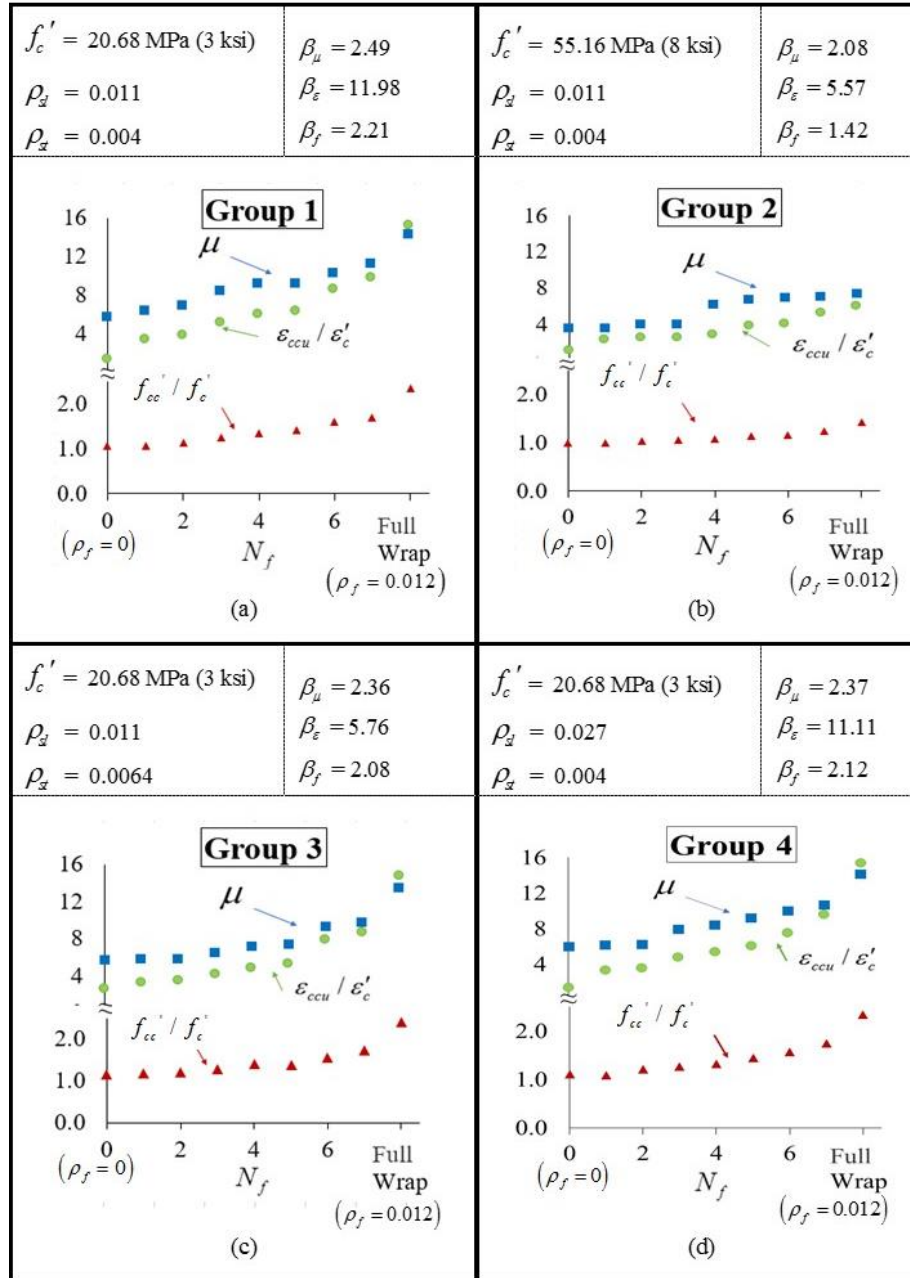
Figure 4.4 – Strengthening ratio (f'_{cc} / f'_c), strain ratio ($\varepsilon_{ccu} / \varepsilon'_c$), and ductility factor (μ) vs number of strips (N_f) for the columns in (a) Group 1, (b) Group 2, (c) Group 3, and (d) Group 4. Note: Refer to Table 4.2 for information on Groups 1 to 4, to Eq. 4.3 for β expressions, and to Figure 4.2 for ρ_f values

Table 4.3 – Stresses, strains and ductility factors for the unwrapped columns (UW) and columns in Groups 1 to 4 [a]   (1 MPa= 0.145 ksi)

Group # [a]		Columns [a]								
		UW	S1	S2	S3	S4	S5	S6	S7	FW
1	f'_{cc} (MPa)	22.13	22.32	23.51	26.22	27.81	29.23	33.18	35.24	48.80
	ε_{ccu}	0.0025	0.0068	0.0076	0.0102	0.0120	0.0126	0.0171	0.0195	0.0303
	ε_{lu}	-	0.003	0.0035	0.0055	0.0061	0.0070	0.0089	0.0102	0.0179
	f'_{cc} / f'_{c}	1.079	1.070	1.137	1.268	1.345	1.414	1.604	1.704	2.360
	$\varepsilon_{ccu} / \varepsilon'_{c}$	1.266	3.390	3.808	5.088	5.995	6.321	8.562	9.741	15.166
	μ	5.744	6.357	6.952	8.422	9.215	9.219	10.269	11.266	14.327
2	f'_{cc} (MPa)	55.20	55.22	57.52	28.35	59.86	62.35	63.39	68.06	78.27
	ε_{ccu}	0.0028	0.0058	0.0065	0.0066	0.0074	0.0098	0.0104	0.0135	0.0154
	ε_{lu}	-	0.0021	0.0025	0.0029	0.0032	0.0044	0.0045	0.0068	0.0077
	f'_{cc} / f'_{c}	1.001	1.001	1.043	1.058	1.085	1.130	1.149	1.234	1.419
	$\varepsilon_{ccu} / \varepsilon'_{c}$	1.083	2.267	2.534	2.580	2.903	3.840	4.062	5.273	6.036
	μ	3.53	3.552	3.970	4.041	6.177	6.762	6.915	7.087	7.339
3	f'_{cc} (MPa)	23.89	24.55	24.78	26.65	28.80	28.83	32.04	35.99	49.79
	ε_{ccu}	0.0051	0.0066	0.0070	0.0083	0.0084	0.0106	0.0157	0.0173	0.0294
	ε_{lu}	-	0.0023	0.0028	0.0035	0.0044	0.0052	0.0077	0.0096	0.0178
	f'_{cc} / f'_{c}	1.155	1.187	1.198	1.289	1.393	1.394	1.549	1.740	2.408
	$\varepsilon_{ccu} / \varepsilon'_{c}$	2.554	3.313	3.491	4.129	4.194	5.309	7.841	8.650	14.717
	μ	5.674	5.796	5.813	6.446	6.983	7.315	9.271	9.765	13.426
4	f'_{cc} (MPa)	22.2	22.38	25.02	26.22	27.31	29.89	32.54	36.16	48.49
	ε_{ccu}	0.0028	0.0066	0.0072	0.0096	0.0108	0.0122	0.0150	0.0193	0.0307
	ε_{lu}	-	0.0031	0.0033	0.0053	0.0056	0.0067	0.0088	0.0113	0.0187
	f'_{cc} / f'_{c}	1.074	1.082	1.210	1.268	1.320	1.445	1.573	1.749	2.345
	$\varepsilon_{ccu} / \varepsilon'_{c}$	1.384	3.323	3.618	4.795	5.391	6.082	7.527	9.637	15.374
	μ	5.972	6.205	6.231	7.918	8.415	9.206	10.026	10.697	14.155

[a] Refer to Tables 4.1 and 4.2, and Figure 4.2 for column dimensions and properties

84

4.5.1 FRP volumetric ratio, ρ_f

In all column groups, as the FRP volumetric ratio in Eq. 4.1 increases from $\rho_f = 0.0$

for the unwrapped column to $\rho_f = 0.012$ for the fully wrapped column (Figure 4.3), and as

expected, there is an increase in the ultimate confined concrete compressive stress ($f_{cc}^{'}$),

the ultimate confined axial strain (ε_{ccu}), and the ultimate lateral strain of confined concrete

(ε_{lu}). Figure 4.4 and Table 4.3 provide more detailed results that clearly show the influence

of the number of strips in Groups 1 to 4 on the strengthening ratio ($f_{cc}^{'}/f_c^{'}$), strain ratio

(ε_{ccu} / $\varepsilon_c^{'}$), and ductility factor (μ). As the number of strips is increased, the

aforementioned ratios also increase.

4.5.2 Unconfined concrete compressive strength, $f_c^{'}$

The influence of $f_c^{'}$ is studied by comparing Group 1 (Figures 4.3a and 4.4a, and

Table 4.3) and Group 2 (Figures 4.3b and 4.4b, and Table 4.3). Figures 4.3a and 4.4a

show the increase in ultimate confined concrete compressive stress ($f_{cc}^{'}$) and the reduction

in the ultimate confined axial strain (ε_{ccu}) as the unconfined concrete compressive strength

$f_c^{'}$ is increased. All nine columns in Group 1 have strengthening ratios ($f_{cc}^{'}/f_c^{'}$), strain

ratios ($\varepsilon_{ccu}/\varepsilon_c^{'}$), ductility factors ($\mu$), and efficiency factors, β (Eq. 4.3), larger than the

one for the corresponding columns in Group 2 (Figures 4.3b and 4.4b, and Table 4.3).

For column S1 (Figures 4.2), the concrete stress-strain (f_c-ε_c) relationship is presented in

Figure 4.5a for Groups 1 to 4 (Table 4.2) to show the influence of the different parameters.

The influence of increasing the unconfined compressive strength from 20.8 MPa (3ksi) in

85

Groups 1, 3, and 4 to 55.16 MPa (8 ksi) in Group 2 has a pronounced effect on the confined

concrete compressive strength $f_{cc}{}'$. Similar behavior is observed for remaining columns

(S2 to FW in Figure 4.2). In order to graphically evaluate the influence of the other

parameters (ρ_{st} and ρ_{sl}) on $f_{cc}{}'$, the results for Group 2 are removed from Figure 4.5b for

column S1, Figure 4.6a for column S4, and Figure 4.6b for the FW column.
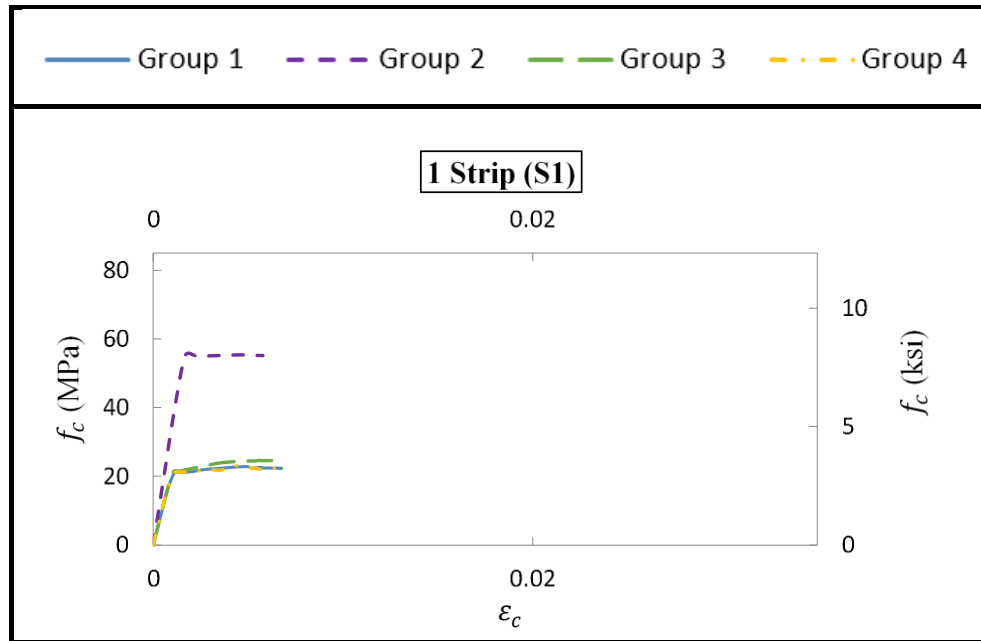
(a)
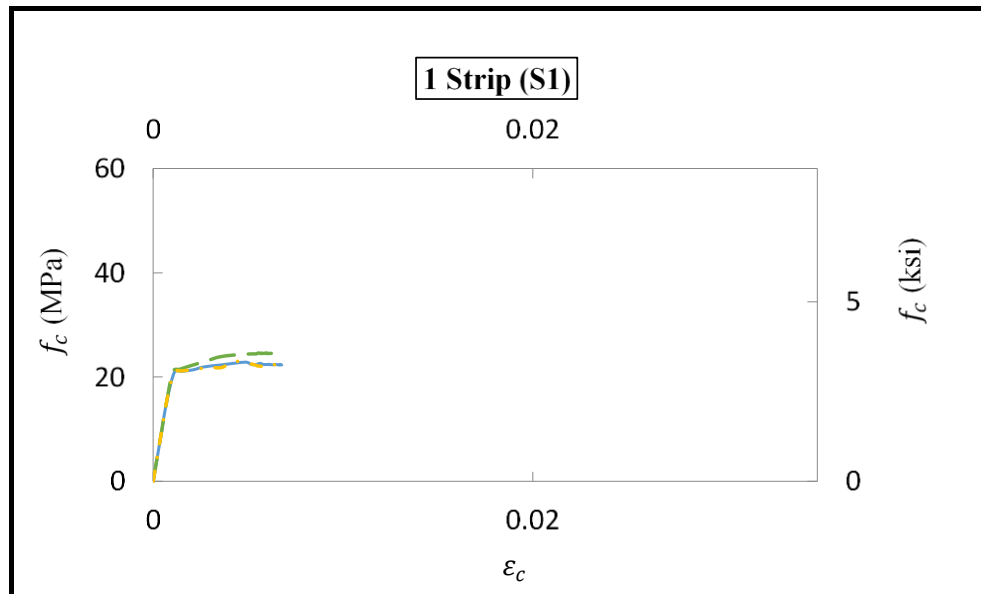
(b)

Figure 4.5 – Comparison of compressive stress (f_c) vs axial strain (ε_c)
for the column with 1-Strip (S1 in Figure 4.2) for: (a) Groups 1
to 4, and (b) for Groups 1, 3 and 4 (Table 4.2)
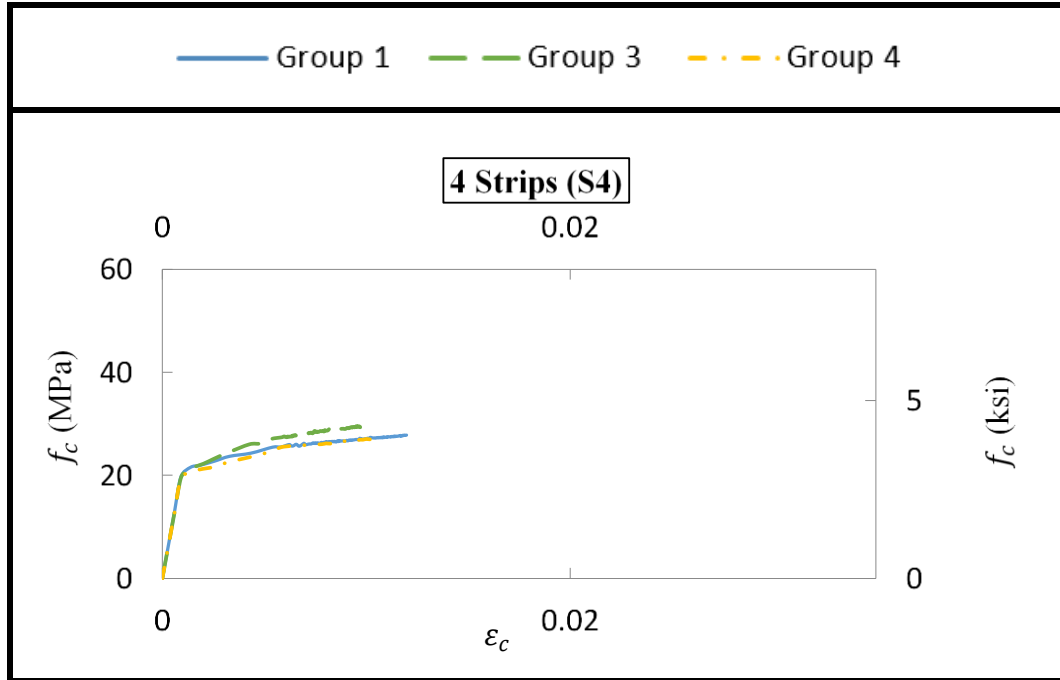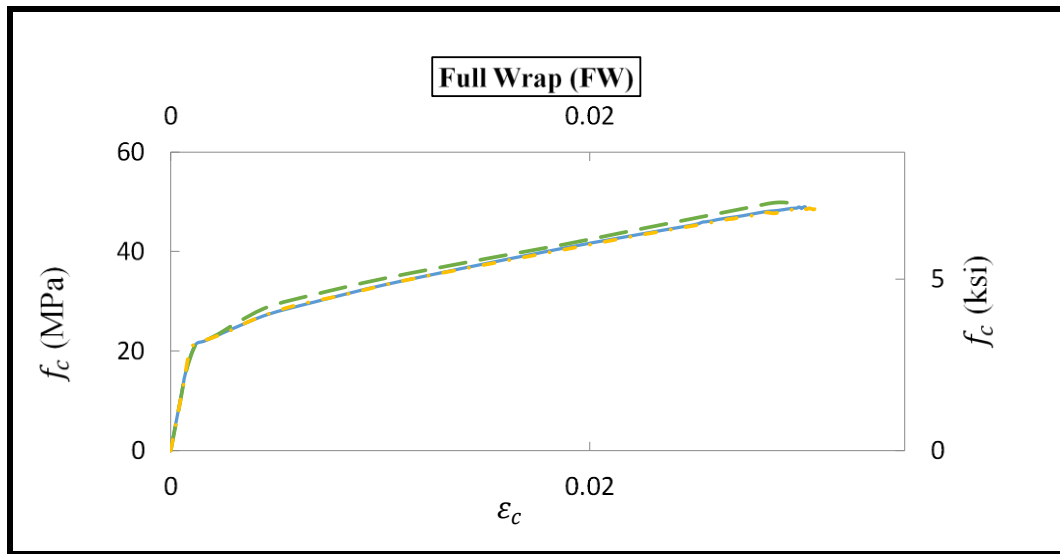
Figure 4.6 – Comparison of compressive stress (f_c) vs axial strain (ε_c) for Groups 1, 3 and 4 (Table 4.2) for: (a) column with 4 Strips (S4 in Figure 4.2), and (b) for column with Full Wrap (FW in Figure 4.2)

88

4.5.3 Transverse steel reinforcement ratio, ρ_{st}

The influence of ρ_{st} is studied by comparing the columns in Group 1 (Figure 4.3a and Table 4.3), with $\rho_{st} = 0.004$, and Group 3 (Figure 4.3c and Table 4.3) with $\rho_{st} = 0.0064$. Except for columns S5 and S6, the columns in Group 1 have a lower ultimate confined concrete compressive stress $f_{cc}^{'}$. For columns S5 and S6 in Group 3, there is an overlap between the FRP and transverse steel leading to a decrease in the volume of confined concrete, and in turn to a lower $f_{cc}^{'}$. The columns in Group 1 also have a higher ultimate confined concrete axial strain, ε_{ccu}, compared to the ones in Group 3 (Table 4.3). The ductility factor, μ, and the efficiency factors, β in Eq. 4.3, are reduced by increasing ρ_{st} (Table 4.3 and Figure 4.4). The influence of increasing ρ_{st} on $f_{cc}^{'}$ can be seen in Figure 4.5b for the column with one strip (S1), in Figure 4.6a for the column with four strips (S4), and in Figure 4.6b for the fully wrapped column. As the number of strips or the lateral FRP confinement (ρ_f) increases, the influence of the transverse steel confinement (ρ_{st}) decreases as can be seen from the post linear behavior when the f_c-ε_c curve for Group 1 ($\rho_{st} = 0.004$) approaches that of Group 3 ($\rho_{st} = 0.0064$).

4.5.4 Longitudinal steel reinforcement ratio, ρ_{sl}

The effect of ρ_{sl} is studied by comparing the columns in Group 1 ($\rho_{sl} = 0.011$) and Group 4 ($\rho_{sl} = 0.027$) in Figures 4.4a and 4.4d, Table 4.3, and Figures 4.5 and 4.6. At ultimate conditions, the columns in Group 1 have a slightly lower ultimate confined concrete compressive stress and higher ultimate axial concrete strain (Table 4.3). The

89

www.manaraa.com

efficiency factors, β (Eq. 4.3), for Group 1 are slightly larger than the ones for Group 4 (Figures 4.4a and 4.4d). In general, the change in the strengthening ratios ($f_{cc}{}'/f_c{}'$), strain ratios ($\varepsilon_{ccu} / \varepsilon'_c$), and ductility factors (μ), due to the increase in the longitudinal steel reinforcement ratio has a little influence on concrete confinement for the columns under consideration (Figures 4.4a and 4.4d, Figures 4.5b, 4.6a, and 4.6b). Figures 4.5 and 4.6 clearly show that the f_c-ε_c plots for Groups 1 and 4 are difficult to separate. Consequently, the contribution of the longitudinal steel is neglected in the derivation of the confined concrete stress-strain model in the following sections.

4.5.5   Strip Arrangement

The effect of the number of strips on the behavior of confined columns is evaluated in Figure 4.7 for two FRP volumetric ratios, ρ_f = 0.003 and ρ_f = 0.006 (Eq. 4.1). One unwrapped (ρ_f = 0.0) and one fully wrapped column, and three columns wrapped with 1, 3, and 6 strips are compared in Figure 4.7. All columns have the same cross section and material properties as the columns in Group 1 (Table 4.2).

Figure 4.7 clearly shows that, for the same volume of CFRP material bonded to the column, the fully wrapped is more effective in increasing the ultimate compressive stress and strain, and thus, ductility. The effectiveness is more pronounced when the CFRP volumetric ratio is increased to 0.006 in Figure 4.7b. The increase in the number of strips, from 1 to 6, leads to an increase in the ultimate compressive stress and strain, and ductility. Although the fully wrapped column is more effective, in certain instances, a specific number of strips could satisfy the design requirements. This may be of interest when

90

retrofitting columns that are not easily accessible (e.g. over a waterway) where the placement of strips maybe more economical than placing a full wrap.

$f_c{}' = 20.68$ MPa (3 ksi)	$f_y = 413.68$ MPa (60ksi)	$f_{fu} = 2848$ MPa (413 ksi)	$E_f = 139$ GPa (20160 ksi)
— ·· Unwrapped (UW)	– – – 1 Strip (S1)	— · — · 3 Strips (S3)	
- - - - - 6Strips (S6)	■ Full Wrap (FW)		

(a)

(b)

Figure 4.7 – Comparison of compressive stress (f_c) vs axial strain (ε_c) relationships for the unwrapped column and columns having the same CFRP volumetric ratio, ρ_f: (a) $\rho_f = 0.003$, and (b) $\rho_f = 0.006$

91

4.6   Current FRP Confined Concrete Stress-Strain Models

A number of models are available in the literature for the confined concrete stress-strain relationships (Popovics 1973, Richard and Abbott 1975, and Mander et al. 1988). The following three models for FRP confined concrete columns are highlighted and are used for comparison with the proposed model presented in the following sections.

Lam and Teng's stress–strain model (2003) has an initial parabolic portion and a linear portion (Table 4.4a and Figure 4.8a). The model accounts for FRP confinement only and ignores the contribution of the transverse steel confinement.

Pellegrino and Modena 2010 proposed an analytical model (Table 4.4b and Figure 4.8b) based on Richard and Abbott's model (1975) that accounts for steel reinforcement contribution to confinement in circular and rectangular columns. The partial wraps are accounted for by modifying the discontinuity coefficient used for transverse steel in Mander's model. The total lateral confining pressure, f_l, is derived by combining that of the transverse steel and FRP.

Lee et al. (2010) introduced an empirical model for concrete confined with both steel spirals and FRP wraps (Table 4.4c and Figure 4.8c). The model accounts for yielding of transverse steel and its contribution to the confining pressure.

92

Table 4.4a – Stress-strain relationship for FRP confined concrete, Lam and Teng 2003

Model	Stress- Strain Relationship
Lam and Teng (2003) **Model Considerations:** - Full Wrap **Model does not account for:** - Partial Wrap - Longitudinal Steel - Transverse Steel - Yielding of Transverse Steel	$-for\ 0 \le \varepsilon_c \le \varepsilon_t\ ,\ f_c = E_c\,\varepsilon_c - \dfrac{(E_c - E_2)^2}{4f_c'}\,\varepsilon_c^{\,2}$ $-for\ \varepsilon_t \le \varepsilon_c\ ,\ f_c = f_c' + E_2\,\varepsilon_c$ $\varepsilon_t = \dfrac{2f_c'}{E_c - E_2}$ $E_2 = \dfrac{f_{cc}' - f_c'}{\varepsilon_{ccu}}$ $f_{cc}' = f_c'\left(1 + 3.3\dfrac{f_l}{f_c'}\right)$ $\varepsilon_c'\left[1.75 + 12\left(\dfrac{f_l}{f_c'}\right)\left(\dfrac{0.586.\varepsilon_{fu}}{\varepsilon_c'}\right)^{0.45}\right]$

93

Table 4.4b – Stress-strain relationship for FRP confined concrete, Pellegrino and Modena (2010)

Model	Stress- Strain Relationship
Pellegrino and Modena (2010) **Model Considerations:** - Full Wrap - Partial Wrap - Longitudinal Steel - Transverse Steel [a] **Model does not account for:** - Yielding of Transverse Steel	$- for\ 0 \leq \varepsilon_c \leq \varepsilon_{ccu}\ ,\ f_c = \dfrac{(E_c - E_1)\varepsilon_c}{\left[1 + \left(\dfrac{(E_c - E_1)\varepsilon_c}{f_0} \right)^n \right]^{1/n}} + E_1 \varepsilon_c$ $n = 1 + \dfrac{1}{(E_c \varepsilon_c' / f_c') - 1}$ $f_0 = f_{cc}' - E_1 \varepsilon_{ccu}$ $E_1 = \dfrac{f_{cc}' - f_c'}{\varepsilon_{ccu} - \varepsilon_c'}$ $f_{cc}' = f_c' \left[1 + A \left(\dfrac{f_l}{f_c'} \right)^{-\alpha} \left(\dfrac{f_l}{f_c'} \right) \right]$ $\varepsilon_{ccu} = \varepsilon_c' \left[2 + B \left(\dfrac{f_l}{f_c'} \right) \right]$ A, B and α are coefficients defined in Tables 3, 4, and 5 in Pellegrino and Modena (2010)

[a] The lateral confining pressures of transverse steel and FRP are combined

94

Table 4.4c – Stress-strain relationship for FRP confined concrete, Lee et. al. 2010

Model	Stress- Strain Relationship
Lee et. al. 2010 **Model Considerations:** - Full Wrap - Transverse Steel - Yielding of Transverse Steel **Model does not account for:** - Partial Wrap - Longitudinal Steel	$-for \quad 0 \le \varepsilon_c \le \varepsilon_c' \;,\; f_c = E_c \varepsilon_c + (f_c' - E_c \varepsilon_c')\left(\dfrac{\varepsilon_c}{\varepsilon_c'}\right)^2$ $-for \quad \varepsilon_c' \le \varepsilon_c \le \varepsilon_{c,s} \;,\; f_c = f_c' + (f_{c,s} - f_c')\left(\dfrac{\varepsilon_c - \varepsilon_c'}{\varepsilon_{c,s} - \varepsilon_c'}\right)^{0.7}$ $-for \quad \varepsilon_{c,s} \le \varepsilon_c \le \varepsilon_{ccu} \;,\; f_c = f_{c,s} + (f_{cc}' - f_{c,s})\left(\dfrac{\varepsilon_c - \varepsilon_{c,s}}{\varepsilon_{ccu} - \varepsilon_{c,s}}\right)^{0.7}$ $\left.\begin{array}{c} \varepsilon_{c,s} = \varepsilon_{ccu}\left[0.85 + 0.03\left(\dfrac{f_{l,f,max}}{f_{l,s,max}}\right)\right] \\ f_{c,s} = 0.95 f_{cc}' \end{array}\right\} \quad f_{l,f,max} \ge f_{l,s,max}$ $\left.\begin{array}{c} \varepsilon_{c,s} = 0.7\varepsilon_{ccu} \\ f_{c,s} = \left(\dfrac{\varepsilon_{c,s}}{\varepsilon_{ccu}}\right)^{0.4} f_{cc}' \end{array}\right\} \quad f_{l,f,max} < f_{l,s,max}$ $k_s = \begin{cases} 2 - \dfrac{f_{l,f,max}}{f_{l,s,max}} & for\, f_{l,f,max} \le f_{l,s,max} \\ 1 & for\, f_{l,f,max} > f_{l,s,max} \end{cases}$ $f_{cc}' = f_c'\left(1 + 2\dfrac{f_l}{f_c'}\right)$ $\varepsilon_{ccu} = \varepsilon_c'\left[1.75 + 5.25\left(\dfrac{f_{l,f,max} + k_s f_{l,s,max}}{f_c'}\right)\left(\dfrac{\varepsilon_{fu}}{\varepsilon_c'}\right)^{0.45}\right]$

95
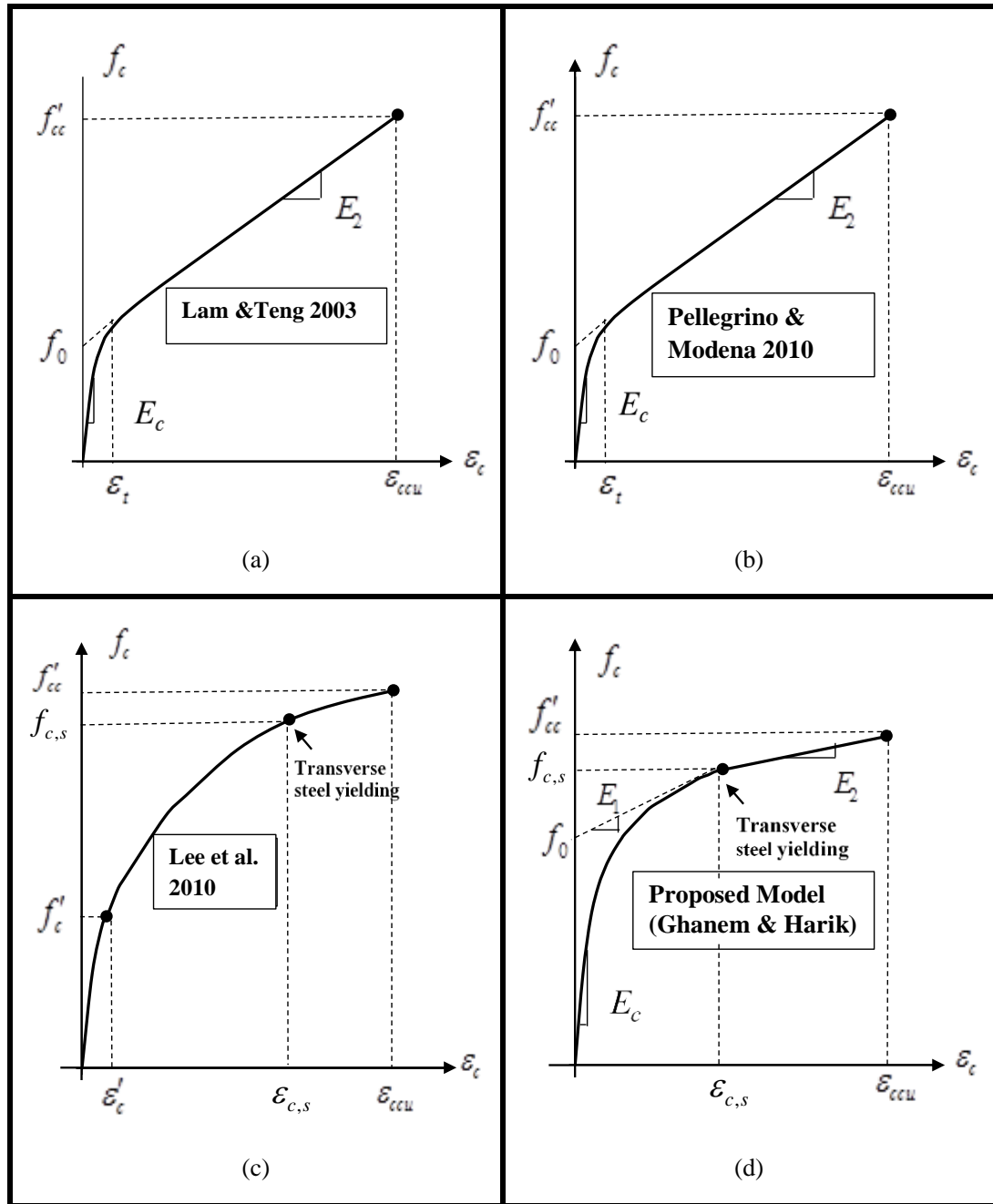
Figure 4.8 – Confined concrete stress-strain models

4.7   Proposed Confined $f_c - \varepsilon_c$ Model

Richard and Abbott's model (Richard and Abbott 1975), which was adopted and modified by others for concrete columns confined by FRP (Samaan et al. 1998, Wu et al. 2009, Pellegrino and Modena 2010) is also adopted herein and modified based on the aforementioned parametric study. Since the contribution of longitudinal steel is minimal (Figures 4.5 and 4.6), it is not considered in the model generation.

The proposed $f_c - \varepsilon_c$ model comprises a nonlinear portion for the strain range of $0 \leq \varepsilon_c \leq \varepsilon_{c,s}$ and a linear portion for $\varepsilon_{c,s} < \varepsilon_c \leq \varepsilon_{ccu}$ (Figure 4.8d). $\varepsilon_{c,s}$ is the confined concrete axial strain at yielding of the transverse steel and ε_{ccu} is the ultimate confined concrete axial strain. The $f_c - \varepsilon_c$ relationship is expressed as follows:

$$f_c = \frac{(E_c - E_1)\varepsilon_c}{\left[1 + \left(\dfrac{(E_c - E_1)\varepsilon_c}{f_0}\right)^n\right]^{1/n}} + E_1 \varepsilon_c^m \qquad\qquad 0 \leq \varepsilon_c \leq \varepsilon_{c,s} \qquad\qquad (4.4)$$

$$f_c = f_{c,s} + E_2(\varepsilon_c - \varepsilon_{c,s}) \qquad\qquad \varepsilon_{c,s} \leq \varepsilon_c \leq \varepsilon_{ccu} \qquad\qquad (4.5)$$

Where f_c and ε_c are the concrete compressive stress and axial strain of FRP-confined concrete, respectively; f_0 is the reference plastic stress at the intercept of the slope at yielding of transverse steel with the stress axis (Figure 4.8d); n is a shape parameter in the transition zone and is expressed as

$$n = 1 + \frac{1}{(E_c \varepsilon_c' / f_c') - 1} \qquad\qquad (4.6)$$

E_c is the concrete modulus of elasticity and, for normal-weight concrete (ACI 2011)

$$E_c = 4700\sqrt{f_c'} \ \ (\text{MPa}) \qquad\qquad (4.7)$$

97

E_1 is the slope of the stress strain curve at the yielding of transverse steel

$$E_1 = \frac{f_{c,s} - f_0}{\varepsilon_{c,s}}$$ (4.8)

Where $f_{c,s}$ and $\varepsilon_{c,s}$ are the compressive stress and strain in confined concrete at yielding of

transverse steel

E_2 is the slope of the stress strain curve after yielding of transverse steel, and is expressed

as

$$E_2 = \frac{f'_{cc} - f_{c,s}}{\varepsilon_{ccu} - \varepsilon_{c,s}}$$ (4.9)

In Eq. (4.4), m can be determined by setting the $f_c(\varepsilon_{c,s}) = f_{c,s}$ at the point of yielding of

transverse steel

$$m = \left[\frac{1}{\ln(\varepsilon_{c,s})}\right]\left\{\ln\left[\frac{1}{E_1}\left(f_{c,s} - \frac{(E_c - E_1)\varepsilon_{c,s}}{\left\{1 + \left[\frac{(E_c - E_1)\varepsilon_{c,s}}{f_0}\right]^n\right\}^{1/n}}\right)\right]\right\}$$ (4.10)

From the parametric study, the average value of the normalized plastic stress intercept $f_0/$

f'_c is 0.97 with a standard deviation 0.038. Consequently, f_0 is replaced by f'_c.

4.7.1 Ultimate confined concrete stress and strain, f_{cc}' and ε_{ccu}

The ultimate confined concrete stress and strain are dependent on the unconfined

compressive concrete strength (f'_c), the maximum lateral confining pressure due to FRP

only ($f_{l,f,max}$), the maximum lateral confining pressure due to transverse steel only ($f_{l,s,}$

$_{max}$) and the ratio between the length of FRP wrap ($N_f\, w_f$) and the unbraced length of the column (l_u). Based on the regression analysis conducted on the data generated in the parametric study, the ultimate confined concrete stress $f_{cc}{}'$ and strain ε_{ccu} can be presented as follows

$$f'_{cc} = f'_c\left[1 + 1.55\left(\frac{f_{l,f,\max}}{f'_c}\right)\left(\frac{N_f w_f}{l_u}\right)^{0.3} + 1.55\left(\frac{f_{l,s,\max}}{f'_c}\right)\right]$$

(4.11)

$$\varepsilon_{ccu} = \varepsilon'_c\left[2.4 + 15\left(\frac{f_{l,f,\max}}{f'_c}\right)\left(\frac{N_f w_f}{l_u}\right)^{0.3} + 7.7\left(\frac{f_{l,s,\max}}{f'_c}\right)\right]$$

(4.12)

$$f_{l,f,\max} = \frac{2t_f E_f \varepsilon_{fu} n_f w_f N_f}{D l_u}$$

(4.13)

$$f_{l,s,\max} = \frac{2A_{st} f_y}{s d_s}$$

(4.14)

where f_y is the specified yield strength of non-prestressed steel reinforcement; A_{st} is the area of transverse steel; d_s is the concrete core diameter to center line of transverse steel; S is the center to center spacing between transverse steel; ε_{fu} is the design rupture strain of FRP wrap.

4.7.2   Concrete stress and strain at yielding of transverse steel, $f_{c,s}$ and $\varepsilon_{c,s}$

The point defined by $f_{c,s}$ and strain $\varepsilon_{c,s}$ (Figure 4.8d) is the transition between the nonlinear and linear stress-strain relationships. The increase in the compressive strength of concrete confined by the two materials can be derived by summing the increments of the

99

compressive strength for each material (Lee et al. 2010). Consequently, $f_{c,s}$ and $\varepsilon_{c,s}$ can be determined by summing the strength of concrete due to FRP confinement and strength of concrete due transverse steel at yielding of the transverse steel. Considering that the transverse steel yield occurred at a lateral strain $\varepsilon_{l,y}$, then

$$\varepsilon_{l,y} = \frac{f_y}{E_s} \tag{4.15}$$

where $\varepsilon_{l,\,y}$ is the confined concrete lateral strain at yielding of transverse steel and E_s is modulus of elasticity of the transverse steel. The strain in the confined concrete at yielding of the transverse steel may now be determined using the relationship introduced by Teng et al 2007 for the lateral strain-axial strain relationship of FRP confined concrete

$$\varepsilon_{c,s} = 0.85\varepsilon_c' \left[1 + 8 \frac{(f_{l,fy} + f_{l,s,\max}')}{f_c'} \right] \cdot \left\{ \left[1 + 0.75 \left(\frac{\varepsilon_{l,y}}{\varepsilon_c'} \right) \right]^{0.7} - \exp\left[-7 \left(\frac{\varepsilon_{l,y}}{\varepsilon_c'} \right) \right] \right\} \tag{4.16}$$

where $f_{l,fy}$ is the lateral confining pressure exerted by FRP at yielding of transverse steel

$$f_{l,fy} = \frac{2t_f E_f \varepsilon_{l,y} w_f n_f N_f}{D l_u} \tag{4.17}$$

$$f_{l,s,\max}' = f_{l,s,\max} \frac{\left(1 - \frac{s'}{2d_s} \right)^2}{1 - (A_{sl}/A_{core})} \tag{4.18}$$

where s' is the clear spacing between the transverse steel (stirrups), and A_{core} is the column core area.

   The concrete core is confined by transverse steel and FRP while the concrete cover is confined by FRP only, therefore

100

$$f_{c,s} = \frac{f_{core}A_{core} + f_{cover}A_{cover}}{A_g} \tag{4.19}$$

$$f_{core} = f_{c,sy} + f_{c,fy} - f_c' \tag{4.20}$$

$$f_{cover} = f_{c,fy} \tag{4.21}$$

$$A_{cover} = A_g - A_{core} \tag{4.22}$$

where A_{core} is the column cover area; f_{core} and f_{cover} are the compressive stresses of confined concrete for the column core and cover, respectively; $f_{c,\,fy}$ is the component of confined concrete compressive stress at yielding of transverse steel due to FRP confinement only; $f_{c,sy}$ is the component of the confined concrete compressive stress at yielding of transverse steel due to transverse steel confinement only.

Mander's model (Mander et al.1988) is used to calculate stress of confined concrete due to transverse steel

$$f_{c,sy} = \frac{f_{cc,s}'(\varepsilon_{c,s} / \varepsilon_{ccu,s})r_s}{r_s - 1 + (\varepsilon_{c,s} / \varepsilon_{ccu,s})^{r_s}} \tag{4.23}$$

in which r_s is a constant to account for the brittleness of concrete and is determined by (Mander et al.1988)

$$r_s = \frac{E_c}{E_c - f_{cc,s}' / \varepsilon_{ccu,s}} \tag{4.24}$$

where $f'_{cc,s}$ and $\varepsilon_{ccu,s}$ are the peak compressive stress and strain, respectively, of confined concrete under the transverse steel confining pressure at yielding of transverse steel and can be calculated using the following equations (Mander et al.1988)

101

$$f'_{cc,s} = f'_c \left(2.254 \sqrt{1 + 7.94 \frac{f'_{l,s,max}}{f'_c}} - 2\frac{f'_{l,s,max}}{f'_c} - 1.254 \right) \tag{4.25}$$

$$\varepsilon_{ccu,s} = \varepsilon'_c \left[1 + 5\left(\frac{f'_{cc,s}}{f'_c} \right) \right] \tag{4.26}$$

The confined concrete stress due to FRP, $f_{c,fy}$, can be expressed as follows

$$f_{c,fy} = \frac{f'_{cc,f}(\varepsilon_{c,s} / \varepsilon_{ccu,f})r_f}{r_f - 1 + (\varepsilon_{c,s} / \varepsilon_{ccu,f})^{r_f}} \tag{4.27}$$

in which, r_f is a constant that accounts for the brittleness of concrete and can be calculated as (Mander et al.1988)

$$r_f = \frac{E_c}{E_c - f'_{cc,f} / \varepsilon_{ccu,f}} \tag{4.28}$$

Where $f'_{cc,f}$ and $\varepsilon_{ccu,f}$ are the peak compressive stress and strain, respectively, of FRP confined concrete at yielding of transverse steel. They can be determined using the following equations (Teng et al 2007)

$$f'_{cc,f} = f'_c \left(1 + 3.5 \frac{f_{l,fy}}{f'_c} \right) \tag{4.29}$$

$$\varepsilon_{ccu,f} = \varepsilon'_c \left[1 + 17.5\left(\frac{f_{l,fy}}{f'_c} \right) \right] \tag{4.30}$$

A summary of the proposed confined concrete stress-strain model is presented in Figure 4.9 and Table 4.4d .

102

Given: A_{core}, A_g, A_{st}, A_{sl}, D, d_s, E_f, f_c', f_y, l_u, n_f, N_f, s, t_f, w_f, ε_{fu}

A_{cover}	Eq. (4.22)
E_c	Eq. (4.7)
$f_{l,f,max}$	Eq. (4.13)
$f_{l,s,max}$	Eq. (4.14)
$\varepsilon_{l,y}$	Eq. (4.15)

f_{cc}'	Eq. (4.11)
$f_{l,fy}$	Eq. (4.17)
$f_{l,s,max}'$	Eq. (4.18)
ε_{ccu}	Eq. (4.12)
n	Eq. (4.6)

$f_{cc,f}'$	Eq. (4.29)
$f_{cc,s}'$	Eq. (4.25)
$\varepsilon_{c,s}$	Eq. (4.16)

$\varepsilon_{ccu,f}$	Eq. (4.30)
$\varepsilon_{ccu,s}$	Eq. (4.26)

r_f	Eq. (4.28)
r_s	Eq. (4.24)

$f_{c,fy}$	Eq. (4.27)
$f_{c,sy}$	Eq. (4.23)

$f_{c,s}$	Eq. (4.19)

E_1	Eq. (4.8)
E_2	Eq. (4.9)

m Eq. (4.10)

Check $\varepsilon_c \leq \varepsilon_{c,s}$

Yes

$$f_c = \frac{(E_c - E_1)\varepsilon_c}{\left[1 + \left(\frac{(E_c - E_1)\varepsilon_c}{f_0}\right)^n\right]^{1/n}} + E_1\varepsilon_c \quad \text{Eq. (4.4)}$$

No

$$f_c = f_{c,s} + E_2(\varepsilon_c - \varepsilon_{c,s}) \quad \text{Eq. (4.5)}$$

w_f

s

l_u

D

d_s

A_{core}

$n_f t_f$

Figure 4.9– Summary of the proposed confined concrete stress-strain model

103

www.manaraa.com

Table 4.4d – Stress-strain relationship for FRP confined concrete, Proposed Model

Model	Stress- Strain Relationship
Proposed Model **(Ghanem and Harik)** **Model Considerations:** - Full Wrap - Partial Wrap - Transverse Steel [a] - Yielding of Transverse Steel **Model does not account for:** - Longitudinal Steel [b]	$- for \; , \; 0 \le \varepsilon_c \le \varepsilon_{c,s} \; , \; f_c = \dfrac{(E_c - E_1)\varepsilon_c}{\left[1 + \left(\dfrac{(E_c - E_1)\varepsilon_c}{f_0}\right)^n\right]^{1/n}} + E_1 \varepsilon_c^m$ $- for \; \varepsilon_{c,s} \le \varepsilon_c \le \varepsilon_{ccu} \; , \; f_c = f_{c,s} + E_2(\varepsilon_c - \varepsilon_{c,s})$ $E_1 = \dfrac{f_{c,s} - f_0}{\varepsilon_{c,s}} ; \quad E_2 = \dfrac{f_{cc}' - f_{c,s}}{\varepsilon_{ccu} - \varepsilon_{c,s}} ; \; n = 1 + \dfrac{1}{(E_c \varepsilon_c' / f_c') - 1}$ $m = \left[\dfrac{1}{\ln(\varepsilon_{c,s})}\right] \left\{ \ln\left[\dfrac{1}{E_1}\left(f_{c,s} - \dfrac{(E_c - E_1)\varepsilon_{c,s}}{\left\{1 + \left[\dfrac{(E_c - E_1)\varepsilon_{c,s}}{f_0}\right]^n\right\}^{1/n}}\right)\right]\right\}$ $f_{c,s} = \dfrac{f_{core} A_{core} + f_{cover} A_{cover}}{A_g}$ $\varepsilon_{c,s} = 0.85\varepsilon_c'\left(1 + 8\dfrac{(f_{l,fy} + f_{l,s,max}')}{f_c'}\right) \cdot \left\{\left[1 + 0.75\left(\dfrac{\varepsilon_{l,y}}{\varepsilon_c'}\right)\right]^{0.7} - \exp\left[-7\left(\dfrac{\varepsilon_{l,y}}{\varepsilon_c'}\right)\right]\right\}$ $f_{cc}' = f_c'\left[1 + 1.55\left(\dfrac{f_{l,f,max}}{f_c'}\right)\left(\dfrac{N_f w_f}{l_u}\right)^{0.3} + 1.55\left(\dfrac{f_{l,s,max}}{f_c'}\right)\right]$ $\varepsilon_{ccu} = \varepsilon_c'\left[2.4 + 15\left(\dfrac{f_{l,f,max}}{f_c'}\right)\left(\dfrac{N_f w_f}{l_u}\right)^{0.3} + 7.7\left(\dfrac{f_{l,s,max}}{f_c'}\right)\right]$

[a] The lateral confining pressures of transverse steel and FRP are treated independently

[b] Refer to the discussion of Figures 4.4a, 4.4d, 4.5, and 4.6 in the text. It concluded that

the increase in the longitudinal steel reinforcement ratio (ρ_{sl}) had little influence on

concrete confinement.

4.8   Comparison of Proposed Model with FE and Experimental Results

A comparison between the proposed confined concrete stress-strain model and the finite element model is presented in Figure 4.10 for RC columns in Group 1 that are partially and fully wrapped with FRP. The comparison shows that, as the stress approaches the ultimate confined compressive concrete stress, the model accurately predict the overall behavior of the columns as well as stress and strain at ultimate. Comparison between the proposed model and FE compressive stress (f_c) vs axial strain (ε_c) for all columns (S1 to FW) in all groups (group 1 to group 4) are in Appendix A.

The proposed model is also compared with experimental results for fully wrapped circular columns in Figure 4.11a (Lee et al. 2010 and Demers and Neale 1999) and for partially wrapped columns (Varma et al. 2009 and Rocca et al. 2006) in Figure 4.12. The detailed calculations of the proposed stress strain relationship of a partially confined circular column W45S6L3F8 (Varma et al. 2009) are in Appendix B.

The results are also compared with ones generated from the three models presented in Tables 4.4a to 4.4c (Lam and Teng 2003, Pellegrino and Modena 2010, and Lee et al. 2010). Except for column U25-2 (Demers and Neale 1999) in Figure 4.11b, the proposed model predicted the stress at ultimate for fully and partially wrapped columns. The other models overestimated the stress at ultimate for all columns.

Figures 4.11 and 4.12 show that the consideration of yielding of transverse steel in the model leads to better prediction of the column behavior beyond that point. Although the model by Pellegrino and Modena 2010 accounts for transverse steel, its influence cannot be separated from that of the FRP strips since the total lateral confining pressure, f_l, combines the transverse steel and FRP pressures as one single equation. In the proposed

105

model, the contribution of the lateral confining pressures for transverse steel and FRP are treated separately.
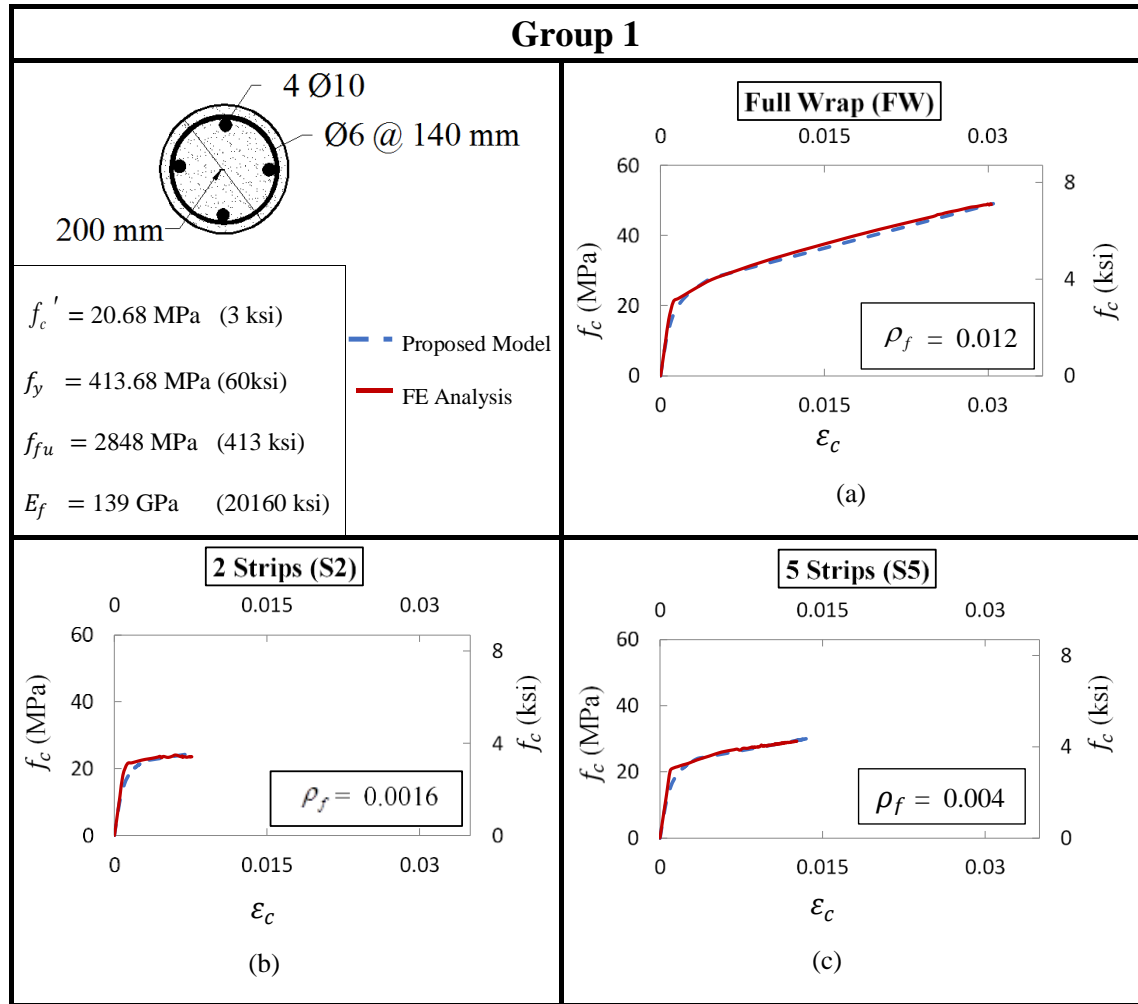
Figure 4.10 – Comparison between the proposed model and FE compressive stress (f_c) vs axial strain (ε_c) for Group 1: (a) fully wrapped (FW in Figure 4.2) column; (b) column with 2 strips (S2 in Figure 4.2); and (c) column with 5 strips (S5 in Figure 4.5)
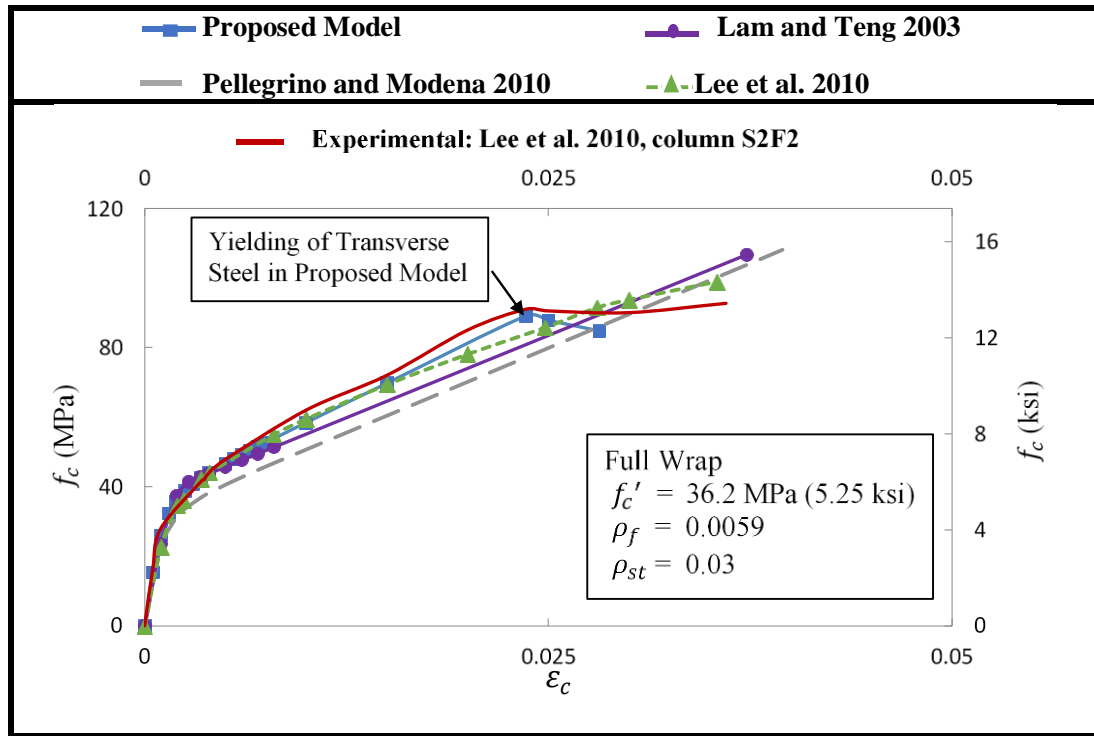
(a)
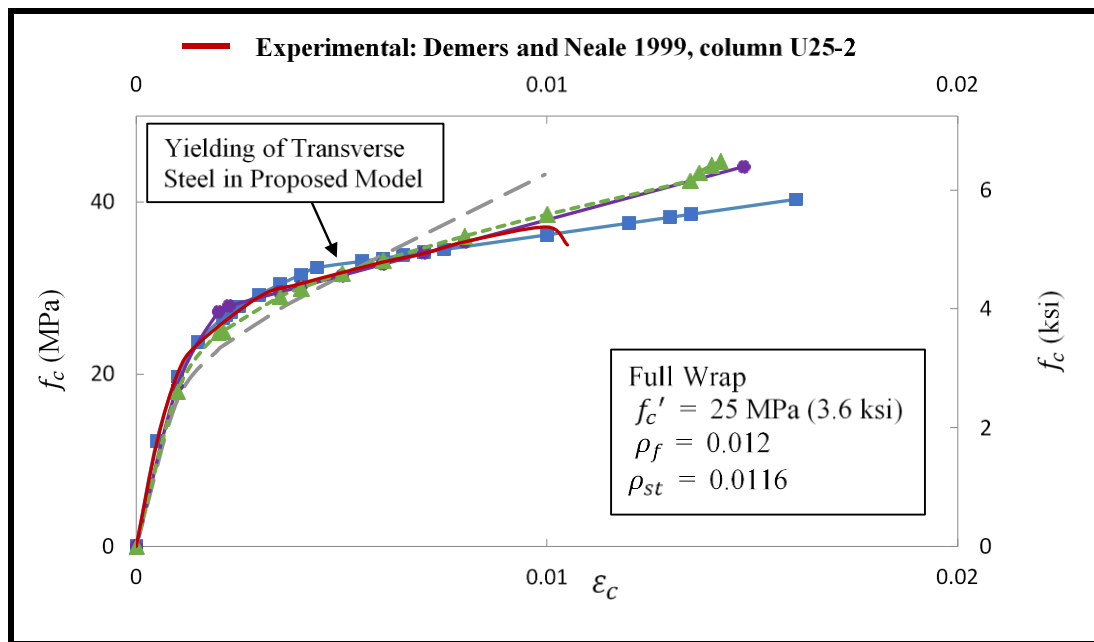
(b)

Figure 4.11 – Comparison between the proposed model and experimental
compressive stress (f_c) vs axial strain (ε_c) for fully wrapped circular
RC columns

107
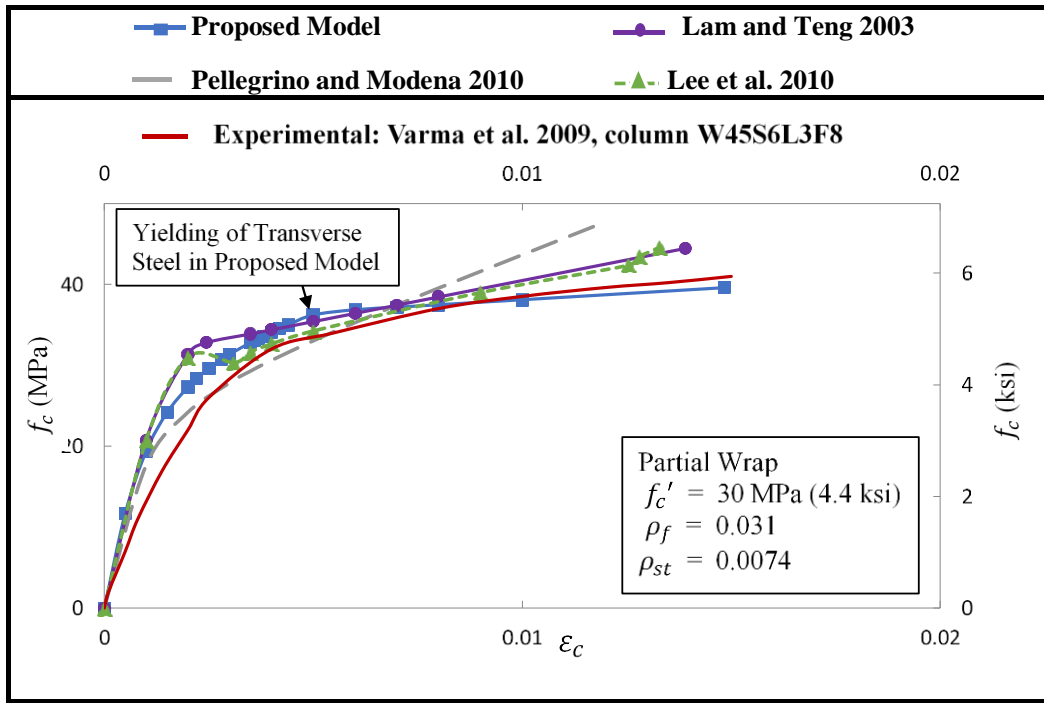
(a)
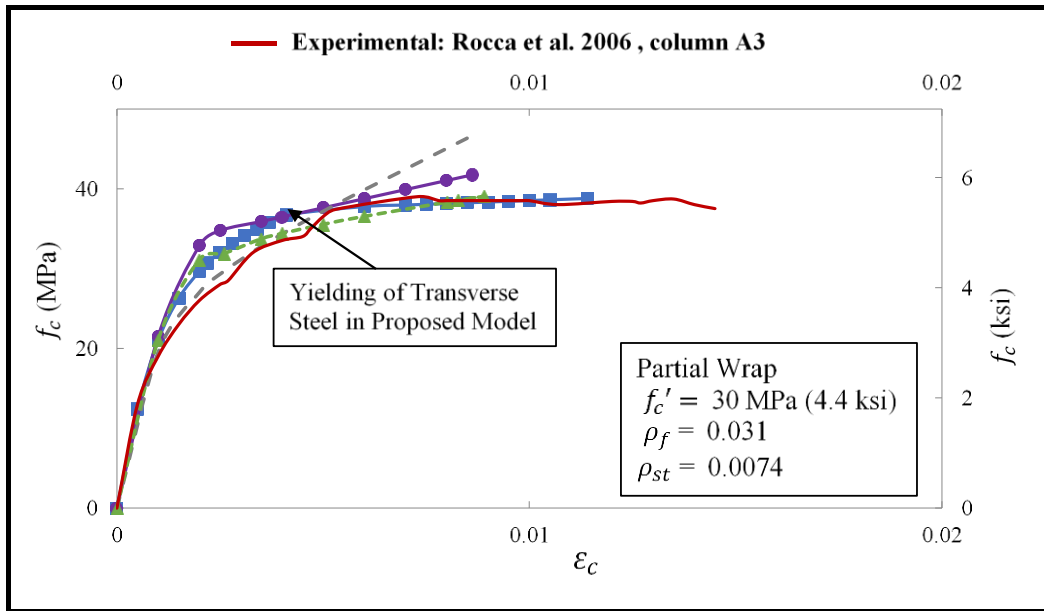
(b)

Figure 4.12 – Comparison between the proposed model and experimental
compressive stress (f_c) vs axial strain (ε_c) for partially wrapped
circular RC columns

4.9   Conclusions

This chapter evaluated the effectiveness of partial wraps (or strips) and proposed an analytical model for describing the compressive behavior of RC columns partially and fully wrapped with FRP. Three dimensional finite element (FE) models were generated to study the influence on the behavior of the concentrically loaded columns of the unconfined compressive strength (f_c'), the number of strips (N_f), the FRP volumetric ratio (ρ_f), the transverse steel reinforcement ratio (ρ_{st}), and the longitudinal steel reinforcement ratio (ρ_{sl}). It should be noted that the columns wrapped with one, two, or three strips are not of practical interest and are used herein to illustrate the influence of partial wrapping as the analysis transitions from an unwrapped column to a partially wrapped column with one to seven strips, to a fully wrapped column.

For the columns evaluated in here, the parametric study indicated the following: (1) The influence of increasing the unconfined compressive strength has a pronounced effect on the increase in the confined concrete compressive strength (f_{cc}'); (2) as the number of identical strips increases (or ρ_f increases), the influence of the transverse steel confinement (ρ_{st}) decreases; (3) the contribution of the longitudinal steel has little influence on the confined concrete stress-strain behavior; and (4) the increase in the number of strips $(N_f = 1$ to 7), while keeping the FRP volumetric ratio (ρ_f) constant, leads to an increase in the ultimate compressive stress and strain, and ductility. This indicates that, for a specific ρ_f, it is more effective to fully wrap the column in order to increase the ultimate confined concrete compressive stress and axial strain.

Based on the parametric study, a new model is proposed for the confined concrete compressive stress and axial strain in partially and fully wrapped columns. The primary

advantage of the model, compared to other models, is its separate account of the yielding of transverse steel which influences the behavior of the stress-strain relationship beyond that point. Compared to experimental data on partially and fully wrapped columns, the proposed model was capable of predicting the stress at ultimate while the other models overestimated its magnitude

CHAPTER 5
ECCENTRICALLY LOADED CONFINED COLUMNS

5.1   Introduction

The current state of art concentrates on FRP confined columns subjected to concentric axial loads. The behavior of FRP confined reinforced concrete columns subjected to eccentric loads are not well understood and the majority of studies concentrated on plain concrete (Wu and Jiang 2014, Parvin and Wang 2001).

Eccentrically loaded FRP confined concrete showed an increase in strength and ductility compared with unconfined concrete (Li and Hadi 2003), and the increase in the stiffness of the FRP wrap would result in an increase in strength and flexural ductility of the column (Li and Hadi 2003, Fitzwilliam and Bisby 2006). The axial load-moment interaction diagrams were developed for FRP wrapped columns eccentrically loaded using layer-by-layer approach.

The confined concrete model developed for concentrically loaded circular RC columns partially confined with FRP, in chapter 4, will be used to develop the axial load-moment (*P-M*) interaction diagrams for eccentrically loaded columns partially wrapped with FRP.

The results are compared with results obtained from finite element models of the FRP confined RC column developed using ANSYS 14 the finite element software.

5.2   Finite Element Model

The Finite Element Model used in chapter 3 is used here, with the same element types and material properties. Due to unsymmetrical load, the full column will be modeled

111

and the load will be applied as a force with different eccentricities. In order to avoid local premature failure at the location of applied load, the top of the column was covered by a rigid plate modeled using the Solid 185 element. Solid 185 element is an 8-node brick element with three translations degrees of freedom at each node in the global X, Y, and Z directions, and is capable of considering nonlinear properties such as multi-linear material model, plasticity, stress stiffening, and large deformations (ANSYS 2012).

The plate has a circular shape with diameter equal to the column diameter, $D = 200$ mm (7.9 in.), and thickness equal to 5 mm (0.2 in.). It is assumed that the plates behaved as a linear elastic material where modulus of elasticity is 200 GPa (29000 ksi) and Poisson ratio of 0.3.

In the model, the Z-axis of the coordinate system coincides with the axis of the circular column. The X and Y axis represent the radial and hoop directions of the circular column respectively. At the bottom of the column, all three degrees of freedom at each node are constrained.

5.3   Finite Element Analysis Results

5.3.1   Columns with different FRP volumetric ratios

Eight columns having the same length of $l_u = 600$ mm (23.62 in.) and a diameter $D = 200$ mm (7.9 in.) are presented (Figure 5.1). One column is fully wrapped and the remaining seven columns are partially wrapped with strips varying from one strip ($N_f = 1$) on column S1 to seven strips on column S7 ($N_f = 7$), as shown in Figure 5.2. Each strip has a width $w_f = 40$ mm (1.6 in.). The full wrap, when $w_f = l_u$ and $N_f = 1$, and each of the strips have four layers of CFRP fabric ($n_f = 4$). The thickness of each layer $t_f = 0.15$ mm

112

(0.0059 in.). All columns have the cross section and material properties of Group 1 in Chapter 3 (Figure 5.2).
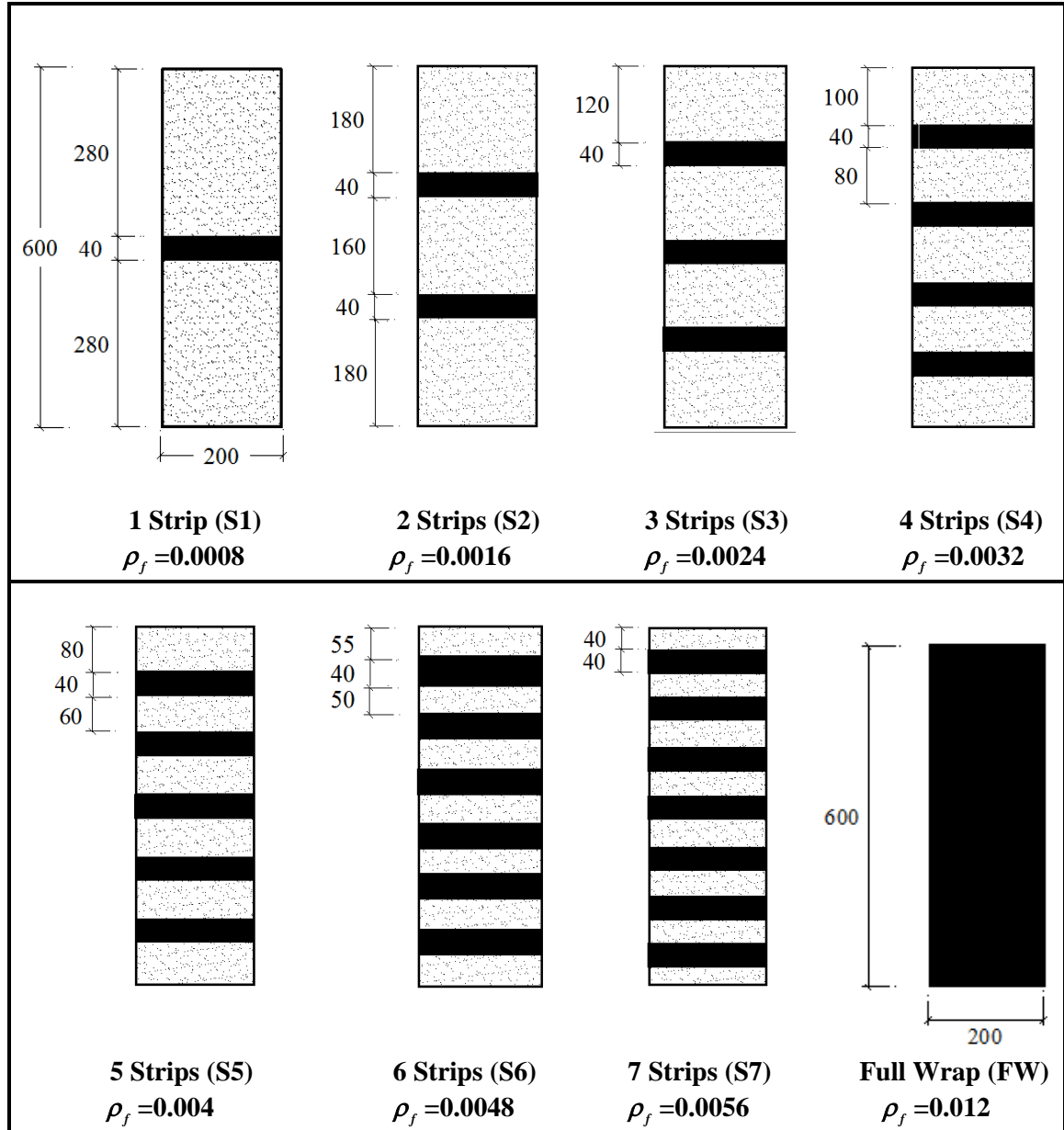
Figure 5.1 – FRP Wraps Layouts (All dimensions are in mm; 1 mm = 0.039 in.)
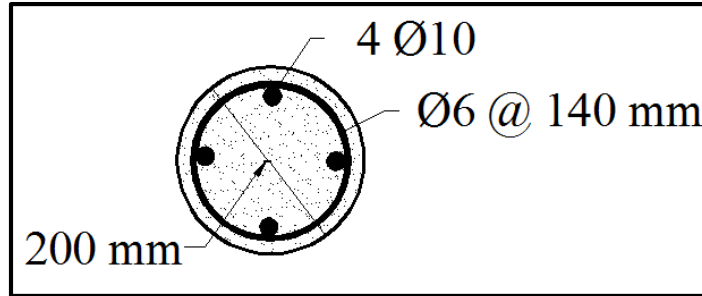
Figure 5.2– Cross sections of tested columns

Axial load -Moment (*P-M*) interaction diagrams are commonly used in the analysis and design of reinforced concrete columns in order to establish a column's ability to withstand a combination of axial load and bending moment.

In the finite element (FE) analysis, the axial load (*P*) is applied at a specific eccentricity (*e*). The magnitude of the axial load is increased until failure. The axial load and moment (*M* = *Pe*) at failure identify a single point on the *P-M* diagram. The process is repeated by specifying a different eccentricity and calculating a *P* and an *M* for another point until an adequate number of points are generated to plot the *P-M* diagram.

Figure 5.4 presents the *P-M* interaction diagrams for columns with different FRP volumetric ratio from $\rho_f = 0$ (unwrapped column) to $\rho_f = 0.012$ (fully wrapped column). As the FRP volumetric ratio (ρ_f) increases, both axial load and flexural capacity increase. Figure 5.3 clearly shows that FRP wraps influence the capacity of the columns. This influence is more pronounced in the compression controlled zone when the axial load (*P*) is larger than that at balance (P_b). At balance conditions ($\varepsilon_c = \varepsilon_{ccu}$ and $e_s = \varepsilon_y$)

114

f'_c = 20.68 MPa (3 ksi)	f_y =413.68 MPa (60ksi)	f_{fu} =2848 MPa (413 ksi)	E_f =139 GPa (20160 ksi)
Unwrapped (ρ_f = 0.0)	1 Strip (ρ_f = 0.08 %)	2 Strips (ρ_f = 0.16 %)	
3 Strips (ρ_f = 0.24 %)	4 Strip (ρ_f = 0.32 %)	5 Strips (ρ_f = 0.4 %)	
6 Strips (ρ_f = 0.48 %)	7 Strips (ρ_f = 0.56 %)	Full Wrap (ρ_f = 1.2 %)	
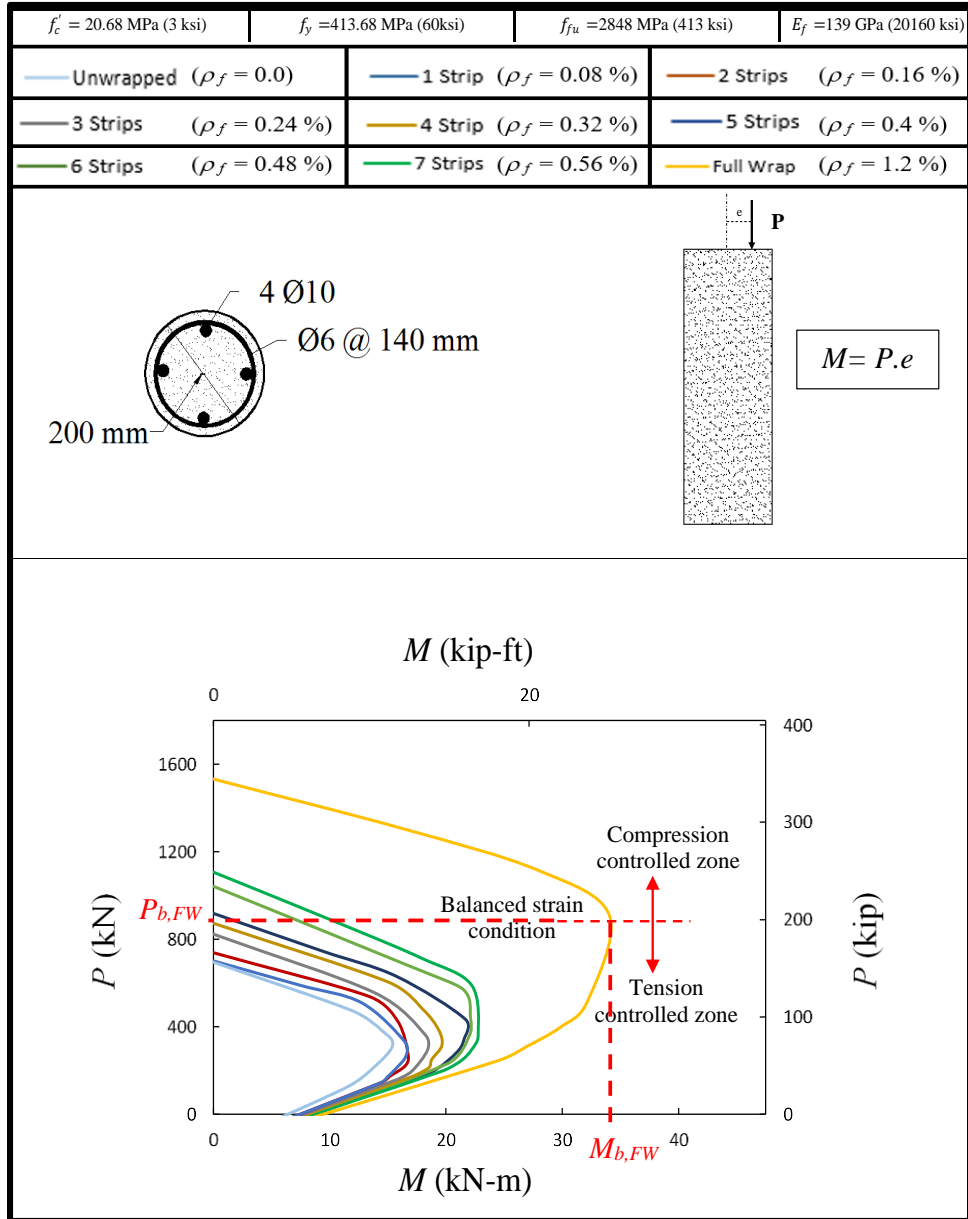
Figure 5.3 – (P-M) interaction diagrams for unwrapped column and columns having different CFRP volumetric ratio (ρ_f) for Group1

5.3.2   Columns with the same FRP volumetric ratio

The effect of the number of strips on the behavior of confined columns under eccentric load is evaluated for two FRP volumetric ratios, $\rho_f = 0.003$ and $\rho_f = 0.006$. A total of four columns are considered, one fully wrapped column and three columns wrapped with 1, 3, and 6 strips (Figure 5.4). All columns have the cross section and material properties of Group 1 in Chapter 3 (Figure 5.2).
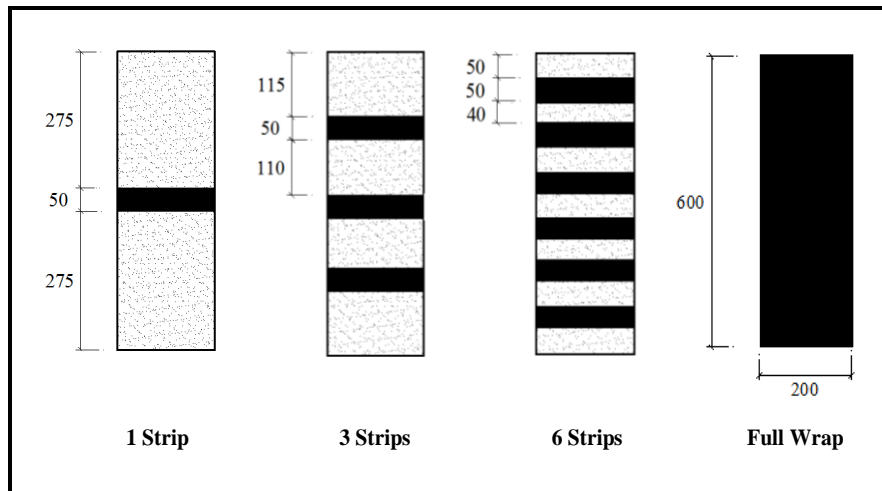
Figure 5.4 – FRP Wraps Layouts to test columns with same FRP reinforcement ratios (ρ_f) (1 *mm* = 0.039 *in*.)

Figure 5.5 shows the (*P-M*) interaction diagrams for columns having the same FRP volumetric ratio (ρ_f), i.e., the same amount of FRP material for the entire column distributed over 1, 3, or 6-strips or over the entire column (full wrap). The unwrapped column ($\rho_f = 0$) along with the fully wrapped columns are used to identify the lower and upper bounds for the column capacity, respectively. Figure 5.5 clearly shows that the optimum use of material is in the fully wrapped columns. The effectiveness of full wrap

116

is more pronounces for the higher FRP volumetric ratio (Figure 5.5b). The influence of the distribution of the FRP material is more pronounced in the compression controlled zone when the axial load (P) is larger than that at balance (P_b). As the axial load magnitude is reduced from $P = P_b$ to $P = 0$ (or the tension controlled zone), the influence of distributing the FRP material on the column capacity becomes negligible.

117
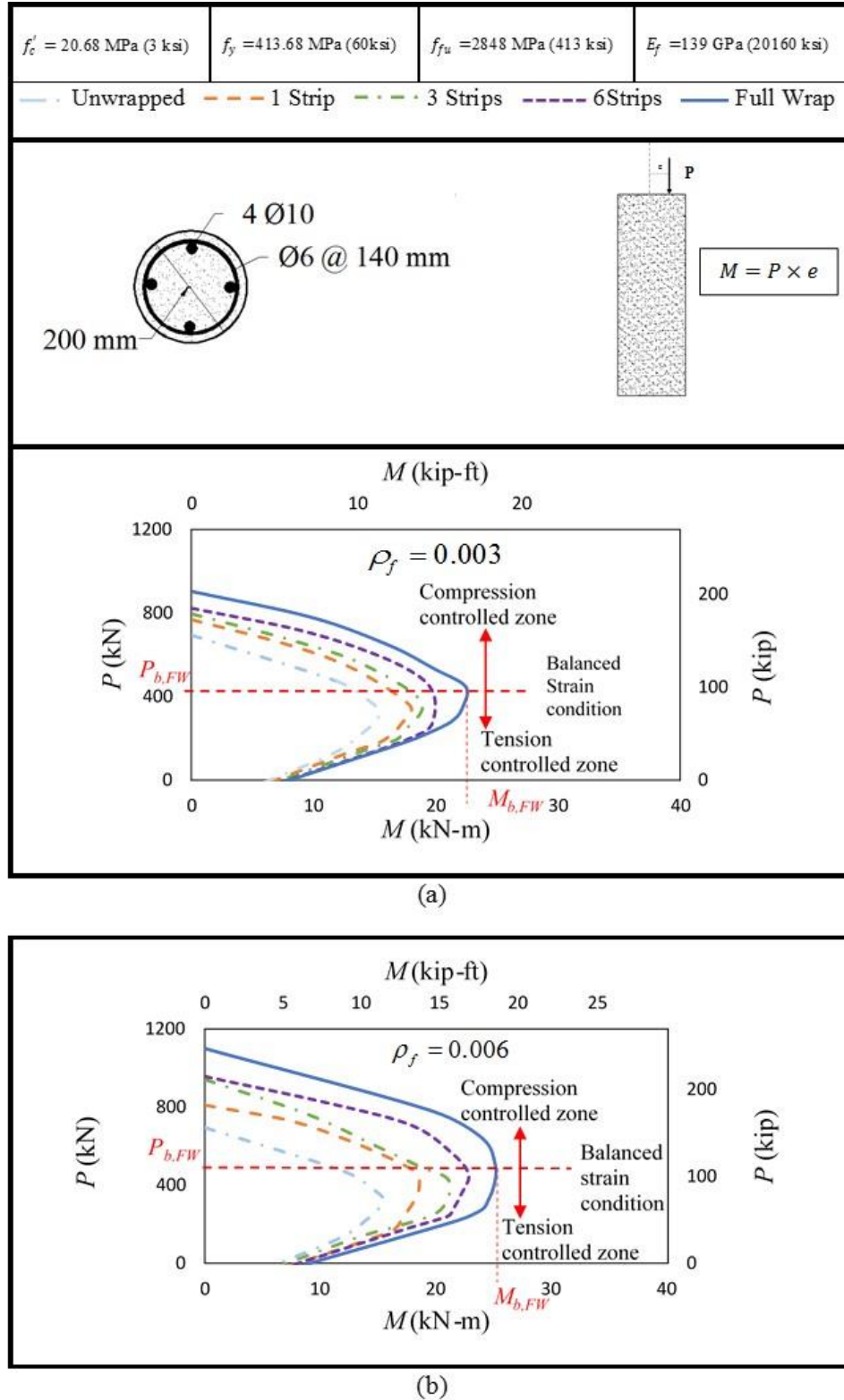
Figure 5.5 – Comparison of (*P-M*) interaction diagrams for the unwrapped column and columns having the same CFRP volumetric ratio, (a) $\rho_f = 0.003$, and (b) $\rho_f = 0.006$

118

5.4   Comparison between the FE Results and the Proposed Model

The model developed in Chapter 4 for concentrically loaded circular RC columns partially confined with FRP, is used to develop the axial load-moment (*P-M*) interaction diagrams for eccentrically loaded columns partially wrapped with FRP. Since the *P-M* diagram is being generated at ultimate conditions, the concrete tensile strength is ignored and plane section before bending are assumed to remain plane after bending. The axial load (*P*) and the bending moment (*M*) are determined by integrating the stress equation over the column area (Figure 5.6).
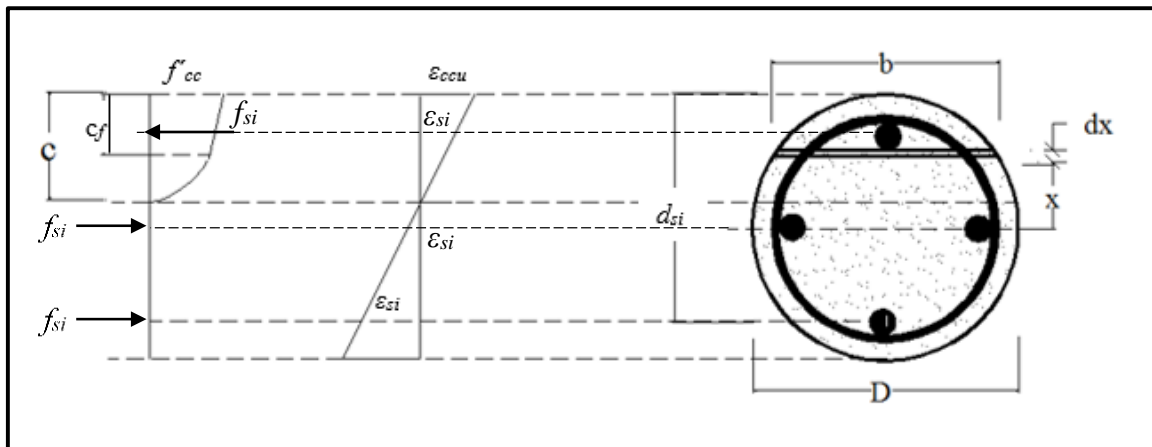
Figure 5.6 –Strains and stresses over column depth at ultimate condition

Since the proposed stress strain ($f_c - \varepsilon_c$) model has a non-linear and a linear portion, the integration will be carried out over two continuous regions: $0 \leq \varepsilon_c \leq \varepsilon_{c,s}$ (prior to yielding of the transverse steel), and $\varepsilon_{c,s} \leq \varepsilon_c \leq \varepsilon_{ccu}$ (following yielding of the transverse steel).   *P* and *M* are derived using the following equations:

119

$$P = \int_{R-c}^{R} (f_c b).dx + \sum_{i=1}^{n_s} (f_{si} - f_c) A_{si} \qquad (5.1 \text{ a})$$

$$P = \int_{R-c}^{R-c+c_f} \left(\frac{(E_c - E_1)(c - R + x)(\varepsilon_{ccu}/c)}{\left\{ 1 + \left[\frac{(E_c - E_1)(c - R + x)(\varepsilon_{ccu}/c)}{f_0} \right]^n \right\}^{1/n}} + E_1 \left[(c - R + x)(\varepsilon_{ccu}/c) \right]^m \right) (2\sqrt{R^2 - x^2}) dx$$

$$+ \int_{R-c+c_f}^{R} \left\{ f_{c,s} + E_2 \left[(c - R + x)(\varepsilon_{ccu}/c) - (\varepsilon_{ccu} c_f / c) \right] \right\} (2\sqrt{R^2 - x^2}) dx + \sum_{i=1}^{n_s} (f_{si} - f_c) A_{si} \qquad (5.1 \text{ b})$$

$$M = \int_{R-c}^{R} (f_c b) x.dx + \sum_{i=1}^{n_s} (f_{si} - f_c)(R - d_{si}) A_{si} \qquad (5.2 \text{ a})$$

$$M = \int_{R-c}^{R-c+c_f} \left(\frac{(E_c - E_1)(c - R + x)(\varepsilon_{ccu}/c)}{\left\{ 1 + \left[\frac{(E_c - E_1)(c - R + x)(\varepsilon_{ccu}/c)}{f_0} \right]^n \right\}^{1/n}} + E_1 \left[(c - R + x)(\varepsilon_{ccu}/c) \right]^m \right) (2\sqrt{R^2 - x^2}) x.dx$$

$$+ \int_{R-c+c_f}^{R} \left\{ f_{c,s} + E_2 \left[(c - R + x)(\varepsilon_{ccu}/c) - (\varepsilon_{ccu} c_f / c) \right] \right\} (2\sqrt{R^2 - x^2}) x dx + \sum_{i=1}^{n_s} (f_{si} - f_c)(R - d_{si}) A_{si} \qquad (5.2 \text{ b})$$

where P is the axial load carried by the section; R is the radius of the column; b is the width of section at distance x from the center of the column cross section; f_{si} is the normal stress of the ''ith'' layer of longitudinal steel reinforcement; n_s is the number of longitudinal bars; A_{si} is the cross-sectional area of the ''ith'' layer of longitudinal steel reinforcement; f_c is the concrete stress in the compression zone; c is the distance from the neutral axis to the extreme compression fiber in the cross-section; c_f is the distance

120

from the center of stirrup (or lateral) steel to the extreme concrete compression fiber in the cross-section; d_{si} is the distance from the position of the ''ith'' layer of longitudinal steel reinforcement to the geometric centroid of the cross-section.

Figures 5.7 and 5.8 compares the finite element results with ones derived using the proposed model (Eqs. 5.1 and 5.2) to generate the *P-M* interaction diagrams for the columns in Group 1 for different FRP volumetric ratios. In Figures 5.9 and 5.10, the columns in Group 1 have the same FRP volumetric ratio ($\rho_f = 0.003$ in Figure 5.9 and $\rho_f = 0.006$ in Figure 5.10). Figures 5.7 to 5.10 show that the results using the proposed model compare very well with ones generated using the FE model of the columns.
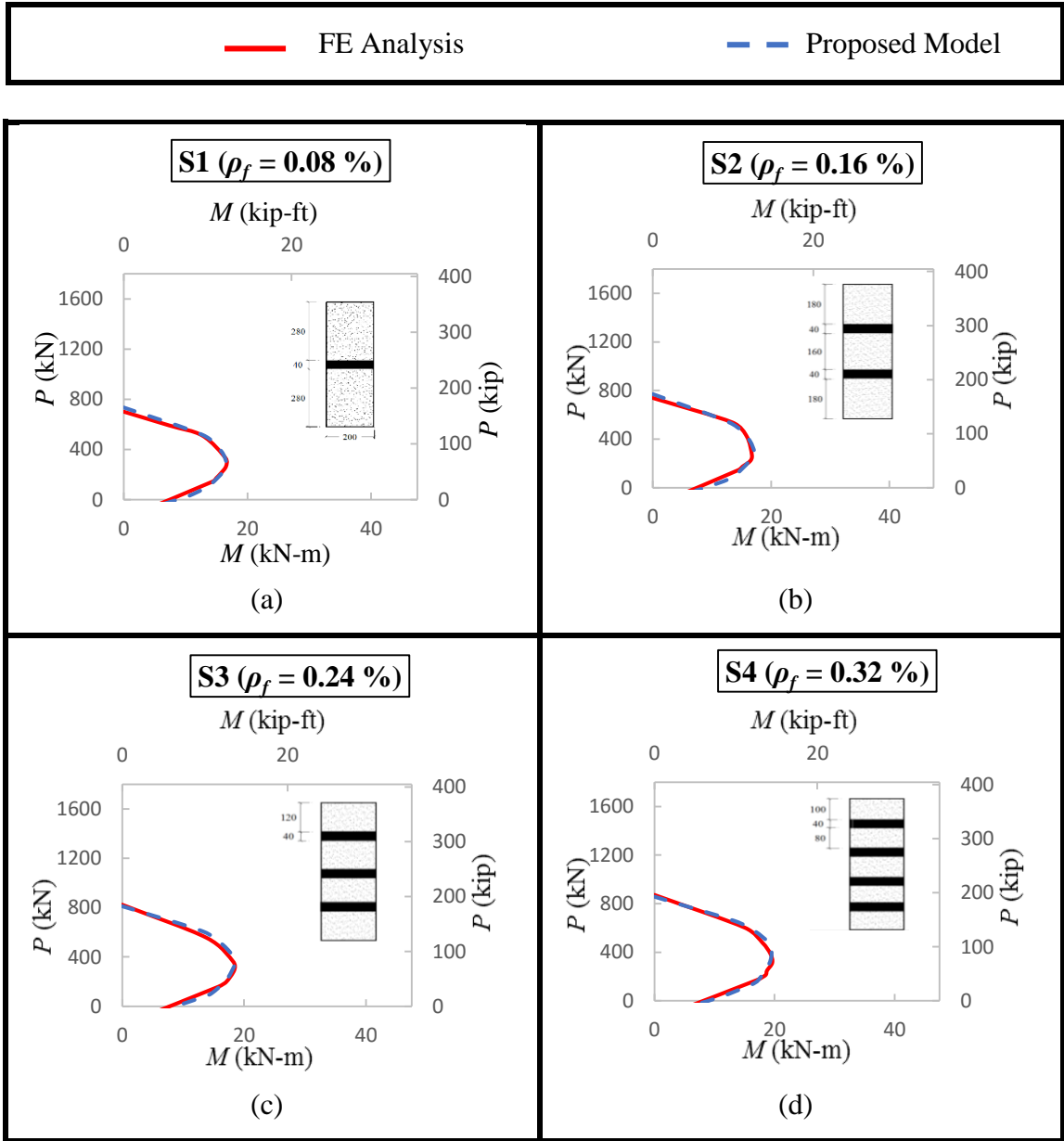
Figure 5.7 – Comparison between the proposed model [Eqs. 5.1 and 5.2] and FE results
for columns in Group 1: (a) S1; (b) S2; and (c) S3; and (d) S4

www.manaraa.com
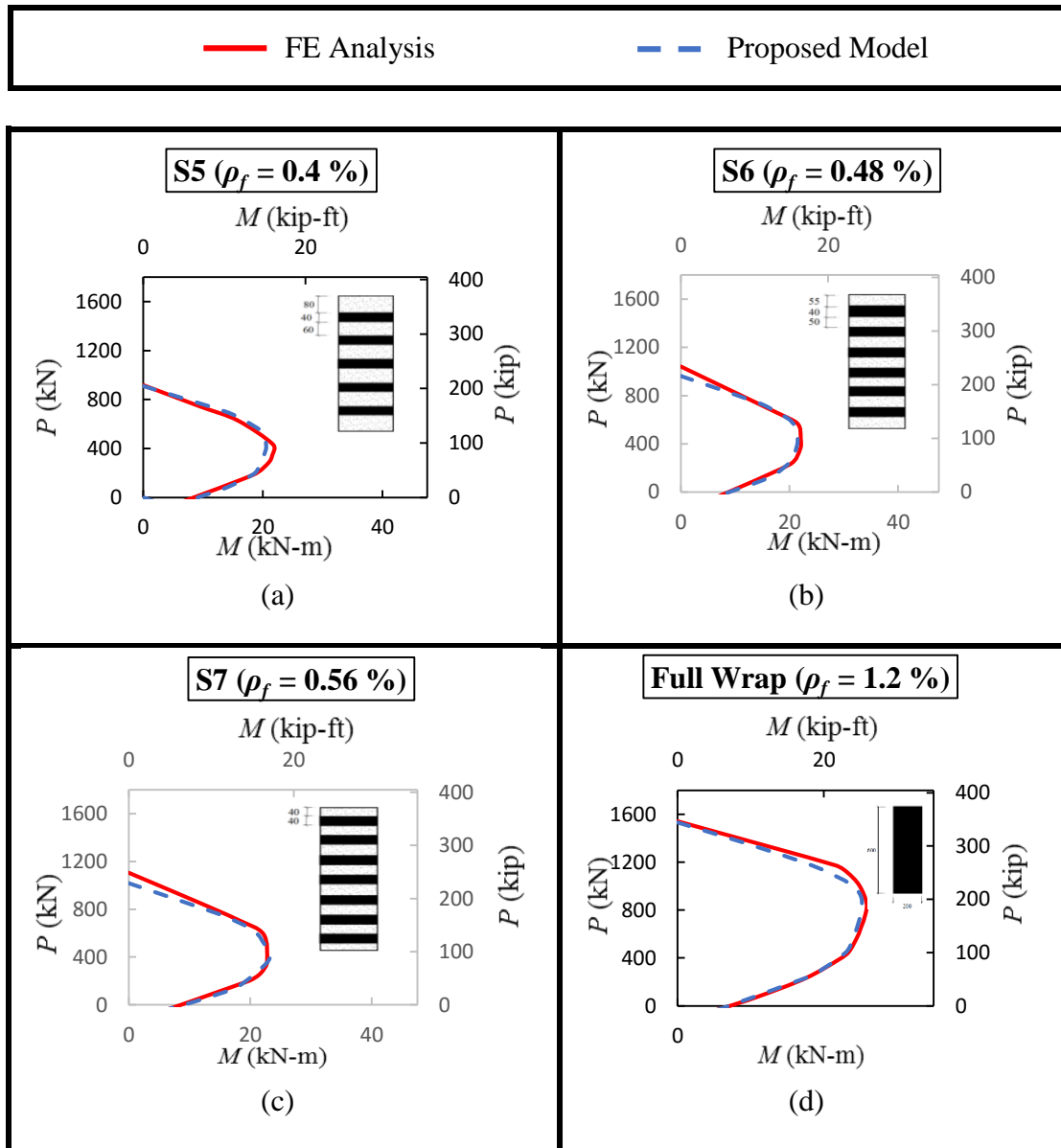
Figure 5.8 – Comparison between the proposed model [Eqs. 5.1 and 5.2] and FE results for columns in Group 1: (a) S5; (b) S6; and (c) S7; and (d) FW
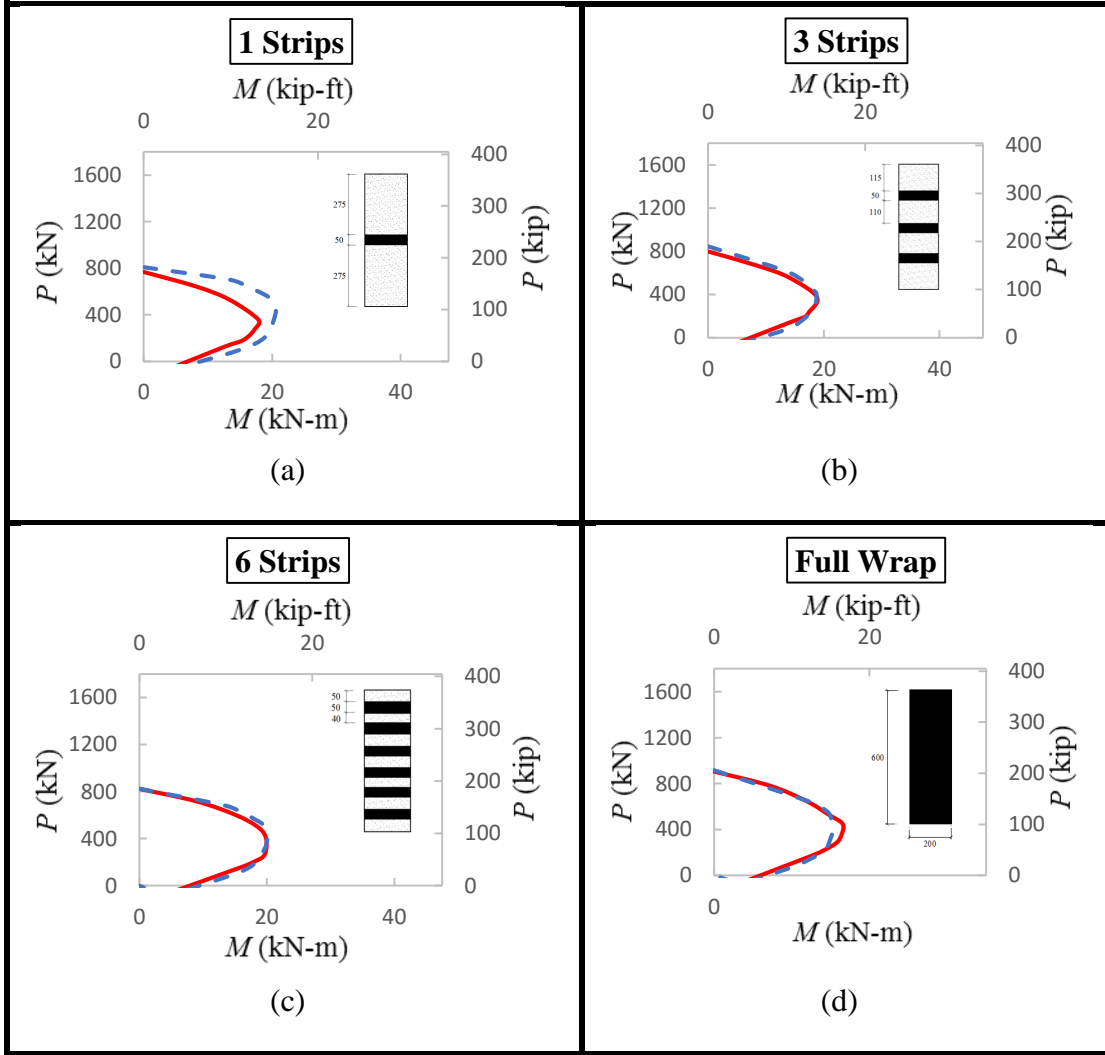
Figure 5.9 – Comparison between the proposed model [Eqs. 5.1 and 5.2] and FE results the same FRP volumetric ratio, $\rho_f = 0.003$ (a) S1 (b) S3 and (c) S6 and (d) FW

$\rho_f = 0.006$

1 Strips

M (kip-ft)

3 Strips

M (kip-ft)

6 Strips

M (kip-ft)

Full Wrap

M (kip-ft)

P (kN) P (kip) M (kN-m)

(a) (b) (c) (d)
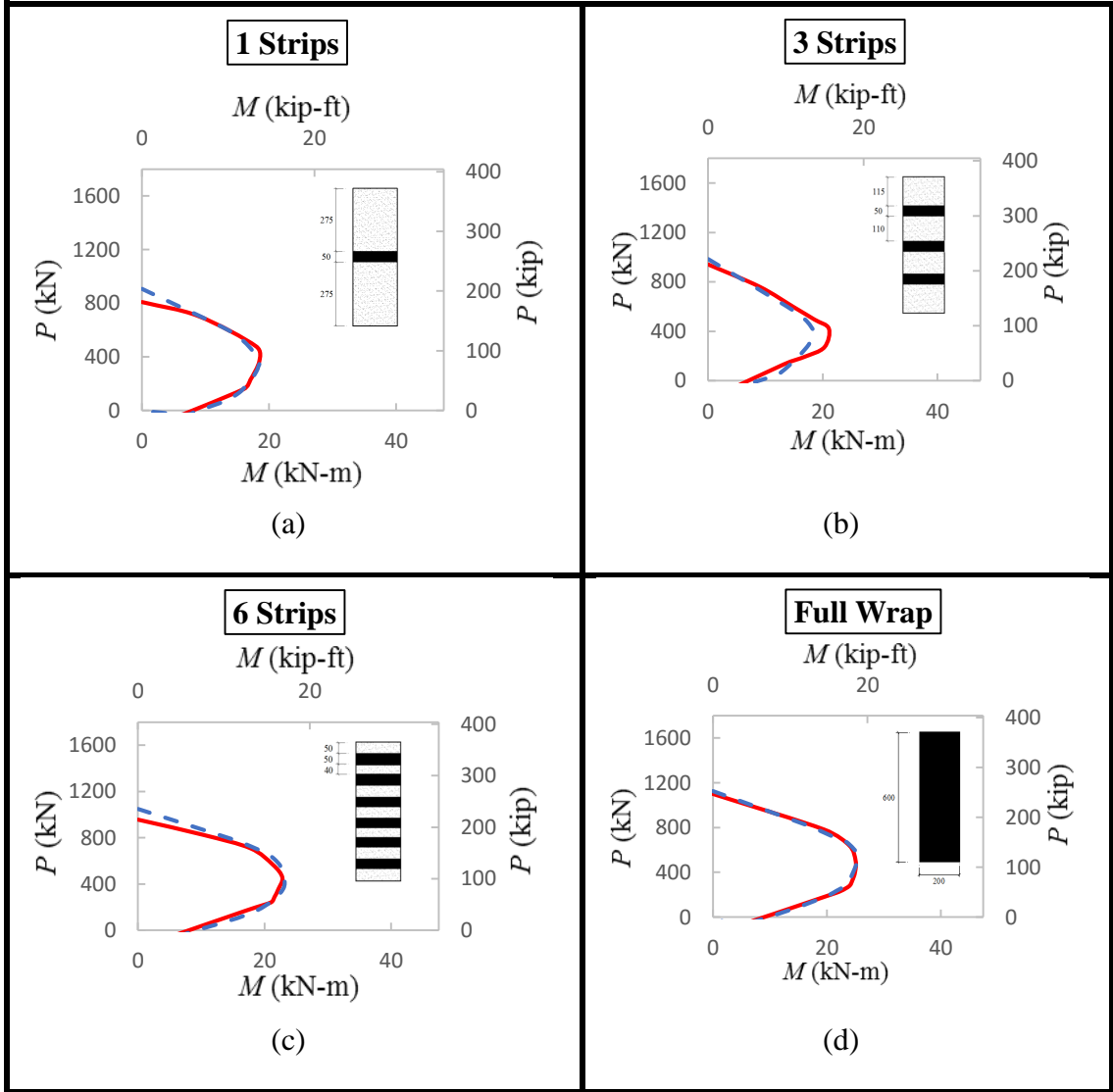
Figure 5.10 – Comparison between the proposed model [Eqs. 5.1 and 5.2] and FE results the same FRP volumetric ratio, $\rho_f = 0.006$ (a) S1 (b) S3 and (c) S6 and (d) FW

5.5 Case Study

5.5.1 Introduction

In order to investigate FRP wrapped RC column under eccentric load, it was deemed beneficial to investigate a retrofitted RC column on an active bridge. The Elrod road bridge that passes over William H. Natcher Pkwy in Warren County in Kentucky is studied herein. One of the columns in an intermediate pier was impacted by a truck. The pier was repaired and wrapped with unidirectional carbon fiber reinforced polymer (CFRP) fabric. The column will be analyzed in this section using the finite element program ANSYS (2012) to determine its capacity, before the impact and after the retrofit in order to determine the effectiveness of the retrofit.

5.5.2 Bridge details

The Elrod road bridge over Natcher Pkwy is a four span bridge and has a reinforced concrete (RC) superstructure and substructure (Figure 5.11). In September 2015, one of the columns in pier to the right of the northbound lanes was impacted by a Semi Trailer (Figure 5.12). The concrete cover spalled at the point of impact, and numerous cracks developed along the length of column and on the pier cap (Figures 5.13 and 5.14). Since cold was approaching, there was concern that deicing agents will seep into the cracks and cause the steel reinforcement to rust and cause premature deterioration of the bridge pier. It was decided to retrofit the bridge in October 2016.

126
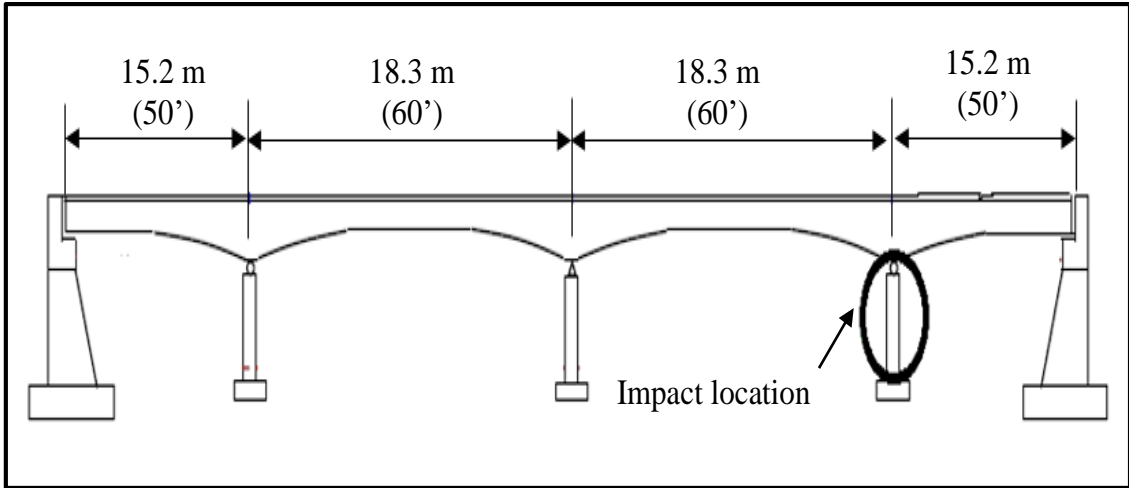
Figure 5.11 – Bridge Layout and Impact Location

Figure 5.12 – Unloaded Semi Trailer that Impacted the Bridge Pier

المنارة للاستشارات

www.manaraa.com

Figure 5.13- Spalling and cracks observed at the point of impact
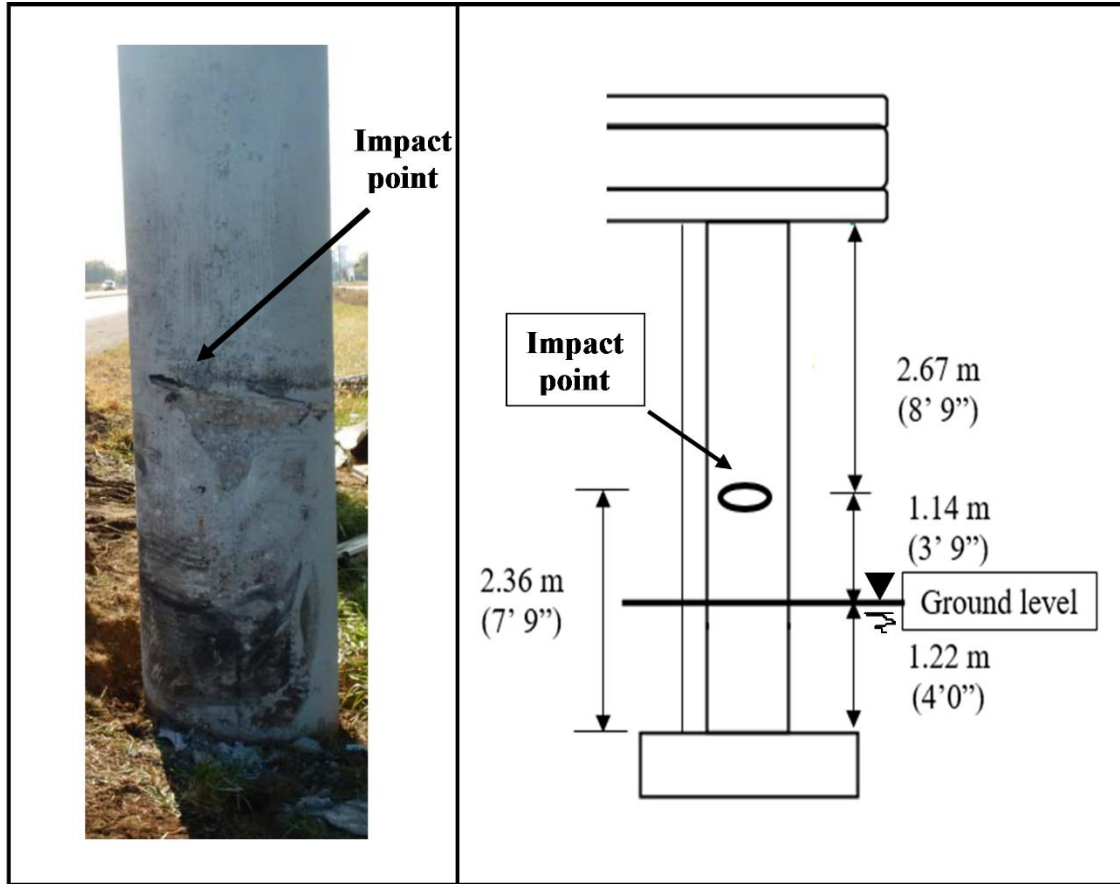
Figure 5.14 – Point of impact on the column

5.5.3 Bridge Repair Plan

After inspecting the column, a repair plan was proposed and it consisted of the following steps:

1. Remove all loose concrete and any coating on the concrete surface by sandblasting or other mechanical means (Figure 5.15)

2. Place repair mortar over the spalled and cleaned area to bring the column to its original shape (Figure 5.16)

3. Use stiff-bristled brush, or spraying equipment, to apply a primer coating to column surface (Figure 5.17)

4. Application of one layer of one Unidirectional Carbon (Figure 5.18)

5. Application of one layer of Triaxial Carbon with fibers oriented at 0^0 and $+/- 60^0$ (Figure 5.19).

6. Application of UV protective coating on retrofit surfaces

Figure 5.15 – Removing loose concrete material

Figure 5.16 – Placement of repair mortar

www.manaraa.com

Figure 5.17 – Application of primer coating on the concrete surface

Figure 5.18 – Application of Unidirectional Carbon Fabric

132

Figure 5.19 –Application of Triaxial Carbon Fabric

5.5.4 Finite element modeling

The column's dimensions, reinforcement, and material properties are taken from the bridge plans and are presented in Figure 5.20 and Table 5.1. The column has an unbraced length l_u = 5030 mm (16' 6") and a diameter D = 762 mm (30 in.), and it is fully wrapped (FW) with one layer of unidirectional carbon fabric (CatStrong UCF 120) and another layer of triaxial Carbon fabric (CatStrong TCF 012).

The FRP material properties are obtained from the manufacturer website (A & P Technology 2014, Bowman 2003) (Table 5.1). In case of unidirectional FRP, the properties are listed in term of ultimate strength (f_{fu}) and tensile modulus of elasticity $\left(E_f\right)$ in the direction of fiber (0°).

www.manaraa.com

The Triaxial FRP Fabric has transverse properties different than the longitudinal properties. Therefore, the properties are listed as ultimate strength ($f_{fu,l}$) and tensile modulus of elasticity $(E_{f,l})$ in longitudinal direction, and ultimate strength ($f_{fu,t}$) and tensile modulus of elasticity $(E_{f,t})$ in the transverse direction.

The FE model details presented in chapter 3 is used herein to model the impacted column. The triaxial CFRP fabric is modeled as a linear orthotropic material where material properties are logged in the longitudinal and transverse directions.

Due to unsymmetrical loading, the entire column is modeled and the load is applied as an axial force, *P*, at a specific eccentricity, *e*. In order to avoid local premature failure at the location of the applied load, a solid plate is introduced at the top of the column using Solid 185 element in ANSYS (2012).
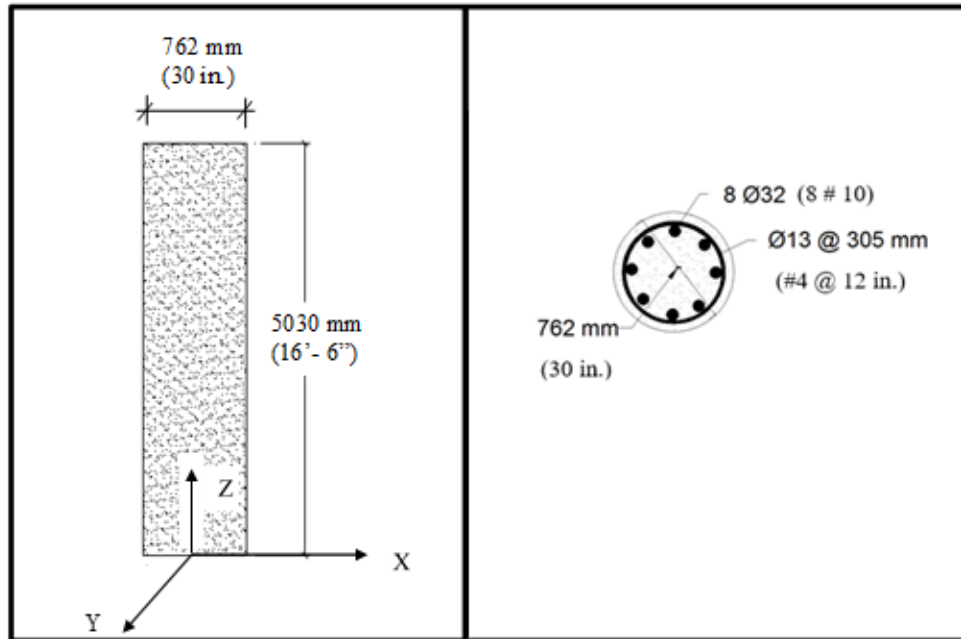
Figure 5.20 – Column dimensions and cross section

Table 5.1: Material properties for the impacted column

Material	Parameter			
Concrete	f'_c		20.68 MPa	3 ksi
	E_c		21.50 GPa	3118 ksi
Steel	f_y		413.68 MPa	60 ksi
	A_s	$\phi\,13$	129 mm^2	0.2 in.^{2}
		$\phi\,32$	819 mm^2	1.27 in.^{2}
Unidirectional CFRP Fabric	t_f		0.76 mm	0.03 in.
	f_{fu}		2848 MPa	413 ksi
	E_f		139 GPa	20160 ksi
Triaxial CFRP Fabric	t_f		0.28 mm	0.011 in.
	$f_{fu,l}$		800 MPa	117 ksi
	$E_{f,l}$		47 GPa	6816 ksi
	$f_{fu,t}$		800 MPa	116 ksi
	$E_{f,t}$		44 GPa	6382 ksi

In the column model, the Z-axis coincides with the axis of the column. The X and Y axes are in the radial and hoop directions of the column, respectively. At the column base, the three degrees of freedom at each of the nodes in each element are restrained. At the top of the column, the nodes are restrained in the X and Z directions.

5.5.5   Column Loading

The loads applied on the column (Figure 5.21) are calculated using the bridge plans to identify the attributed concentric axial load (*P*) and bending moment (*M*). The axial load *P* = 1104 kN (248 kips) and the bending moment *M* = 304.5 kN-m (224.6 kips-ft.).

135
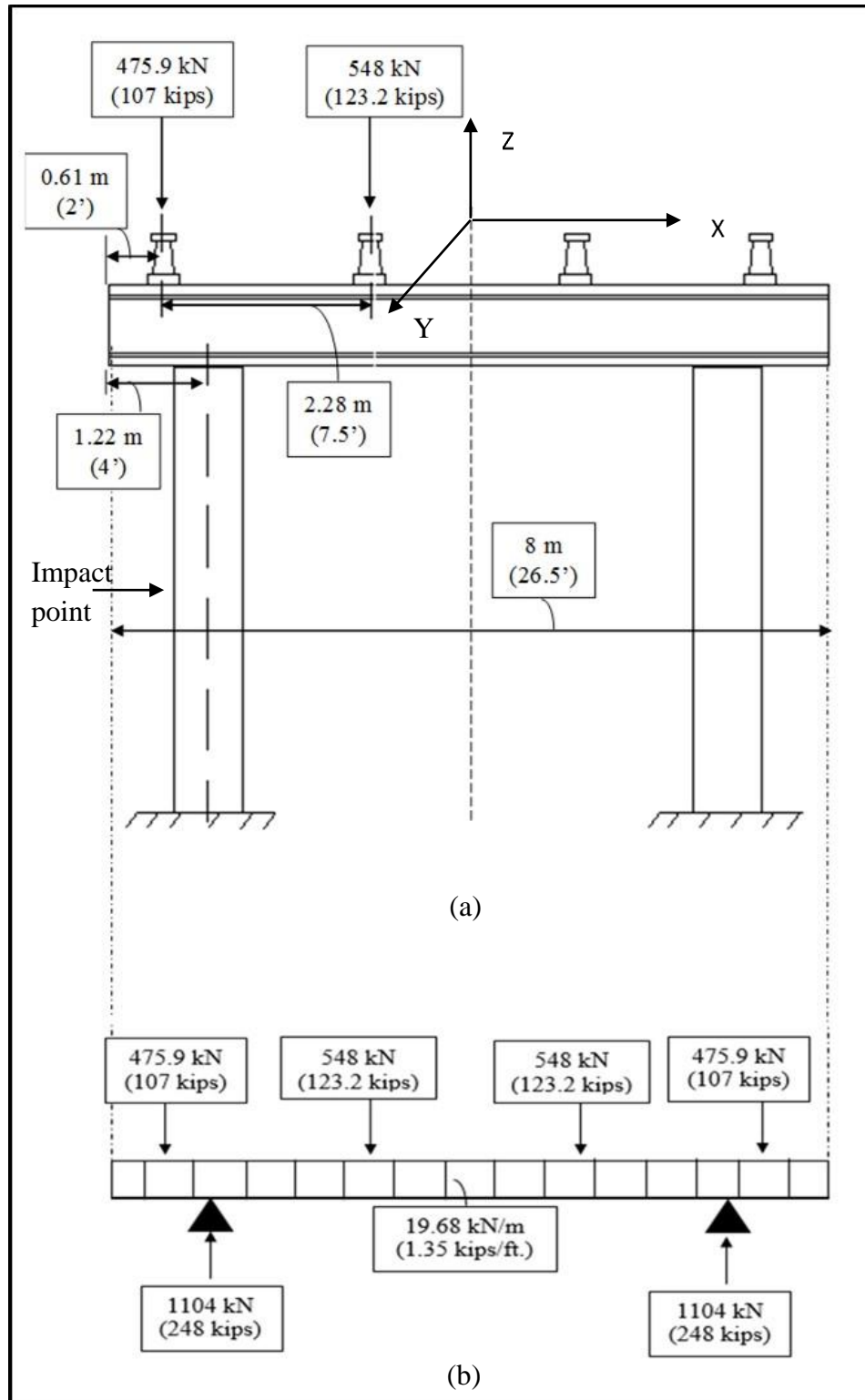
Figure 5.21– (a) Loading on the bridge pier (b) structural model used to determine the loads on the impacted pier

The combination of axial load and bending moment will be replaced with an eccentric load of magnitude P = 1104 kN (248 kips) applied at an eccentricity

$e = \dfrac{M}{P} = 276$ mm (10.86 in.). Figure 5.22 shows the original (i.e., prior to impact) column

model used in the FE analysis.
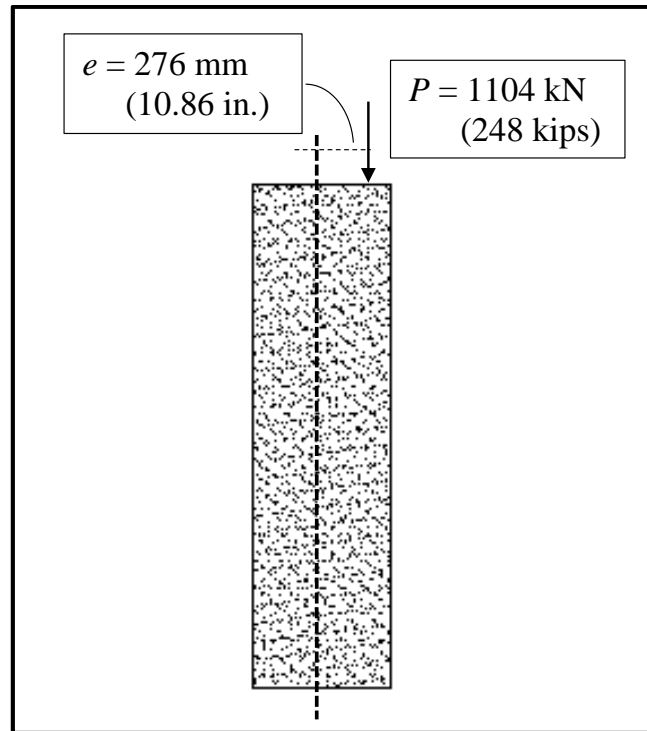
Figure 5.22 – Applied dead load on the column

5.5.6   Results

The capacities of the original, or as constructed, column and the CFRP wrapped column are presented in Figure 5.23. The axial capacity, at an eccentricity e = 276 mm, increased from 2448 kN (505 kips) for the original column (Figure 5.23a) to 8104 kN (1821 kips) for the CFRP wrapped column (Figure 5.23b). That is a 260% increase in axial capacity.

137

Original column (without FRP)	Repaired column (wrapped with CFRP)
$e = 276$ mm (10.86 in.) $P_u = 2058$ kN (462.6 kips)	$e = 276$ mm (10.86 in) $P_u = 8104$ kN (1821 kips) 3810 mm (12'- 6") 5030 mm (16'- 6")
(a)	(b)
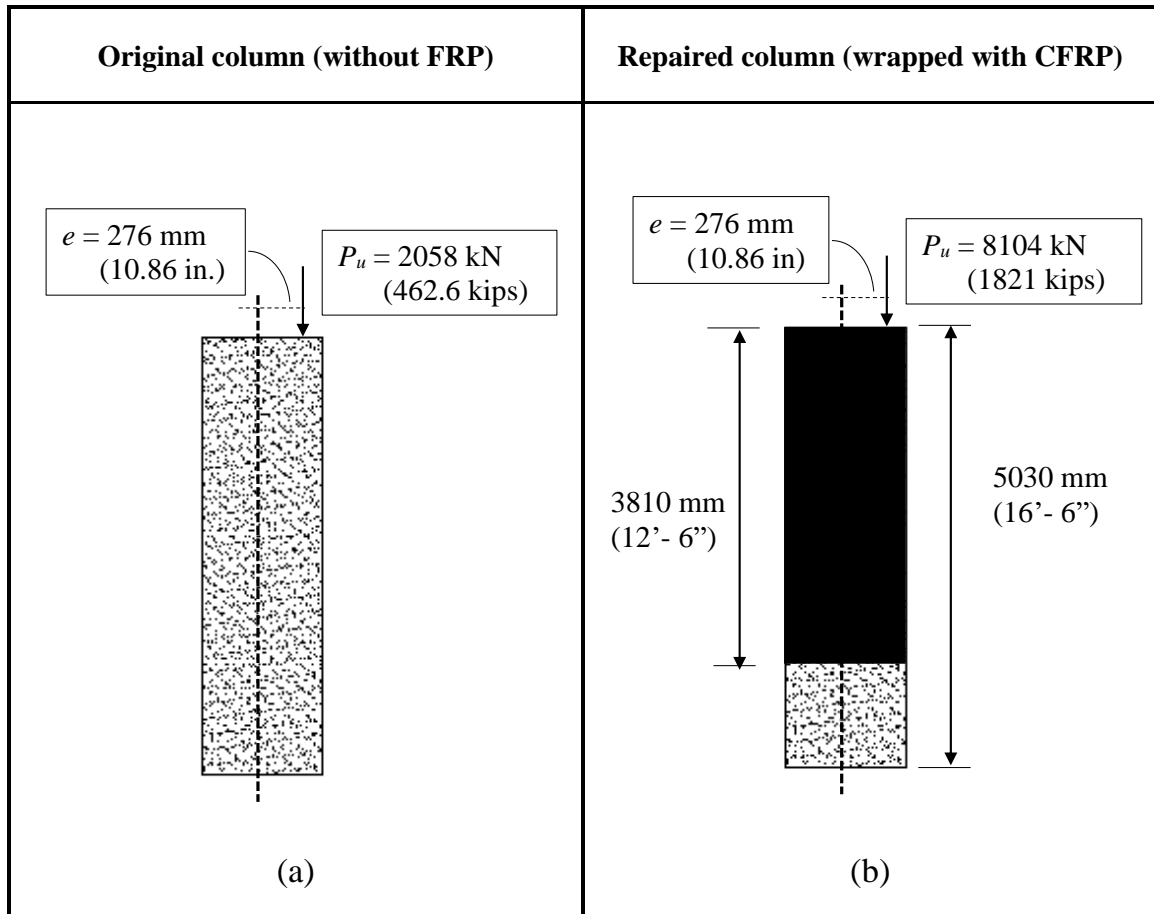
Figure 5.23 – The axial capacity of the bridge column: (a) original or as constructed column; and (b) CFRP wrapped column

5.6   Conclusions

The confined concrete model developed for concentrically loaded circular RC columns, in chapter 4, was used to generate the axial load-moment (*P-M*) interaction diagrams for eccentrically loaded columns that are partially and fully wrapped with FRP. The results compared very well with ones derived using finite element models of developed using the program ANSYS 14. As the FRP volumetric ratio (ρ_f) increases,

both axial and flexural capacities increase. These changes were more noticeable for columns with four FRP strips or more.

The influence of the distribution of the FRP material is more pronounced in the compression controlled zone when the axial load (P) is larger than that at balance (P_b). As the axial load magnitude is reduced from $P = P_b$ to $P = 0$ (or the tension controlled zone), the influence of distributing the FRP material on the column capacity becomes negligible.

A case study of an eccentrically loaded column in a bridge pier was used to evaluate the effectiveness of FRP confinement. The pier axial load capacity was increase by 260%.

139

CHAPTER 6
CONCLUSIONS

6.1   Summary

This study evaluated the effectiveness of partial fiber reinforced polymer (FRP) wraps (or strips) for increasing the strength and ductility of circular reinforced concrete (RC) columns subjected concentric compressive loads. Three dimensional finite element (FE) models were generated using ANSYS and validated by comparing the results with published experimental data. The FE results compared very well.

Three dimensional FE models were generated for concentrically loaded RC columns to study the influence of various parameters on the confined stress-strain relationship. The parameters included the unconfined compressive strength $(f_c^{'})$, the number of strips (N_f), the FRP volumetric ratio (ρ_f), the transverse steel reinforcement ratio (ρ_{st}), the longitudinal steel reinforcement ratio (ρ_{sl}), and the strip arrangement. The results of the parametric study were used to develop a confined concrete compressive stress-strain $(f_c - \varepsilon_c)$ model for concentrically loaded RC columns partially and fully wrapped with FRP with fibers oriented in the hoop direction.   In addition to the effect of partial and full confinement and the unconfined concrete strength $f_c^{'}$, the proposed $f_c - \varepsilon_c$ model accounts for yielding of transverse steel. Comparison of the results generated using the proposed model with FE and experimental results are in good agreement.

The proposed model was used to develop the axial load-moment (*P-M*) interaction diagrams for eccentrically loaded columns partially wrapped with FRP. The results were compared with finite element results. The results showed an increase in the columns

140

www.manaraa.com

capacities as the number of FRP strips is increased, and that columns fully wrapped with FRP are more effective than columns partially wrapped with the same FRP volumetric ratio. A case study of a column in a bridge substructure subjected to eccentric load was presented. The column was impacted by a semi-trailer, and was repaired and wrapped using FRP materials. The column was analyzed using finite element modeling, and the results showed a significant enhancement in the axial capacity and ductility of the column.

6.2   General Conclusions

- The FE model generated in this study successfully simulated the behavior of partially and fully wrapped RC columns with FRP. There is good agreement between FE predictions and experimental results published in the literature when comparing the confined concrete compressive stress-strain (f_c – ε_c) relationships. The FE model gives a reasonable values for the column the ultimate confined concrete compressive stress (f'_{cc}) and the ultimate confined concrete axial strain (ε_{ccu}) corresponding to the ultimate confined concrete compressive stress.

- As the number of FRP Strips are increased, corresponding to an increase in the FRP volumetric ratio, an increase is reported in the ultimate confined concrete compressive stress (f_{cc}'), the ultimate confined axial strain (ε_{ccu}), and the ultimate lateral strain of confined concrete (ε_{lu}). Additionally, the strengthening ratio (f'_{cc}/f_c'), strain ratio ($\varepsilon_{ccu}/\varepsilon_c'$), and ductility factor (μ) also increased.

141

- The ultimate lateral strains (ε_{lu}) increases with increasing FRP volumetric ratio, leading to a higher effective lateral confining pressure. The reported values did not reach the maximum FRP tensile strain (or FRP rupture) in either fully or partially wrapped columns.

- The influence of increasing the unconfined compressive concrete strength has a pronounced effect on the confined columns. As the unconfined compressive strength increases, the strengthening ratios ($f_{cc}{'} / f_c{'}$), strain ratios ($\varepsilon_{ccu} / \varepsilon_c{'}$), and ductility factors (μ) decrease.

- The increase in the number of strips, while keeping the FRP volumetric ratio (ρ_f) constant, leads to an increase in the ultimate compressive stress and strain, and ductility. This indicates that, for a specific ρ_f, it is more effective to fully wrap the column in order to increase the ultimate confined concrete compressive stress and axial strain. Although the fully wrapped column is more effective, in certain instances, a specific number of strips could satisfy the design requirements. This may be of interest when retrofitting columns that are not easily accessible (e.g. over a waterway) where the placement of strips maybe more economical than placing a full wrap.

- As the column Transverse steel reinforcement ratio (ρ_{st}) increases, the ultimate confined concrete ultimate stress ($f_{cc}{'}$) increases. On the other hand, the ultimate axial strain (ε_{ccu}) and ductility factor (μ) are reduced by increasing (ρ_{st}). It should

142

be noted that, as the number of strips or the lateral FRP confinement (ρ_f) increases, the influence of the transverse steel confinement (ρ_{st}) decreases.

- The FE results showed that the compressive response of concrete, when confined with two materials (transverse steel and FRP), is quite different from the compressive response of concrete confined with only one material. Taking into account the characteristics of the stress strain curves of confining materials, the slope of the confined concrete compressive stress-strain ($f_c - \varepsilon_c$) curve decreases after the transverse steel yields.

- As the longitudinal steel reinforcement ratio ρ_{st} is increased, there is a slight increase in the ultimate confined concrete compressive stress and the ultimate axial concrete strain (f_{cc}' and ε_{ccu}, respectively). However, in general, the change in the strengthening ratios (f_{cc}'/f_c'), strain ratios ($\varepsilon_{ccu}/\varepsilon_c'$), and ductility factors (μ) due to the increase in the longitudinal steel reinforcement ratio, has little influence on concrete confinement for the columns under consideration. Consequently, the contribution of the longitudinal steel is neglected in the derivation of the confined concrete stress-strain model.

- A new model is proposed for the confined concrete compressive stress and axial strain in partially and fully wrapped columns. The model accounts for the effect of partial and full confinement, the unconfined concrete strength f_c', and yielding of transverse steel. Based on the parametric study, the longitudinal steel has little

143

influence on the confined concrete, and the contribution of the longitudinal steel was neglected in the derivation of the model.

- The primary advantage of the model, compared to other models in the literature, is its separate account of the yielding of transverse steel which influences the behavior of the stress-strain relationship beyond that point, and the lateral confining pressures of transverse steel and FRP are treated independently. FRP strips were modeled individually and the Strips' arrangement contribution in the columns behavior was considered.

- A comparison between the proposed confined concrete stress-strain model and the finite element results shows that, as the stress approaches the ultimate confined compressive concrete stress, the model accurately predicts the overall behavior of the columns as well as the stress and strain at ultimate.

- The proposed model was compared with experimental results for partially and fully wrapped circular columns. The results were also compared with ones generated from the three existing models presented in literature. The proposed model predicted the stress at ultimate condition for fully and partially wrapped columns, while the other models overestimated the stress at ultimate for all columns. The consideration of yielding of transverse steel in the model leads to better prediction of the column behavior beyond the yielding point.

- The proposed model was successfully used to develop the *P-M* interaction diagrams for FRP partially and fully wrapped column. The model show values that are close

144

to those of the finite element results, except at the balance point. Therefore, further improvements in the finite element model are needed.

- As the FRP volumetric ratio (ρ_f) increases, both the axial load and flexural capacities increase. These changes were more noticeable for columns with four or more FRP strips. FRP wrapping has a more pronounced effect on increasing the column strength when a compression mode failure is dominated.

- For the same volume of FRP bonded to the column, the fully wrapped column is more effective than partially wrapped columns in increasing axial load and moment capacities within the compression control zone. The effectiveness is more pronounced when the CFRP volumetric ratio is increased.

6.3   Study Limitations and Future Research Recommendations

The primary focus of this research study was to evaluate the effectiveness of partial FRP wraps (or strips) in increasing the strength and ductility of reinforced concrete circular columns under concentric compressive load. A new confined concrete compressive stress-strain ($f_c - \varepsilon_c$) model was developed to account for partial wrapping of concentrically loaded RC columns that are partially and fully wrapped with FRP with fibers oriented in the hoop direction. The model is restricted to circular RC columns.

During the course of the study, numerous areas of research were identified for future research:

145

- Expand the parametric study to account for creep and shrinkage.

- Cyclic loading is a consideration for structures subjected to earthquakes and other extreme loads.

- The inelastic buckling of longitudinal steel reinforcement leads to a post yield softening branch in compression that strongly influences its behavior. A model for the softening branch of longitudinal steel in partially and fully wrapped columns that accounts for the phenomena is another topic requiring further research.

- A model that accounts for yielding of transverse steel for confined rectangular columns is an area requiring further research.

146

APPENDIX A

COMPARISON BETWEEN THE PROPOSED MODEL AND FE COMPRESSIVE

STRESS (f_c) VS AXIAL STRAIN (ε_c) FOR ALL COLUMNS (S1 TO FW) IN ALL

GROUPS (GROUP 1 TO GROUP 4)

Full Wrap (FW)		

Group 1	Group 2
$f_c' =$20.68 MPa (3 ksi)	$f_c' =$55.16 MPa (8 ksi)

Group 3	Group 4
$f_c' =$20.68 MPa (3 ksi)	$f_c' =$20.68 MPa (3 ksi)
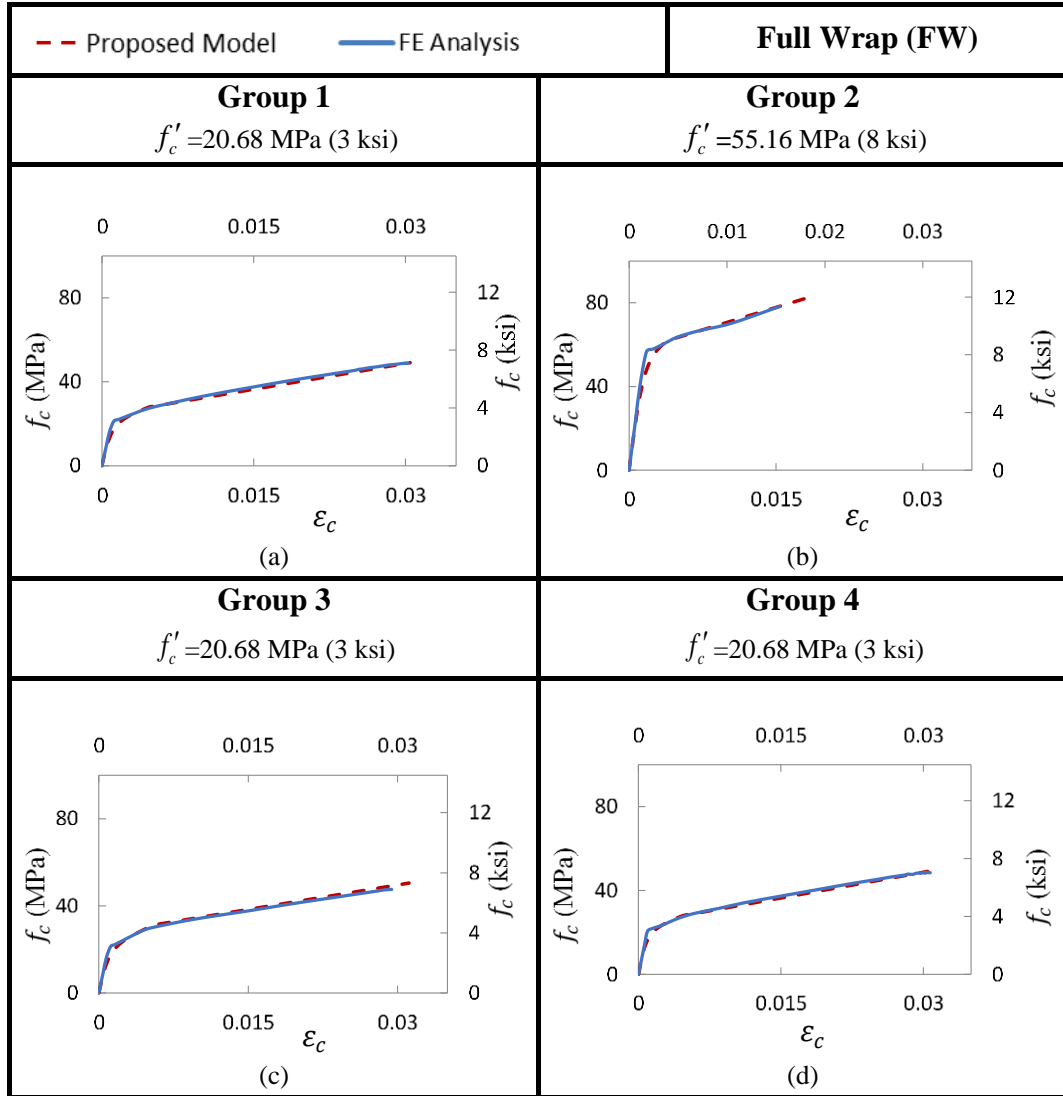
Figure A.1 – Comparison between the proposed model and FE compressive stress (f_c) vs axial strain (ε_c) for column (FW) in (a) Group 1 (b) Group 2 (c) Group 3 (d) Group 4

148

- - Proposed Model ━━ FE Analysis	**1 Strip (S1)**
Group 1 $f_c' =20.68$ MPa (3 ksi)	**Group 2** $f_c' =55.16$ MPa (8 ksi)

(a)

(b)

Group 3 $f_c' =20.68$ MPa (3 ksi)	**Group 4** $f_c' =20.68$ MPa (3 ksi)

(c)

(d)
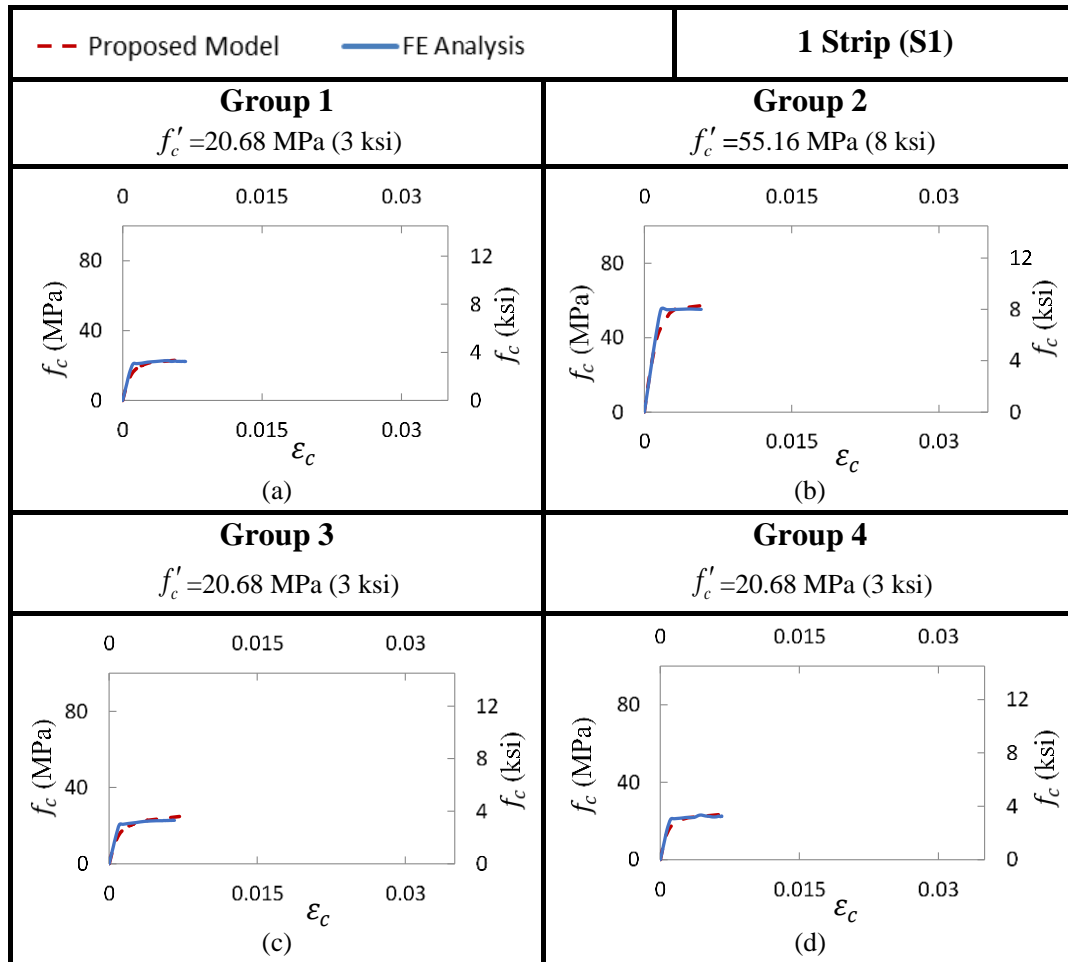
Figure A.2 – Comparison between the proposed model and FE compressive stress (f_c) vs axial strain (ε_c) for column (S1) in (a) Group 1 (b) Group 2 (c) Group 3 (d) Group 4

www.manaraa.com

- - Proposed Model —— FE Analysis	**2 Strips (S2)**
Group 1 f'_c =20.68 MPa (3 ksi)	**Group 2** f'_c =55.16 MPa (8 ksi)

(a)

(b)

Group 3 f'_c =20.68 MPa (3 ksi)	**Group 4** f'_c =20.68 MPa (3 ksi)

(c)

(d)
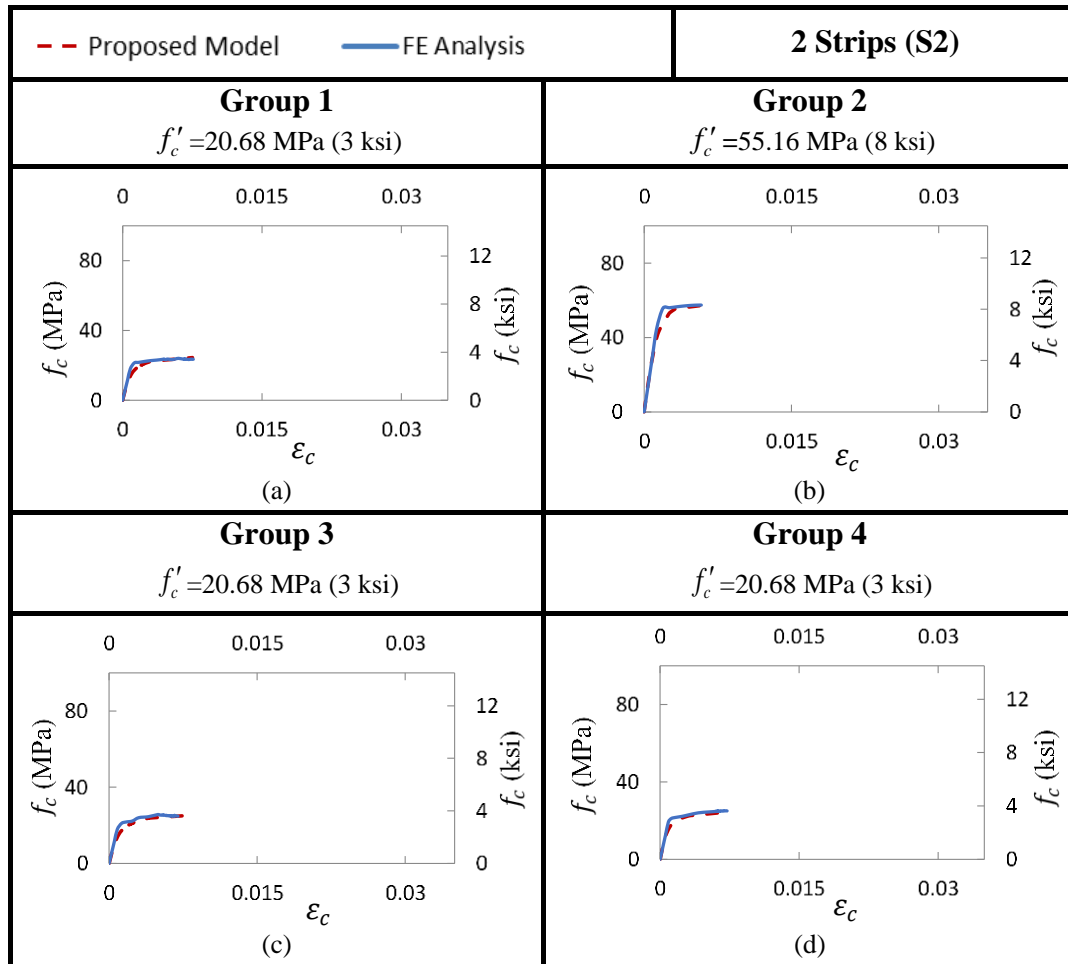
Figure A.3 – Comparison between the proposed model and FE compressive stress (f_c) vs axial strain (ε_c) for column (S2) in (a) Group 1 (b) Group 2 (c) Group 3 (d) Group 4

	3 Strips (S3)
- - Proposed Model ——FE Analysis	
Group 1 f'_c =20.68 MPa (3 ksi)	**Group 2** f'_c =55.16 MPa (8 ksi)
(a)	(b)
Group 3 f'_c =20.68 MPa (3 ksi)	**Group 4** f'_c =20.68 MPa (3 ksi)
(c)	(d)
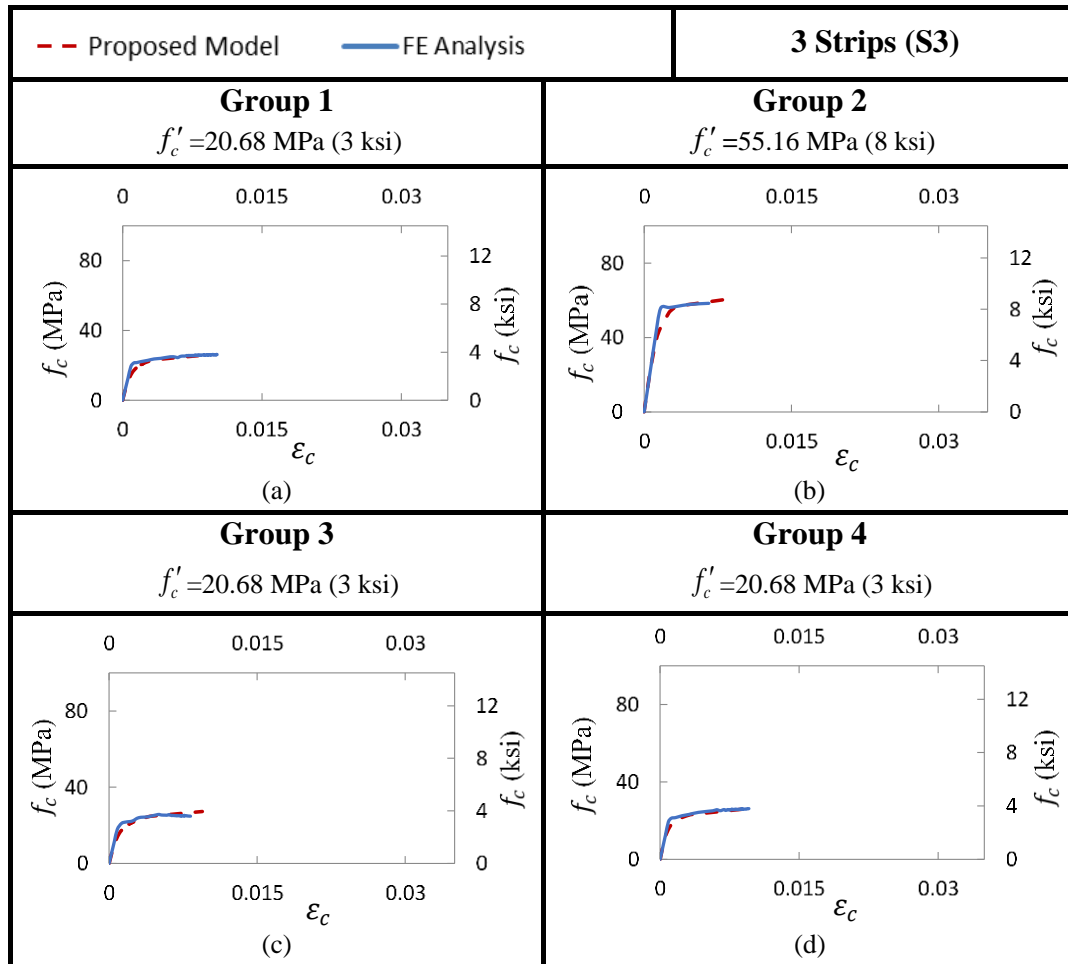
Figure A.4 – Comparison between the proposed model and FE compressive stress (f_c) vs axial strain (ε_c) for column (S3) in (a) Group 1 (b) Group 2 (c) Group 3 (d) Group 4
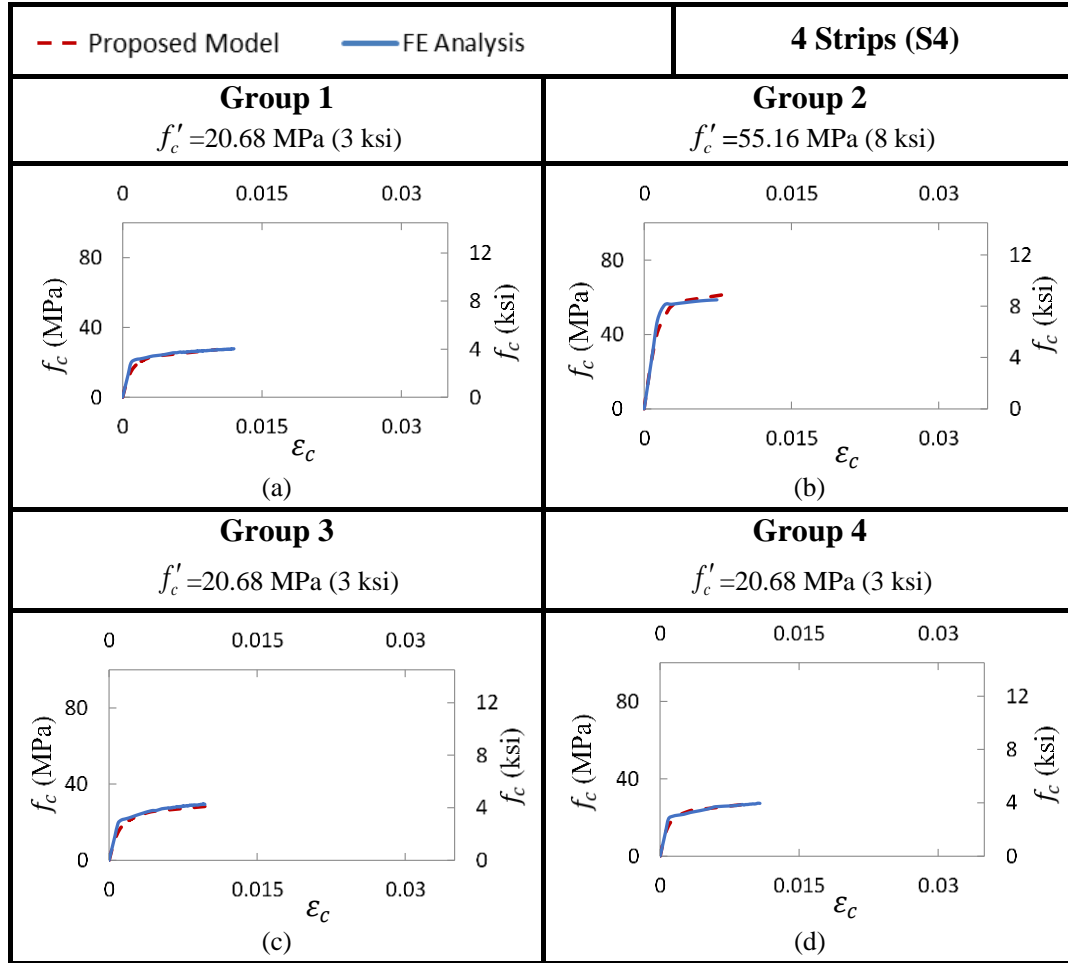
Figure A.5 – Comparison between the proposed model and FE compressive stress (f_c) vs axial strain (ε_c) for column (S4) in (a) Group 1 (b) Group 2 (c) Group 3 (d) Group 4

– – Proposed Model ━━━ FE Analysis	**5 Strips (S5)**
Group 1 f'_c =20.68 MPa (3 ksi)	**Group 2** f'_c =55.16 MPa (8 ksi)
(a)	(b)
Group 3 f'_c =20.68 MPa (3 ksi)	**Group 4** f'_c =20.68 MPa (3 ksi)
(c)	(d)
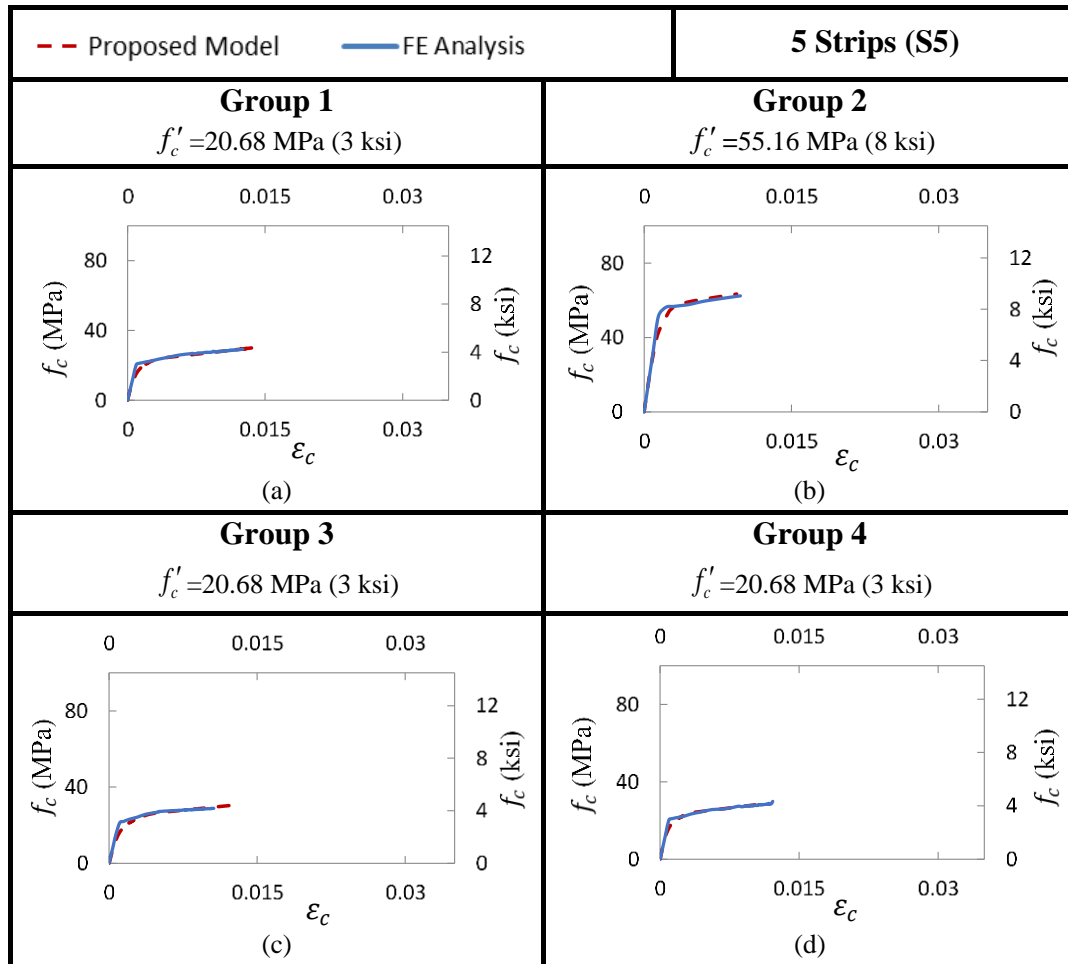
Figure A.6 – Comparison between the proposed model and FE compressive stress (f_c) vs axial strain (ε_c) for column (S5) in (a) Group 1 (b) Group 2 (c) Group 3 (d) Group 4
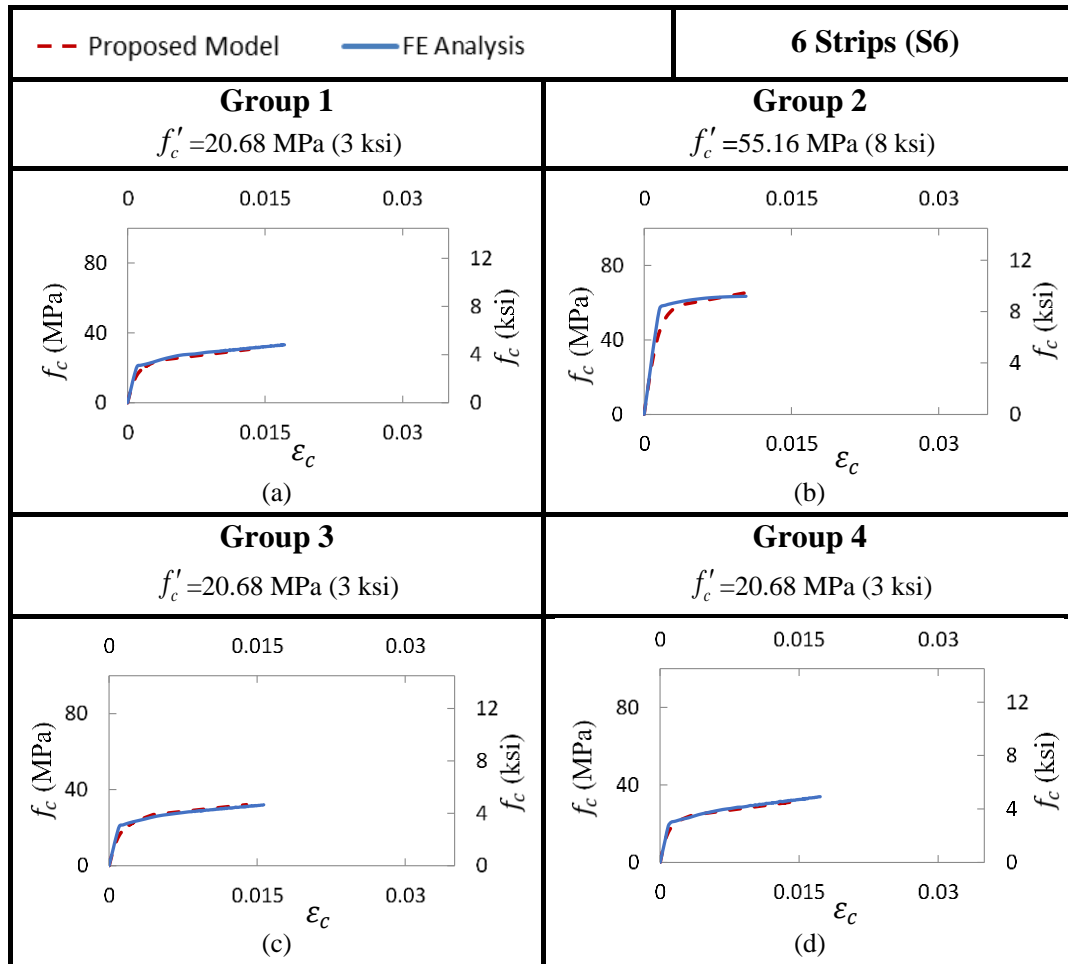
Figure A.7 – Comparison between the proposed model and FE compressive stress (f_c) vs axial strain (ε_c) for column (S6) in (a) Group 1 (b) Group 2 (c) Group 3 (d) Group 4

154

	7 Strips (S7)
− − Proposed Model ⎯⎯ FE Analysis	

Group 1 f'_c =20.68 MPa (3 ksi)	Group 2 f'_c =55.16 MPa (8 ksi)
(a)	(b)

Group 3 f'_c =20.68 MPa (3 ksi)	Group 4 f'_c =20.68 MPa (3 ksi)
(c)	(d)
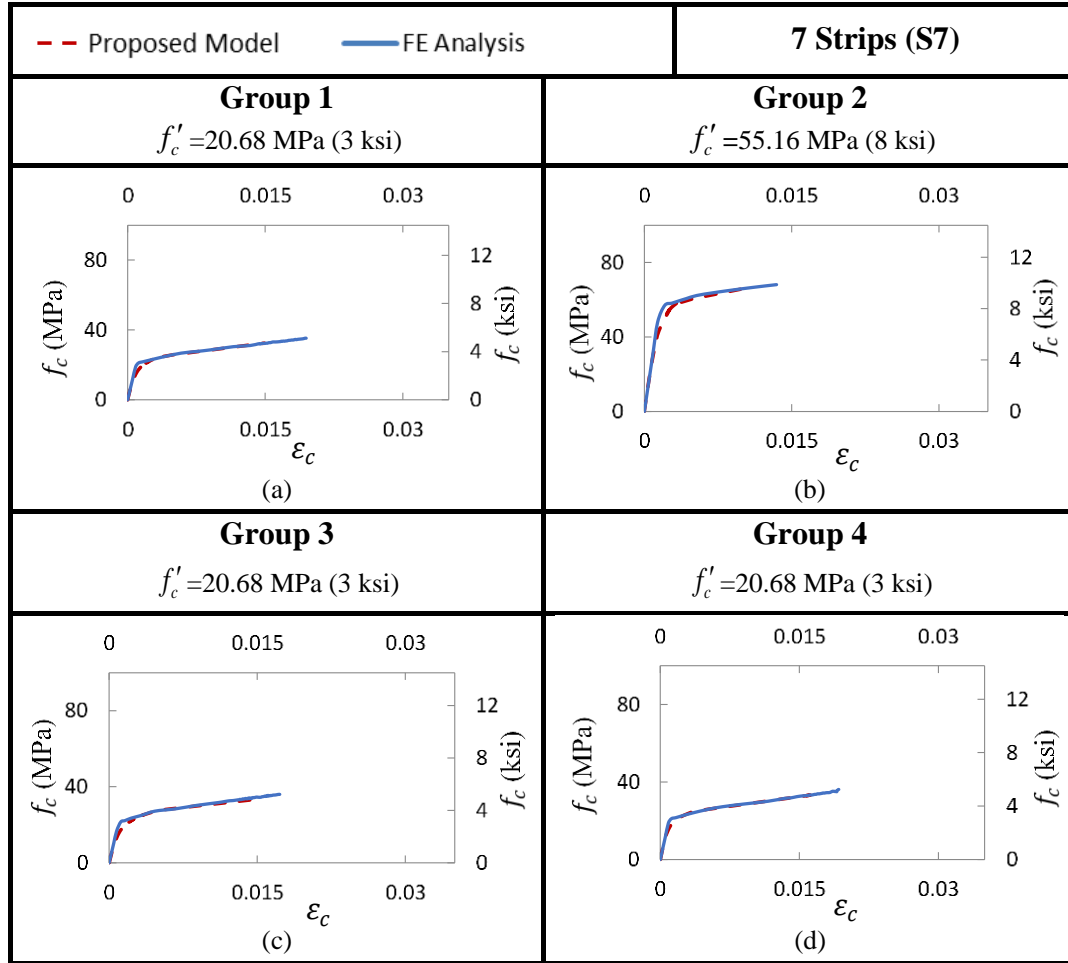
Figure A.8 – Comparison between the proposed model and FE compressive stress (f_c) vs axial strain (ε_c) for column (S7) in (a) Group 1 (b) Group 2 (c) Group 3 (d) Group 4

155

APPENDIX B

EXAMPLE:

CONFINED CONCRETE STRESS STRAIN RELATIONSHIP OF A PARTIALLY

CONFINED CIRCULAR COLUMN USING THE PROPOSED MODEL

156

The procedure of deriving the stress strain (f_c – ε_c) relationship using the proposed model is presented in this appendix. Column W45S6L3F8 (Figure 4.12a in chapter 4), is selected to illustrate the process. The column was tested by Varma et al. (2009) as part of an experimental program to investigate the behaviour of RC columns wrapped with FRP strips. It has a circular cross section with a diameter $D = 200$ mm (7.9 in.) and unbraced length $l_u = 600$ mm (23.62 in.), as shown in Figure B.1. The column is partially wrapped with 6 strips ($N_f = 6$). Each strip has a width $w_f = 45$ mm (1.77 in.) and three layers of CFRP fabric ($n_f = 3$). The thickness of each layer $t_f = 0.113$ mm (0.0044 in.).

Figure B.1 and Table B.1 summarizes the column data given in Varma et al (2009). The detailed derivation steps are in Table B.2 for SI metric units, and in Table B.3 for inch-pound units.
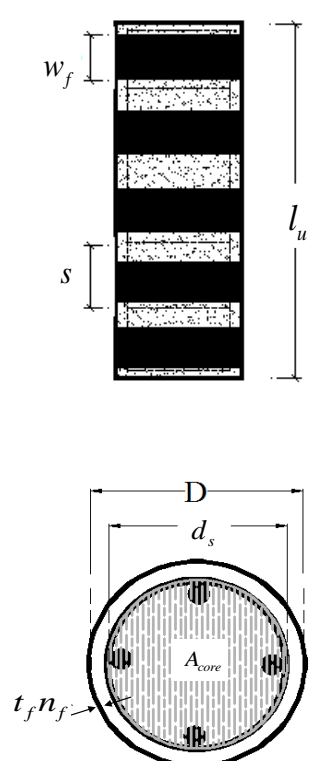
	Parameter	
D	200 mm	7.9 in.
l_u	600 mm	23.62 in.
w_f	45 mm	1.77 in.
s	96 mm	3.78 in.
s'	90 mm	3.54 in.
d_s	160 mm	6.3 in.
A_g	31400 mm^2	48.67 in.^{2}
A_{core}	20096 mm^2	31.15 in.^{2}
A_{cover}	11304 mm^2	17.52 in.^{2}
n_f	3	3
N_f	6	6

Figure B.1- FRP Wrap Layout and column's cross section
[Varma et al (2009)]

158

Table B. 1: Material properties for column
W45S6L3F8 [Varma et al (2009)]

Material	Parameter		
Concrete	f_c'	30 MPa	4.4 ksi
	E_c	25.87 GPa	3752 ksi
Steel	f_y	468.3 MPa	68 ksi
	A_{st}	28.3 mm^2	0.044 in^2
	A_{sl}	200.96 mm^2	0.312 in^2
FRP	t_f	0.113 mm	0.0044 in
	f_{fu}	3539 MPa	513 ksi
	E_f	232 GPa	33648 ksi
	ε_{fu}	0.0153	0.0153

159

Table B.2: Derivation of the stress strain ($f_c - \varepsilon_c$) relationship for Column W45S6L3F8 in SI metric units

Procedure	Calculations in SI metric units
Calculate the maximum lateral confining pressure due to FRP only $$f_{l,f,\max} = \frac{2 t_f E_f \varepsilon_{fu} n_f w_f N_f}{D l_u} \qquad \text{Eq. (4.13)}$$	$2(0.113\ mm)(232000\ MPa)\dfrac{(0.0153\ )(3)(45\ mm)(6)}{(200\ mm)(600\ mm)}$ $f_{l,f,\max} = 5.4\ MPa$
Calculate the maximum and lateral confining pressure due to transverse steel only $$f_{l,s,\max} = \frac{2 A_{st} f_y}{s d_s} \qquad \text{Eq. (4.14)}$$ **The effective lateral confining stress on the concrete due to steel only** $$f'_{l,s,\max} = \frac{\left(1 - \dfrac{s'}{2 d_s}\right)^2}{1 - (A_{sl}/A_{core})} f_{l,s,\max} \qquad \text{Eq. (4.18)}$$	$\dfrac{2\,(28.3\ mm^2)(468.3\ MPa)}{(96\ mm)(160\ mm)}$ $f_{l,s,max} = 1.72\ MPa$ $\dfrac{\{1 - [90\ mm/2(160\ mm)]\}^2}{1 - \left(\dfrac{200.96\ mm^2}{20096\ mm^2}\right)}$ $\times (1.72\ MPa)$ $f'_{l,s,max} = 0.9\ MPa$
Confined Concrete Ultimate Stress (f'_{cc}) $$f'_{cc} = f'_c \times [1 + 1.55 \left(\frac{f_{l,f,max}}{f'_c}\right)$$ $$\times \left(\frac{N_f w_f}{l_u}\right)^{0.3} + 1.55 \left(\frac{f_{l,s,max}}{f'_c}\right)] \qquad \text{Eq. (4.11)}$$	$(30\ MPa)\left[1 + 1.55\left(\dfrac{5.4\ MPa}{30\ MPa}\right)\left(\dfrac{6\ \times 45\ mm}{600\ mm}\right)^{0.3}\right.$ $\left. + 1.55\left(\dfrac{1.72\ MPa}{30\ MPa}\right)\right]$ $f'_{cc} = 39.6\ MPa$
Axial Ultimate Strain (ε_{ccu}) $$\varepsilon_{ccu} = \varepsilon'_c \times \left[2.44 + 15 \left(\frac{f_{l,f,max}}{f'_c}\right)\left(\frac{N_f w_f}{l_u}\right)^{0.3}\right.$$ $$\left. + 7.7 \left(\frac{f_{l,s,max}}{f'_c}\right)\right]$$ Eq. (4.12)	$(0.003)\left[2.44 + 15\left(\dfrac{5.4\ MPa}{30\ MPa}\right)\left(\dfrac{6\ \times 45\ mm}{600\ mm}\right)^{0.3}\right.$ $\left. + 7.7\left(\dfrac{1.72\ MPa}{30\ MPa}\right)\right]$ $\varepsilon_{ccu} = 0.0148$

160

Axial strain at yielding of transverse steel ($\varepsilon_{c,s}$) $\varepsilon_{l,y} = \dfrac{f_y}{E_s}$ Eq. (4.15) $f_{l,fy} = \dfrac{2t_f E_f \varepsilon_{l,y} w_f n_f N_f}{Dl_u}$ Eq. (4.17) $\varepsilon_{c,s} = 0.85\, \varepsilon_c' \times \left[1 + 8\left(\dfrac{f_{l,fy} + f_{l,s,max}'}{f_c'}\right)\right]$ $\times \left\{\left[1 + 0.75\left(\dfrac{\varepsilon_{l,y}}{\varepsilon_c'}\right)\right]^{0.7} - exp\left[-7\left(\dfrac{\varepsilon_{l,y}}{\varepsilon_c'}\right)\right]\right\}$ Eq. (4.16)	$\dfrac{468\ MPa}{200{,}000\ MPa}$ $\varepsilon_{l,y} = 0.00234$ $2(0.113\ mm)(232000\ MPa)\dfrac{(0.00234)(3)(45\ mm)(6)}{(200\ mm)(600\ mm)}$ $\dfrac{(0.00234)(3)(45\ mm)(6)}{(200\ mm)(600\ mm)}$ $f_{l,fy} = 0.78\ MPa$ $0.85\,(0.003) \times \left[1 + 8\left(\dfrac{0.78\ MPa + 0.9\ MPa}{30\ MPa}\right)\right]$ $\times \left\{\left[1 + 0.75\left(\dfrac{0.00234}{0.003}\right)\right]^{0.7} - exp\left[-7\left(\dfrac{0.00234}{0.003}\right)\right]\right\}$ $\varepsilon_{c,s} = 0.005$
Component of confined concrete compressive stress at yielding of transverse steel due to steel confinement only ($f_{c,sy}$) $f_{cc,s}' = f_c'\left[2.254\sqrt{1 + 7.94\dfrac{f_{l,s,max}'}{f_c'}} - 2\left(\dfrac{f_{l,s,max}'}{f_c'}\right)\right.$ $\left. - 1.254\right]$ Eq.(4.25) $\varepsilon_{ccu,s} = \varepsilon_c'\left[1 + 5\left(\dfrac{f_{cc,s}'}{f_c'}\right)\right]$ Eq.(4.26) $r_s = \dfrac{E_c}{E_c - f_{cc,s}'/\varepsilon_{ccu,s}}$ Eq.(4.24) $f_{c,sy} = \dfrac{f_{cc,s}'(\varepsilon_{c,s}/\varepsilon_{ccu,s})r_s}{r_s - 1 + (\varepsilon_{c,s}/\varepsilon_{ccu,s})^{r_s}}$ Eq.(4.23)	$30\ MPa\left[2.254 \times \sqrt{1 + 7.94\dfrac{0.9\ MPa}{30\ MPa}} - 2\left(\dfrac{0.9\ MPa}{30\ MPa}\right) - 1.254\right]$ $f_{cc,s}' = 36\ MPa$ $0.003\left[1 + 5\left(\dfrac{36\ MPa}{30\ MPa}\right)\right]$ $\varepsilon_{ccu,s} = 0.021$ $\dfrac{25870\ MPa}{25870\ MPa - 36\ MPa/0.021}$ $r_s = 1.07$ $\dfrac{(36\ MPa)(0.005/0.021)(1.07)}{1.07 - 1 + (0.005/0.021)^{1.07}}$ $f_{c,sy} = 32\ MPa$

161

Component of confined concrete compressive stress at yielding of transverse steel due to FRP confinement only $(f_{c,fy})$ $$f'_{cc,f} = f'_c \left(1 + 3.5 \frac{f_{l,fy}}{f'_c}\right) \qquad \text{Eq.(4.29)}$$ $$\varepsilon_{ccu,f} = \varepsilon'_c \left[1 + 17.5 \left(\frac{f_{l,fy}}{f'_c}\right)\right] \qquad \text{Eq.(4.30)}$$ $$r_f = \frac{E_c}{E_c - f'_{cc,f}/\varepsilon_{ccu,f}} \qquad \text{Eq.(4.28)}$$ $$f_{c,fy} = \frac{f'_{cc,f}(\varepsilon_{c,s}/\varepsilon_{ccu,f})r_f}{r_f - 1 + (\varepsilon_{c,s}/\varepsilon_{ccu,f})^{r_f}} \qquad \text{Eq.(4.27)}$$	$$30\ MPa \left[1 + 3.5 \left(\frac{0.78\ MPa}{30\ MPa}\right)\right]$$ $$f'_{cc,s} = 33\ MPa$$ $$0.003 \left[1 + 17.5 \left(\frac{0.78\ MPa}{30\ MPa}\right)\right]$$ $$\varepsilon_{ccu,f} = 0.0044$$ $$\frac{25870\ MPa}{25870\ MPa - 33\ MPa/0.0044}$$ $$r_f = 1.4$$ $$\frac{(33\ MPa)(0.005/0.0044)(1.4)}{1.4 - 1 + (0.005/0.0044)^{1.4}}$$ $$f_{c,fy} = 33\ MPa$$
Confined concrete compressive stress at yielding of transverse steel $(f_{c,s})$ $$f_{core} = f_{c,sy} + f_{c,fy} - f'_c \qquad \text{Eq.(4.20)}$$ $$f_{cover} = f_{c,fy} \qquad \text{Eq. (4.21)}$$ $$f_{c,s} = \frac{f_{core}A_{core} + f_{cover}A_{cover}}{A_g} \qquad \text{Eq. (4.19)}$$	$$32\ MPa + 33\ MPa - 30\ MPa$$ $$f_{core} = 35\ MPa$$ $$f_{cover} = 33\ MPa$$ $$\frac{1}{31400\ mm^2} \times$$ $$[(35\ MPa)(20096\ mm^2) + (33\ MPa)(11304\ mm^2)]$$ $$f_{c,s} = 34.15\ MPa$$

162

Calculate the slope of the stress strain curve at yielding of transverse steel $E_1 = \dfrac{f_{c,s} - f_0}{\varepsilon_{c,s}}$ Eq. (4.8)	$\dfrac{34.15\ MPa - 30\ MPa}{0.005}$ $E_1 = 830\ MPa$
Slope of the stress strain curve after yielding of transverse steel $E_2 = \dfrac{f'_{cc} - f_{c,s}}{\varepsilon_{ccu} - \varepsilon_{c,s}}$ Eq. (4.9)	$\dfrac{39.6\ MPa - 34.15\ MPa}{0.0149}$ $E_2 = 365.7\ MPa$
$n = 1 + \dfrac{1}{(E_c \varepsilon'_c / f'_c) - 1}$ Eq. (4.7) $m = \left(\dfrac{1}{\ln \varepsilon_{c,s}}\right) \ln\left[\dfrac{1}{E_1}\left(f_{c,s} - \dfrac{(E_c - E_1)\varepsilon_{c,s}}{\left\{1 + \left[\frac{(E_c - E_1)\varepsilon_{c,s}}{f_0}\right]^n\right\}^{1/n}}\right)\right]$ Eq. (4.6)	$n = 1 + \dfrac{1}{\left(25870\ MPa \times \frac{0.003}{30 MPa}\right) - 1}$ $n = 1.64$ $(E_c - E_1)\varepsilon_{c,s} = (25870\ MPa - 830\ MPa)(0.005)$ $= 125.2\ MPa$ $\left\{1 + \left[\dfrac{(E_c - E_1)\varepsilon_{c,s}}{f_0}\right]^{1.64}\right\}^{1.64} =$ $\left\{1 + \left[\dfrac{125.2\ MPa}{30\ MPa}\right]^{1.64}\right\}^{\frac{1}{1.64}} = 4.4$ $\left(\dfrac{1}{\ln 0.005}\right) \times \ln\left[\dfrac{1}{830\ MPa}\left(34.15\ MPa - \dfrac{125.2\ MPa}{4.4}\right)\right]$ $m = 0.944$

163

Generate stress – strain curve

$$f_c = \frac{(E_c - E_1)\varepsilon_c}{\left[1 + \left(\frac{(E_c - E_1)\varepsilon_c}{f_0}\right)^n\right]^{1/n}} + E_1\varepsilon_c^m \qquad 0 \leq \varepsilon_c \leq \varepsilon_{c,s} \qquad \text{Eq. (4.4)}$$

$$f_c = f_{c,s} + E_2(\varepsilon_c - \varepsilon_{c,s}) \qquad \varepsilon_{c,s} \leq \varepsilon_c \leq \varepsilon_{ccu} \qquad \text{Eq. (4.5)}$$

164

Table B.2: Derivation of the stress strain ($f_c - \varepsilon_c$) relationship for Column W45S6L3F8 inch-pound units

Procedure	Calculations in inch-pound units
Calculate the maximum lateral confining pressure due to FRP only $f_{l,f,\max} = \dfrac{2t_f E_f \varepsilon_{fu} n_f w_f N_f}{D l_u}$ Eq. (4.13)	$2(0.0044\ in)(33648\ ksi)\dfrac{(0.0153\ )(3)(1.77 in.\ )(6)}{(7.9\ in.\ )(23.62\ in.\ )}$ $f_{l,f,max} = 0.78\ ksi$
Calculate the maximum and lateral confining pressure due to transverse steel only $f_{l,s,\max} = \dfrac{2A_{st}f_y}{s d_s}$ Eq. (4.14) **The effective lateral confining stress on the concrete due to steel only** $f'_{l,s,\max} = \dfrac{\left(1 - \dfrac{s'}{2d_s}\right)^2}{1-(A_{sl}/A_{core})} f_{l,s,\max}$ Eq. (4.18)	$\dfrac{2\ (0.044\ in.^2\ )(68\ ksi)}{(3.78\ in.\ )(6.3\ in,)}$ $f_{l,s,max} = 0.25\ ksi$ $\dfrac{\{1 - [3.5\ in./2(6.3\ in.^2\ ]\}^2}{1 - \left(\dfrac{0.312\ in.^2}{31.15\ in.^2}\right)}(0.25\ ksi)$ $f'_{l,s,max} = 0.035\ ksi$
Confined Concrete Ultimate Stress $f'_{cc} = f'_c \times [1 + 1.55\left(\frac{f_{l,f,max}}{f'_c}\right)$ $\times \left(\frac{N_f w_f}{l_u}\right)^{0.3} +1.55\left(\frac{f_{l,s,max}}{f'_c}\right)]$ Eq. (4.11)	$(4.4\ ksi)\left[1 + 1.55\left(\dfrac{0.78\ ksi}{4.4\ ksi}\right)\left(\dfrac{6 \times 1.77\ in.}{23.6\ in}\right)^{0.3}\right.$ $\left. + 1.55\left(\dfrac{0.25\ ksi}{4.4\ ksi}\right)\right]$ $f'_{cc} = 5.7\ ksi$
Axial Ultimate Strain (ε_{ccu}) $\varepsilon_{ccu} = \varepsilon'_c \times \left[2.44 + 15\left(\frac{f_{l,f,max}}{f'_c}\right)\left(\frac{N_f w_f}{l_u}\right)^{0.3} + 7.7\left(\frac{f_{l,s,max}}{f'_c}\right)\right]$ Eq. (4.12)	$(0.003)\left[2.44 + 15\left(\dfrac{0.78\ ksi}{4.4\ ksi}\right)\left(\dfrac{6 \times 1.77\ in.}{23.6\ in}\right)^{0.3}\right.$ $\left. + 7.7\left(\dfrac{0.25\ ksi}{4.4\ ksi}\right)\right]$ $\varepsilon_{ccu} = 0.0148$

165

Axial strain at yielding of transverse steel ($\varepsilon_{c,s}$) $\varepsilon_{l,y} = \dfrac{f_y}{E_s}$ Eq. (4.15) $f_{l,fy} = \dfrac{2t_f E_f \varepsilon_{l,y} w_f n_f N_f}{D l_u}$ Eq. (4.17) $\varepsilon_{c,s} = 0.85\,\varepsilon_c' \times \left[1 + 8\left(\dfrac{f_{l,fy} + f_{l,s,max}'}{f_c'}\right)\right]$ $\times \left\{\left[1 + 0.75\left(\dfrac{\varepsilon_{l,y}}{\varepsilon_c'}\right)\right]^{0.7} - exp\left[-7\left(\dfrac{\varepsilon_{l,y}}{\varepsilon_c'}\right)\right]\right\}$ Eq. (4.16)	$\dfrac{68\ ksi}{29000\ ksi}$ $\varepsilon_{l,y} = 0.00234$ $2(0.0044\ in)(33648\ ksi)\dfrac{(0.00234\,)(3)(1.77in.)(6)}{(7.9\ in.)(23.62\ in.)}$ $f_{l,fy} = 0.113\ ksi$ $0.85\,(0.003) \times \left[1 + 8\left(\dfrac{0.113\ ksi + .035\ ksi}{4.4\ ksi}\right)\right]$ $\times \left\{\left[1 + 0.75\left(\dfrac{0.00234}{0.003}\right)\right]^{0.7} - exp\left[-7\left(\dfrac{0.00234}{0.003}\right)\right]\right\}$ $\varepsilon_{c,s} = 0.005$
Component of confined concrete compressive stress at yielding of transverse steel due to steel confinement only ($f_{c,sy}$) $f_{cc,s}' = f_c'\left[2.254\sqrt{1 + 7.94\dfrac{f_{l,s,max}'}{f_c'}} - 2\left(\dfrac{f_{l,s,max}'}{f_c'}\right)\right.$ $\left. - 1.254\right]$ Eq.(4.25) $\varepsilon_{ccu,s} = \varepsilon_c'\left[1 + 5\left(\dfrac{f_{cc,s}'}{f_c'}\right)\right]$ Eq.(4.26) $r_s = \dfrac{E_c}{E_c - f_{cc,s}'/\varepsilon_{ccu,s}}$ Eq.(4.24) $f_{c,sy} = \dfrac{f_{cc,s}'(\varepsilon_{c,s}/\varepsilon_{ccu,s})r_s}{r_s - 1 + (\varepsilon_{c,s}/\varepsilon_{ccu,s})^{r_s}}$ Eq.(4.23)	$4.4\ ksi\left[2.254\sqrt{1 + 7.94\dfrac{0.035\ ksi}{4.4\ ksi}} - 2\left(\dfrac{0.035\ ksi}{4.4\ ksi}\right) - 1.254\right]$ $f_{cc,s}' = 5.2\ ksi$ $0.003\left[1 + 5\left(\dfrac{5.2\ ksi}{4.4\ ksi}\right)\right]$ $\varepsilon_{ccu,s} = 0.021$ $\dfrac{3752\ ksi}{3752\ ksi - 5.2\ ksi/0.021}$ $r_s = 1.07$ $\dfrac{(5.2\ ksi)\,(0.005/0.021)(1.07)}{1.07 - 1 + (0.005/0.021)^{1.07}}$ $f_{c,sy} = 4.6\ ksi$

166

Component of confined concrete compressive stress at yielding of transverse steel due to FRP confinement only $(f_{c,fy})$	
$$f'_{cc,f} = f'_c\left(1+3.5\frac{f_{l,fy}}{f'_c}\right) \quad \text{Eq.(4.29)}$$	$$30\ MPa\left[1+3.5\left(\frac{0113\ ksi}{4.4\ ksi}\right)\right]$$ $$f'_{cc,s} = 4.8\ ksi$$
$$\varepsilon_{ccu,f} = \varepsilon'_c\left[1+17.5\left(\frac{f_{l,fy}}{f'_c}\right)\right] \quad \text{Eq.(4.30)}$$	$$0.003\left[1+17.5\left(\frac{0.113\ MPa}{4.4\ MPa}\right)\right]$$ $$\varepsilon_{ccu,f} = 0.0044$$
$$r_f = \frac{E_c}{E_c - f'_{cc,f}/\varepsilon_{ccu,f}} \quad \text{Eq.(4.28)}$$	$$\frac{3752\ ksi}{3752\ ksi - 4.8\ ksi/0.0044}$$ $$r_f = 1.4$$
$$f_{c,fy} = \frac{f'_{cc,f}(\varepsilon_{c,s}/\varepsilon_{ccu,f})r_f}{r_f - 1 + (\varepsilon_{c,s}/\varepsilon_{ccu,f})^{r_f}} \quad \text{Eq.(4.27)}$$	$$\frac{(5.2\ ksi)(0.005/0.0044)(1.4)}{1.4 - 1 + (0.0044)^{1.4}}$$ $$f_{c,fy} = 4.8\ ksi$$
Confined concrete compressive stress at yielding of transverse steel $(f_{c,s})$ $$f_{core} = f_{c,sy} + f_{c,fy} - f'_c \quad \text{Eq.(4.20)}$$ $$f_{cover} = f_{c,fy} \quad \text{Eq. (4.21)}$$	$$4.8\ MPa + 4.8\ MPa - 4.4\ MPa$$ $$f_{core} = 5\ ksi$$ $$f_{cover} = 4.8\ ksi$$
$$f_{c,s} = \frac{f_{core}A_{core} + f_{cover}A_{cover}}{A_g} \quad \text{Eq. (4.19)}$$	$$\frac{1}{48.67\ mm^2} \times$$ $$[(5\ MPa)(31.15\ mm^2) + (4.8\ MPa)(17.52\ mm^2)]$$ $$f_{c,s} = 4.9\ MPa$$

167

Calculate the slope of the stress strain curve at yielding of transverse steel $E_1 = \dfrac{f_{c,s} - f_0}{\varepsilon_{c,s}}$ Eq. (4.8)	$\dfrac{4.9 \; ksi - 4.4 \; ksi}{0.005}$ $E_1 = 120 \; ksi$
Slope of the stress strain curve after yielding of transverse steel $E_2 = \dfrac{f'_{cc} - f_{c,s}}{\varepsilon_{ccu} - \varepsilon_{c,s}}$ Eq. (4.9)	$\dfrac{5.7 \; ksi - 4.9 \; ksi}{0.0149}$ $E_2 = 53 \; ksi$
$n = 1 + \dfrac{1}{(E_c \varepsilon'_c / f'_c) - 1}$ Eq. (4.7) $m = \left(\dfrac{1}{\ln \varepsilon_{c,s}}\right) \ln \left[\dfrac{1}{E_1} \left(f_{c,s-} \dfrac{(E_c - E_1)\varepsilon_{c,s}}{\left\{ 1 + \left[\dfrac{(E_c - E_1)\varepsilon_{c,s}}{f_0} \right]^n \right\}^{1/n}} \right) \right]$ Eq. (4.6)	$n = 1 + \dfrac{1}{\left(3752 \; ksi \times \dfrac{0.003}{4.4 \; ksi}\right) - 1}$ $n = 1.64$ $(E_c - E_1)\varepsilon_{c,s} = (3752 \; ksi - 120 \; ksi)(0.005)$ $= 18.16 \; ksi$ $\left\{ 1 + \left[\dfrac{(E_c - E_1)\varepsilon_{c,s}}{f_0} \right]^{1.64} \right\}^{1.64} =$ $\left\{ 1 + \left[\dfrac{18.16 \; ksi}{4.4 \; ksi} \right]^{1.64} \right\}^{\frac{1}{1.64}} = 4.36$ $\left(\dfrac{1}{\ln 0.005}\right) \times \ln \left[\dfrac{1}{120 \; ksi} \left(4.9 \; ksi - \dfrac{18.16 \; ksi}{4.36} \right) \right]$ $m = 0.944$

168

Generate stress – strain curve

$$f_c = \frac{(E_c - E_1)\varepsilon_c}{\left[1 + \left(\dfrac{(E_c - E_1)\varepsilon_c}{f_0}\right)^n\right]^{1/n}} + E_1\varepsilon_c^m \qquad\qquad 0 \le \varepsilon_c \le \varepsilon_{c,s} \qquad\qquad \text{Eq. (4.4)}$$

$$f_c = f_{c,s} + E_2(\varepsilon_c - \varepsilon_{c,s}) \qquad\qquad \varepsilon_{c,s} \le \varepsilon_c \le \varepsilon_{ccu} \qquad\qquad \text{Eq. (4.5)}$$

169

NOMENCLATURE

A_{core}	= core area of the column measured to the centerline of transverse steel	mm^2	(in.^{2})
A_{cover}	= cover area of the column measured to the centerline of transverse steel	mm^2	(in.^{2})
A_g	= gross area of the column section	mm^2	(in.^{2})
A_{si}	= cross-sectional area of the ''ith'' layer of longitudinal steel reinforcement	mm^2	(in.^{2})
A_{st}	= area of transverse steel	mm^2	(in.^{2})
A_{sl}	= total area of longitudinal reinforcement	mm^2	(in.^{2})
b	= width of section at distance x from the center of the column cross section	mm	(in.)
b''	= width of the confined core	mm	(in.)
c	= distance from the neutral axis position to the extreme compression fiber in the cross-section	mm	(in.)
c_f	= distance from the point of stirrups steel yield to the extreme compression fiber in the cross-section	mm	(in.)
c_{DP}	= the cohesion value of the material in Drucker–Prager plasticity model		
d_s	= concrete core diameter to center line of transverse steel	mm	(in.)
d_{si}	= distance from the position of the ''ith'' layer of longitudinal steel reinforcement to the geometric centroid of the cross-section	mm	(in.)
D	= Column Diameter	mm	(in.)
e	= Eccentricity of axial load	mm	(in.)
E_c	= modulus of elasticity of concrete	GPa	(ksi)
E_f	= tensile modulus of elasticity of the FRP composite	GPa	(ksi)

170

$E_{f,l}$		tensile modulus of elasticity of the FRP composite in the longitudinal direction	GPa (ksi)
$E_{f,t}$		tensile modulus of elasticity of the FRP composite in the transverse direction	GPa (ksi)
E_s	=	modulus of elasticity of the steel	GPa (ksi)
E_1	=	slope of the stress strain curve at yielding of transverse steel	GPa (ksi)
E_2	=	slope of the stress strain curve after yielding of transverse steel	GPa (ksi)
E_2 (Lam & Teng 2003)	=	slope of the linear second portion	GPa (ksi)
f_c	=	the confined concrete stress	MPa (ksi)
$f_{c,fy}$	=	component of confined concrete compressive stress at yielding of transverse steel due to FRP confinement only (Note: this component will be added to the one due to transverse steel confinement only to determine the total stress)	MPa (ksi)
$f_{c,s}$	=	compressive stress in confined concrete at yielding of transverse steel	MPa (ksi)
$f_{c,sy}$	=	component of confined concrete compressive stress at yielding of transverse steel due to transverse steel confinement only	MPa (ksi)
f_{core}	=	compressive stress of confined concrete for core of the column	MPa (ksi)
f_{cover}	=	compressive stress of confined concrete for cover of the column	MPa (ksi)
f_{fu}	=	ultimate strength of FRP material	MPa (ksi)
$f_{fu,l}$	=	ultimate strength of FRP material in the longitudinal direction	MPa (ksi)

171

$f_{fu,t}$	= ultimate strength of FRP material in the transverse direction	MPa	(ksi)
f_l	= total lateral confining pressure	MPa	(ksi)
$f_{l,a}$	= actual maximum confining pressure (Lam &Teng 2003)	MPa	(ksi)
$f_{l,f,\max}$	= maximum lateral confining pressure due to FRP only	MPa	(ksi)
$f_{l,fy}$	= lateral confining pressure exerted by FRP at yielding of transverse steel	MPa	(ksi)
$f_{l,s,\max}$	= maximum lateral confining pressure due to transverse steel only	MPa	(ksi)
f_{si}	= normal stress of the ''ith'' layer of longitudinal steel reinforcement	MPa	(ksi)
f_y	= specified yield strength of nonprestressed steel reinforcement	MPa	(ksi)
f_c'	= compressive strength of unconfined concrete	MPa	(ksi)
f_{cc}'	= ultimate compressive stress in confined concrete	MPa	(ksi)
$f_{cc,f}'$	= peak compressive stress of concrete under FRP confining pressure at yielding of transverse steel	MPa	(ksi)
$f_{cc,s}'$	= Maximum axial compressive strength of partially FRP-confined concrete	MPa	(ksi)
$f_{l,s,\max}'$	= peak compressive stress of confined concrete under transverse steel confining pressure at yielding of transverse steel	MPa	(ksi)
f_0	= is the reference plastic stress at the intercept of the slope at yielding of transverse steel with the stress axis	MPa	(ksi)
$f_{0\,(\text{Lam \& Teng 2003})}$	= is the intercept of the stress axis by the linear second portion		
H	= lateral static load	kN	(kips)
k_s	= Steel confining pressure adjustment coefficient (Lee et al. 2010)		

$k_{e,s}$	=	steel confinement effectiveness coefficient		
l_u	=	column unbraced length	mm	(in)
M	=	The bending moment capacity of eccentrically loaded column	kN-m	(kip-ft)
M_{DP}	=	Special diagonal matrix for Drucker–Prager plasticity model		
M_u	=	ultimate moment in column at failure	kN-m	(kip-ft)
N_f	=	number of FRP strips along the column		
n_f	=	number of FRP sheets per strip		
n_s	=	the number of longitudinal steel bars		
P	=	column axial load	kN	(kips)
P_n	=	nominal axial capacity of the column	kN	(kips)
P_u	=	Ultimate axial load of confined concrete	kN	(kips)
r_f , r_s	=	constants that account for brittleness of concrete		
R	=	the radius of the column	mm	(in.)
s	=	center to center spacing between transverse steel	mm	(in.)
s_v	=	is the deviatoric stress vector	MPa	(ksi)
s'	=	clear spacing between transverse steel	mm	(in.)
s'_f	=	average clear spacing between FRP strips	mm	(in.)
t_f	=	thickness of FRP sheet	mm	(in.)
V_c	=	total volume of concrete in the column	mm^3	(in.^{3})
V_{st}	=	total volume of transverse steel in the column	mm^3	(in.^{3})
w_f	=	FRP strip width	mm	(in.)

173

x	=	the section distance from the center of the column cross section	mm	(in.)
Z	=	the slope of descending curve in Kent and Park model	GPa	(ksi)
β	=	material constant for Drucker–Prager plasticity model		
β_f	=	efficiency factor for confined concrete stress (the ratio between ultimate stress of fully wrapped column to ultimate stress of similar unwrapped column)		
β_ε	=	efficiency factor for confined concrete strain (the ratio between ultimate strain of fully wrapped column to ultimate strain of similar unwrapped column)		
β_μ	=	efficiency factor for confined concrete ductility (the ratio between the ductility of fully wrapped column to the ductility of similar unwrapped column)		
ε_c	=	axial strain in confined concrete		
ε_{ccu}	=	confined concrete ultimate axial strain corresponding to the ultimate confined concrete compressive stress		
$\varepsilon_{ccu,f}$	=	peak axial strain of concrete under FRP confining pressure at yielding of transverse steel		
$\varepsilon_{ccu,s}$	=	peak axial strain of confined concrete under transverse steel confining pressure at yielding of transverse steel		
$\varepsilon_{c,s}$	=	Strain of concrete under a specific constant steel confining pressure at steel yield level		
ε_{fe}	=	effective strain level in FRP wrap attained at failure		
ε_{fu}	=	design rupture strain of FRP wrap		
ε_l	=	the confined concrete lateral strain		
ε_{lu}	=	the ultimate lateral strain of confined concrete		
$\varepsilon_{l,y}$	=	the lateral strain in confined concrete at yielding of transverse steel		
ε'_c	=	axial strain at the peak stress of unconfined		

174

ε_{50h}	=	strain at 50% of compressive strength of unconfined concrete (f'_c)	
ε_{50u}	=	strain increment due to the effects of confinement for confined concrete at 50% f'_c	
μ	=	ductility factor	
ν	=	Poisson's ratio	
ρ_f	=	FRP volumetric ratio	
ρ_{st}	=	transverse steel reinforcement ratio	
ρ_{sl}	=	longitudinal steel reinforcement ratio	
σ_m	=	the mean or hydrostatic stress	MPa (ksi)
σ_y	=	yield parameter of the material in Drucker–Prager plasticity model	
ϕ	=	the angle of internal friction	

175

REFERENCES

A & P Technology. "Typical Properties of Braided Laminates". Cincinnati, OH, USA, 2014. Retrieved from http://braider.com/pdf/Properties.pdf>

ACI 318-11. "Building Code Requirements for Structural Concrete". Farmington, MI: American Concrete Institute, 2011.

ACI 440.2R-08. "Guide for the Design and Construction of Externally Bonded FRP Systems for Strengthening Concrete Structures". Farmington, MI: American Concrete Institute; 2008

ANSYS. Release 14.0 Documentation for ANSYS. Version 14.0, ANSYS Inc. Canonsburg, PA, USA, 2012

"AASHTO LRFD Bridge Design Specifications", 6th ed. American Association of State Highway and Transportation Officials, Washington, D.C., 2012.

Barros, J., and Ferreira, D., "Assessing the Efficiency of CFRP Discrete Confinement Systems for Concrete Cylinders". Journal of Composites for Construction, V. 12, No. 2, 2008, pp. 134–148

Bowman, C.L., Roberts, G.D., Braley, M.S, Xie, M., and Booker, M.J. "Mechanical Properties of Triaxial Braided Carbon/Epoxy Composites". Cincinnati, OH, USA, 2003. Retrieved from <http://braider.com/pdf/Papers-Articles/Mechanical-Properties-of-Triaxial-Braided-Carbon-Epoxy-Composites.pdf>

Chastre, C., and Silva, M. "Monotonic axial behavior and modeling of RC circular columns confined with CFRP". Engineering Structures, V. 32, No.8, 2010, pp. 2268-2277

Colomb, F., Tobbi, H., Ferrier, E., Hamelin, P, "Seismic Retrofit of Reinforced Concrete Short Columns by CFRP Materials". Composite Structures, V.82, 2008, pp. 475-48

Cui, C., Sheikh, S., "Experimental Study of Normal- and High-Strength Concrete Confined with Fiber-Reinforced Polymers." Journal of Composites for Construction, V. 14, No.5, 2010, pp. 553–561.

Demers, M., Neale, K.W., "Confinement of Reinforced Concrete Columns with Fiber-Reinforced Composite Sheets-An Experimental Study" Canadian Journal of Civil, V. 26, No.2, 1999, pp. 226–241

Drucker, D. C. and Prager, W. "Soil mechanics and plastic analysis for limit design". Quarterly of Applied Mathematics, Vol. 10, No. 2, 1952, pp. 157–165

Eid, R., and Paultre, P. "Analytical model for FRP-confined circular reinforced concrete columns". Journal of Composites for Construction, V.12, No.5, 2008, pp. 541-552

Fardis, M. N., and Khalili, H. ''FRP-encased concrete as a structural material.'' Magazine of Concrete Research., V.34, No.121, 1982, pp.191–202

Fam, A.Z.and Rizkalla, S.H. "Confinement model for axially loaded concrete confined by circular fiber-reinforced polymer tubes". ACI Structural Journal, Vol.98, No.4, 2001, pp. 451-461

Fam, A. Z., Flisak, B., and Rizkalla, S. 'Experimental and analytical modeling of concrete-filled Fiber-reinforced polymer tubes subjected to combined bending and axial loads', ACI Structural Journal, Vol. 100, No. 4, 2003, pp.499-509.

Fitzwilliam, J., and Bisby, L., 'Slenderness effects on circular FRP wrapped reinforced concrete columns', Third International Conference on FRP Composites in Civil Engineering (CICE 2006), 2006, Miami, Florida, USA

Harajli, M. H., Hantouche, E., and Soudki, K., "Stress-Strain Model for Fiber-Reinforced Polymer Jacketed Concrete Columns." ACI Structural Journal, V. 103, No. 5, 2006, pp. 672–882.

Hoshikuma, J., Kawashima, K.,Nagaya,K. and Taylor, A.W. "Stress-Strain Model for confined Reinforced Concrete in Bridge Piers". Journal of Structural Engineering, V. 123 No. 5, 1997, pp. 624-633

Ilki, A., Peker, O., Karamuk, E., Demir, C., and Kumbasar, N. "FRP Retrofit of Low and Medium Strength Circular and Rectangular Reinforced Concrete Columns". Journal of Materials in Civil Engineering, V.20, No.2, 2008, pp. 169–188.

177

Karbhari, V. M., and Gao, Y. "Composite jacketed concrete under uniaxial compression-verification of simple design equations." Journal of Materials in Civil Engineering, V.9, No.4, 1997, pp. 185–193.

Kent, D.C. & Park R. "Flexural members with confined concrete". Journal of the Structural Division, V. 97, No.7, 1971, pp. 1969-1990

Lam, L. and Teng, J.-G. "Strength Models for Fiber-Reinforced-Plastic-Confined Concrete, Journal of Structural Engineering, ASCE, V.128, No.5, 2002, pp. 612–623.

Lam, L., Teng, J. G., "Design-Oriented Stress-Strain Model for FRP-Confined Concrete in Rectangular Columns". Journal of Reinforced Plastics and Composites, V.22, No.5, 2003, pp.1149-1186

Lam, L., Teng, J. G., "Design-Oriented Stress-Strain Model for FRP-Confined Concrete." Construction and Building Materials, V. 17, 2003, pp.471–489.

Lee J.-Y.; Kim J.-K.; Yi C.-K.; Jeong H.-S.; Kim S.-W. "Compressive Response of Concrete Confined with Steel Spirals and FRP Composites". Journal of Composite Materials, Vol 44, No.4, 2010, pp. 481-504

Li, G., Kidane, S., Pang, S., Helms, J E, Stubblefield, M A. "Investigation into FRP Repaired RC Column". Composite Structures, V.62, No.1, 2003, pp. 83–89

Li, J., and Hadi, M.N.S. "Behaviour of externally confined high-strength concrete columns under eccentric loading", Composite Structures, V62, No. 2, 2003, pp.145-153.

Mander, J. B. Priestley, M. J. N., Park, R., "Theoretical Stress-Strain Model for Confined Concrete." Journal of Structural Engineering, V.114, No. 8, 1988, pp. 1804-1826

Mander, J. B. Priestley, M. J. N., Park, R., "Observed Stress-Strain Model Behaviour of Confined Concrete." Journal of Structural Engineering, V.114, No. 8, 1988, pp. 1827-1849

Mirmiran A, Shahawy M, "A new concrete filled hollow FRP composite column". Composites: part B, V.27, No. 3, 1996, pp. 263-268.

Mirmiran, A., Shahawy, M., ''Behavior of Concrete Columns Confined by Fiber Composites.'' Journal of Structural Engineering, V.123, No. 5, 1997, pp.583–590

Mirmiran, A., Shahawy, M., Samaan, M. and El Echary, H. "Effect of Column Parameters on FRP-confined Concrete". Journal of Composite for Construction, ASCE, V.2, No.4, 1998, pp.175–185.

Mirmiran A, Zagers K, Yuan W., "Nonlinear Finite Element Modeling of Concrete Confined by Fiber Composites". Finite Elements in Analysis and Design, V. 35, No. 1, 2000, pp.79-96

Nanni, A., and Bradford, N.M. "FRP jacketed concrete under uniaxial compression". Construction and Building Materials, V.9, No.2, 1995, pp.115-124

Pantelides, C., Yan, Z., "Confinement Model of Concrete with Externally Bonded FRP Jackets or Posttensioned FRP Shells". Journal of Structural Engineering, V. 133, No. 9, 2007, pp. 1288–1296

Park, R. and Paulay, T. "Reinforced Concrete Structures, John Wiley & Sons". N.Y., U.S.A., 1975.

Parvin, A. and Wang, W. "Behavior of FRP Jacketed Concrete Columns under Eccentric Loading." Journal of Composites for Construction (ASCE), 2001, Vol. 5, No. 3, pp. 146-152

Pellegrino, C., Modena, C. "Analytical Model for FRP Confinement of Concrete Columns with and without Internal Steel Reinforcement". Journal of Composites for Construction, V. 14, No. 6, 2010, pp. 693-705

Richard, R. M., and Abbott, B. J. "Versatile elastic-plastic stress strain formula." Journal of the Engineering Mechanics Division, V. 101, No. 4, 1975, pp. 511–515

179

Richart, F.E.; Brantzaeg, A.; and Brown, R.L. "A study of the failure of concrete under combined compressive stresses." 1928, Bulletin No. 185, Engineering Experiment Station, University of Illinois, Urbana

Richart, F.E.; Brantzaeg, A.; and Brown, R.L. "The Failure of Plain and Spirally Reinforced Concrete in Compression." 1929, Bulletin No. 190, Engineering Experiment Station, University of Illinois, Urbana

Rocca, S., Galati, N., Nanni, A., "Large-Size Reinforced Concrete Columns Strengthened with Carbon FRP: Experimental Evaluation". Third International Conference on FRP Composites in Civil Engineering (CICE 2006), 2006, Miami, Florida, USA

Rocca, S. "Experimental and Analytical Evaluation of FRP- Confined Large Size Reinforced Concrete Columns." Doctoral dissertation, University of Missouri -Rolla, MO, 2007

Rochette P, Labossiere, P., "A plasticity Approach for Concrete Columns Confined with Composite Materials". Proceeding of the Advanced Composite Materials in Bridges and Structures, CSCE, 1996, pp. 359-66.

Rochette, P. and Labossiere, P. "Axial Testing of Rectangular Column Models Confined with Composites", Journal of Composites for Construction, ASCE, V.4, No.3, 2000, pp.129–136

Saadatmanesh, H., Ehsani, M. R., and Li, M. W, ''Strength and Ductility of Concrete Columns Externally Reinforced with Fiber Composite Straps.'' ACI Structural Journal, V. 91, No.4, 1994, pp.434–447

Samaan, M., Mirmiram, A., and Shahawy, M. ''Model of Concrete Confined by Fiber Composites.'' Journal of Structural Engineering, V. 124, No.9, 1998, pp.1025–1031

Schickert, G., and Winkler, H. "Results of Test Concerning Strength and Strain of Concrete Subjected to Multiaxial Compressive Stresses". Deutscher Ausschuss, Berlin 1977.

Scott, B.D., Park, R., & Priestley, J.N. "Stress-strain behavior of concrete confined by overlapping hoops at low and high strain rates". ACI Journal, V.79, No 1, 1982, pp.13-27

Shahawy, M, Mirmiran, A., and Beitelman, T. "Tests and modeling of carbon-wrapped concrete columns". Composites: Part B 31, 2000, pp. 471-480

Shao, Y., Wu, Z.S. and Bian, J. "Wet-bonding between FRP laminates and cast-in-place concrete", Proceedings of the International Symposium on Bond Behavior of FRP in Structures (BBFS 2005), Hong Kong, China, December , 2005, pp. 91-96.

Sheikh, S. A., and Uzumeri, S. M. "Strength and ductility of tied concrete columns." Journal of. Structural Division. ASCE, V. 106, No.5, 1980, pp. 1079-1102

Spoelstra, M. R., Monti, G., ''FRP-Confined Concrete Model.'' Journal of Composites for Construction, V. 3, No.3, 1999, pp.143–150

Teng, J.G. and Lam, L. "Behavior and Modeling of Fiber Reinforced Polymer-confined concrete". Journal of Structural Engineering, ASCE, V. 130, No. 11, 2004, pp.1713-1723.

Teng, J. G., Huang, Y. L., Lam, L., Ye, L. P. "Theoretical Model for Fiber-Reinforced Polymer-Confined Concrete" Journal of Composites for Construction, V. 11, No.2, 2007, pp. 201–210

Toutanji, H., ''Stress-Strain Characteristics of Concrete Columns Externally Confined with Advanced Fiber Composite Sheets.'' ACI Material Journal, V.96, No.3, 1999, pp.397–404

Varma, R.K., Barros, J.A.O., Sena-Cruz, J.M. "Numerical model for CFRP confined concrete elements subject to monotonic and cyclic loadings", Composites Part B, V40, No.8, 2009, pp. 766-775

William, K. J. and Warnke, E. P. "Constitutive Model for the Triaxial Behavior of Concrete," .Proceedings, International Association for Bridge and Structural Engineering, 1975,V. 19, ISMES, Bergamo, Italy, pp. 174,

Wu, H., Wang, Y., Liu, Y., Li, X., "Experimental and Computational Studies on High-Strength Concrete Circular Columns Confined by Aramid Fiber-Reinforced Polymer Sheets". Journal of Composites for Construction, V.13, No.2, 2009, pp.125-134

181

Wu, Y., Jiang, C. "Stress- Strain Model for Eccentrically Loaded FRP- Confined Concrete Columns". The International Conference on FRP Composites in Civil Engineering (CICE 2014), Vancouver, Canada, 2014.

Xiao, Y., and Wu, H. ''Compressive Behavior of Concrete Confined by Carbon Fiber Composite Jackets.'' Journal of Materials in Civil Engineering., V.12, No.2, 2000, pp.139–146.

Yung, C., Wang, and Restrepo, J. I. "Investigation of Concentrically Loaded Reinforced Concrete Columns Confined with Glass Fiber-Reinforced Polymer Jackets', ACI Structural Journal, V.92,No.3,

VITA
SAHAR GHANEM

EDUCATION

MASTER OF SCIENCE, Civil Engineering   Jun 2009

Stevens Institute of Technology
Hoboken, NJ

BACHELOR OF SCIENCE, Civil Engineering   Jan 2005

Jordan University of Science and Technology
Irbid, Jordan

PUBLICATIONS

Ghanem, S. and Harik, I.E. (2015). "PARTIALLY CONFINED RC COLUMNS."
Proceedings of 2015 The 12th International Symposium on Fiber Reinforced Polymers
for Reinforced Concrete Structures (FRPRCS-12) & The 5th Asia-Pacific Conference on
Fiber Reinforced Polymers in Structures (APFIS-2015). Nanjing, China, pp. 6

Ghanem, S and Harik I.E. (2016). "Concentrically Loaded Circular RC Columns Partially
Confined with FRP". ACI Structural Journal, 2016. (Under review).

SCHOOL AWARDS & MEMBERSHIP IN HONORARY/ PROFESSIONAL SOCIETIES

- Omicron Delta Kappa, The National Leadership Honor Society, Inducted 2014
- Jordanian Engineering Association.
- Honor list: 2002 and 2004.

Sahar Ghanem

April, 2016